UNIVERSITÄTSKLINIKUM HAMBURG-EPPENDORF

Institut für Neurophysiologie und Pathophysiologie

Prof. Dr. med. Andreas K. Engel

INVESTIGATION AND MODULATION OF TEMPORAL PREDICTION USING NON-INVASIVE AND INVASIVE BRAIN STIMULATION

Dissertation

zur Erlangung des Doktorgrades PhD

an der Medizinischen Fakultät der Universität Hamburg

vorgelegt von:

Rebecca Burke

aus Haselünne

Hamburg, 2025

Veröffentlicht mit Genehmigung der
Medizinischen Fakultät der Universität Hamburg

Betreuer:in/Gutachter:in der Dissertation: Prof. Dr. Andreas K. Engel
Gutachter:in der Dissertation: Prof. Dr. Monika Pötter-Nerger

Vorsitz der Prüfungskommission: Prof. Dr. Andreas K. Engel
Mitglied der Prüfungskommission: Prof. Dr. Monika Pötter-Nerger
Mitglied der Prüfungskommission: Prof. Dr. Michael Rose

Datum der mündlichen Prüfung: 09.12.2025

INVESTIGATION AND MODULATION OF TEMPORAL PREDICTION USING NON-INVASIVE AND INVASIVE BRAIN STIMULATION

TABLE OF CONTENTS

Acronyms

D_{KL} Kullback-Leibler divergence 44, 45, 48

DBS deep brain stimulation 6, 7, 66–69, 72, 74–77, 79, 82–87, 93–98, 100, 106, 132

DC direct current 41

DICS Dynamic Imaging of Coherent Sources 18, 76

DLPFC dosolateral prefrontal cortex 26

EEG electroencephalography 3, 66, 68, 74, 76, 77

FAR false alarm rates 44

H&Y Hoehn & Yahr scale 69

HD-tACS high-definition tACS 39

HR hit rates 44

ICA independent component analysis 17, 74

ITPC inter-trial phase consistency 10–13, 19, 22, 28, 29, 35, 36, 47, 55, 66, 76, 77, 79, 82, 83, 86, 93, 94, 99

LFP local field potential 3, 106

LM luminance matching 14, 16, 19, 20, 22, 25–28

MEG magnetencephalography 2, 3, 6, 10, 11, 17, 38, 93, 95, 96, 98, 99, 106, 131

MNI Montreal Neurological Institute 76

mPFC medial prefrontal cortex 26

MTG middle temporal gyrus 26

PD Parkinson's disease 6, 66–69, 72, 74, 77, 79, 82–87, 93, 94, 96–99, 132

PSE point of subjective equality 18, 75, 76

ROT point of right on time 18

RT reaction times 17, 18

rTMS repetitive transcranial magnetic stimulation 55

SDT signal detection theory 42

STN subthalamic nucleus 6, 66–69, 83–85, 93, 94, 96, 100, 106

STS superior temporal sulcus 26, 27

tACS transcranial alternating current stimulation 6, 7, 30, 34, 36, 38, 41, 42, 44, 45, 47–49, 51–53, 55–59, 92–94, 98–100, 106, 131

tDCS transcranial direct current stimulation 55

TP temporal prediction 14, 16, 19, 20, 22, 25–28

UPDRS Unified Parkinson's Disease Rating Scale 69

LIST OF TABLES

LIST OF ILLUSTRATIONS

INTRODUCTION

Temporal prediction, the ability to anticipate when something will happen, is central to how we navigate the world. From catching a ball to waiting at a traffic light, or social interactions and conversations, our experience of time is deeply entwined with our ability to anticipate what comes next. We continuously extract temporal patterns from the environment (Buhusi and Meck, 2005; Kösem and van Wassenhove, 2012; Schroeder et al., 2008), whereby our perception of elapsed time is influenced by various factors, such as bottom-up processes, like physiological arousal or emotional valence (Droit-Volet and Gil, 2009), or top-down influences, like attention (Nobre and Ede, 2018).

0.1. **Rhythmic & non-rhythmic temporal prediction**

Our temporal prediction capacity is thought to be context-sensitive and may be supported by either rhythmic cues (e.g., music, speech) or memory-based cues (Breska and Ivry, 2018). When events occur in a rhythmic pattern, the brain can entrain internal neural oscillations to match the external beat. This alignment of low-frequency oscillatory phase with stimulus periodicity is believed to coincide high-excitability phases with upcoming events (ten Oever et al., 2014; Henry and Obleser, 2012; Cravo et al., 2013; Busch et al., 2009). In the auditory domain, this phase-locking is associated with improved detection and faster responses for *on-beat* events compared to *off-beat* events (Jones et al., 2006; Fujioka et al., 2015) and is consistent with oscillatory entrainment models (Henry et al., 2014). Importantly, neural oscillations do not act in isolation. Cross-frequency dynamics indicate an interaction between slow rhythmic tracking and faster neural processes. Delta-beta coupling has been identified as a hallmark of rhythm-based prediction (Arnal et al., 2015; Morillon et al., 2014). In an magnetencephalography (MEG) study of auditory beat-timing, Arnal et al. (2015) found that slow delta-band oscillations became tightly coupled with beta-band oscillations in anticipation of a target-tone, aligning neural excitability with the expected beat. The strength of this delta-beta coupling predicted whether subjects correctly detected slight timing deviations. No-

tably, the motor system was involved as well: beta oscillations, often originating from motor cortex, were engaged even though the task was purely perceptual. These findings support a framework in which sensorimotor circuits orchestrate oscillatory dynamics to implement rhythmic predictions (Arnal, 2012; Ivry and Schlerf, 2008; Morillon and Baillet, 2017). At the single-neuron level, animal studies reveal ramping and rhythmic firing patterns that likely give rise to the oscillatory dynamics observed in electroencephalography (EEG)/MEG and local field potential (LFP). In rodents, striatal neurons can encode an internally generated beat-frequency. Notably, populations of striatal neurons change their firing rate as a function of elapsed time between rhythmic cues. This ramping or cyclic pattern speeds up or slows down depending on whether the animal perceives an interval as shorter or longer (Gouvêa et al., 2015). Therefore, basal ganglia circuits are intimately involved in rhythm-based temporal prediction. Recent findings support this context-dependent specialization within subcortical circuits: the basal ganglia appear to support temporal prediction in rhythmic contexts, whereas the cerebellum is more engaged in predictions based on single-interval associations (Breska and Ivry, 2018; Terranova et al., 2023). Rhythmic structures facilitate prediction by embedding temporal cues within the sensory stream, thereby reducing memory load (Capizzi et al., 2012; Schroeder et al., 2010). In contrast, interval-based timing requires maintaining and retrieving specific internal representations, making it more susceptible to cognitive interference. Empirical evidence supports this dissociation, showing that concurrent working memory tasks impair memory-based, but not rhythmic, temporal prediction (Capizzi et al., 2012; de la Rosa et al., 2012). Importantly, in many situations, no continuous rhythm is available. Although rhythms are ecologically relevant and often used to study oscillatory contributions to temporal prediction, they present significant methodological and conceptual challenges. Rhythmic stimulation generates a continuous stream of regularly timed, bottom-up evoked responses, which can be hard to disentangle from top-down, phase-aligned neural oscillations occurring at similar frequencies. As a result,

phase alignment observed across trials may not necessarily reflect genuine resets of endogenous oscillations (Doelling et al., 2019; Zoefel et al., 2018). Moreover, although many studies on temporal prediction rely on some form of rhythmic stimulation, this approach captures only a limited aspect of real-world scenarios, neglecting how we form temporal predictions in response to irregular or non-rhythmic events. For this reason, I set out to investigate non-ryhthmic temporal prediction.

0.2. **Unimodal & crossmodal temporal prediction**

Within a single modality, the neural mechanisms of temporal prediction largely resides in that modality's processing stream and associated timing networks. Unimodal visual temporal prediction is associated with phase-resets of low-frequency delta oscillations in occipital areas and domain-general timing areas like the parietal cortices and cerebellum (Daume et al., 2021). Similarly, unimodal auditory temporal prediction employs auditory cortical oscillations and auditory-striatal circuits (Kösem et al., 2018; Lakatos et al., 2005; Bendixen et al., 2009). Thus, within one modality, temporal prediction manifests as a modality-specific modulation: the sensory cortex for that modality enters a state of heightened readiness, often through oscillatory phase alignment or sustained activity (ramping or baseline shift) timed to the expected input. Top-down projections likely mediate this process as well (Engel et al., 2001; Samaha et al., 2015). In crossmodal contexts, the brain must coordinate timing information across different sensory systems. A central question is whether crossmodal temporal prediction recruits the same oscillatory mechanisms as unimodal temporal prediction and how signals in one modality might inform other modalities. Neural synchronization appears to play a key role in crossmodal influences (Senkowski and Engel, 2024; Bauer et al., 2020), where low-frequency oscillations can provide a common temporal frame that links modalities. For example, if a rhythmic auditory cue is presented, it can phase-reset ongoing oscillations in the visual cortex, and thus entrain the visual system to the timing dictated by the auditory rhythm. This was

demonstrated in macaque monkeys by Lakatos et al. (2009): when monkeys attended to a visual task, an irrelevant auditory stimulus could still reset the phase of oscillations in the primary visual cortex, but only if the auditory stimulus was temporally aligned with the expected visual rhythm. Therefore, crossmodal phase resetting is a compelling mechanism of temporal prediction by which a cue aligns the target modality's oscillation into the optimal phase for stimulus processing. Notably, crossmodal influences can occur even in early sensory cortices, indicating that temporal predictions are propagated to very low-level processing stages when modalities are coupled (Bauer et al., 2020; Kayser and Logothetis, 2007; Lakatos et al., 2007). The goal of this thesis is to uncover how the brain supports non-rhythmic temporal prediction by investigating the neural dynamics underlying this ability in both unimodal and crossmodal contexts.

0.3. **Aims and scope of the thesis**

There is a fundamental trade-off between ecological validity, i.e., capturing the richness and complexity of real-world experiences and the need for tight experimental control to ensure that findings are interpretable and comparable within the scientific community. While temporal prediction is central to many everyday activities, such as conversation, listening to music, or motor interactions, studying it in such dynamic settings introduces numerous uncontrolled variables that complicate data interpretation. Therefore, to isolate specific mechanisms and draw reliable conclusions about the neural basis of temporal prediction, it is essential to design experiments that minimize confounding influences and allow for precise manipulation of temporal features, while still being true to everyday experiences. Traditional approaches to studying temporal prediction, such as duration estimation, temporal reproduction, or rhythm-based paradigms, provide structured frameworks that can be systematically varied and replicated. However, the environment does not always entail rhythmic structures. To address this, the present work focuses on non-rhythmic temporal prediction, where the brain must infer the timing of

an event based on motion cues and internal estimates rather than rhythmic regularities. By constraining the temporal structure of stimuli and minimizing external influences, it becomes possible to probe the dynamics of neural activity with both precision and interpretability. This thesis combines correlative and causal approaches to dissect these mechanisms. I focused on an established temporal prediction task (Daume et al., 2021; Roth et al., 2013), which was used with various modifications. In healthy subjects, MEG was used to examine the spatiotemporal patterns of brain activity associated with temporal prediction in a crossmodal context. Furthermore, transcranial alternating current stimulation (tACS) was used to infer the causal relevance of the phase of cortical delta oscillations associated with temporal prediction. So far, there have been few efforts to modulate temporal prediction performance through phase-specific tACS within the delta frequency range, making this study a noteworthy contribution to the field. Furthermore, temporal prediction was studied in Parkinson's disease (PD) patients. A hallmark of neurophysiological alterations in PD is the excessive synchronization of beta oscillations within the basal ganglia, which is linked to the severity of motor symptoms (Kühn et al., 2009; Brown, 2003). Additionally, PD patients exhibit increased beta-band synchronization between the basal ganglia and the frontal cortex, a pathological change that has been suggested to contribute to cognitive impairments (Litvak et al., 2011; Oswal et al., 2013). There is evidence indicating that the basal ganglia, particularly the dopaminergic pathway, play a crucial role in temporal prediction (Tomassini et al., 2019; Breska and Ivry, 2018; Rammsayer and Classen, 1997; Buhusi and Meck, 2005). PD patients are known to experience deficits in various time-related tasks, including duration reproduction and time perception (Smith et al., 2007; Perbal et al., 2005). In addition to conventional dopaminergic therapy, deep brain stimulation (DBS) of the subthalamic nucleus (STN) is a well-established treatment for PD, primarily aimed at alleviating motor symptoms (Deuschl et al., 2006), by decreasing excessive beta synchronization within the cortico-basal ganglia circuits (Oswal et al., 2016). Therefore, Parkinson's disease and

therapeutical DBS offer a rare opportunity to causally investigate the contribution of subcortical structures, specifically the basal ganglia, in temporal prediction.

Together, this multimethod approach leverages the strengths of observational and modulatory techniques, allowing for a more comprehensive and mechanistic understanding of how the brain generates temporal predictions in ecologically relevant, yet experimentally tractable, conditions.

0.3.1. Outline

CHAPTER 1 (Burke et al., 2025a) establishes that the phase of low-frequency delta oscillations tracks temporal prediction performance. Our study demonstrates that cross-modal phase-resets occur even with combination of non-rhythmic and discrete stimulation and thereby highlights the broad applicability of phase resets as a mechanism for predicting time across various types of stimuli.

CHAPTER 2 (Burke et al., 2025b) demonstrates that delta-tACS resulted in phase-dependent modulation of unimodal temporal prediction performance. The dynamic targeting of delta oscillations through tACS is a compelling approach to infer a causal role of the phase of delta oscillations in temporal prediction performance.

CHAPTER 3 (Burke et al., 2025c) uncovers the contribution of the basal ganglia to temporal prediction. We found that pathological oscillatory dynamics of Parkinson's disease disrupted both power and phase-based mechanisms underlying temporal prediction. This chapter highlights that DBS can restore not only motor, but also cognitive functions like temporal prediction.

CHAPTER 1

DIFFERENTIAL CONTRIBUTIONS OF LOW-FREQUENCY PHASE AND POWER IN CROSSMODAL TEMPORAL PREDICTION: A MEG STUDY

Status: *preprint*

R. Burke, J. Daume, T.R. Schneider, A.K. Engel (2025). *bioRxiv*

1.1. ABSTRACT

BACKGROUND

Our representation of time is embedded within multisensory perception, based on sight, sound, or touch. However, despite being a crucial aspect of daily life, the neural dynamics of cross-modal temporal predictions remain elusive. The objective of this study was to investigate neural correlates of tactile-to-visual influences on temporal prediction using MEG. We hypothesized to observe increased inter-trial phase consistency (ITPC) in the low-frequency delta range (0.5-4 Hz) due to their involvement in temporal prediction. In addition, stronger ITPC values should correlate with a steeper slope of the psychometric function, indicating phase alignments as a likely cause of more consistent temporal predictions.

METHODS

The study was conducted within one MEG session employing a modified version of the time prediction task by Roth et al. (2013) and Daume et al. (2021). Participants (N=23) observed a visual stimulus moving towards an occluder. Shortly before reaching the occluder, the visual stimulus faded in luminance to make the visual offset less informative. Instead, participants received a brief tactile stimulus to the ipsilateral hand at the time point of disappearance, generating a temporal expectation regarding its reappearance on the opposite side of the occluder. After variable time intervals, a visual stimulus reappeared, and participants had to indicate whether this was *too early* or *too late* compared to the movement before disappearance. A non-predictive control condition involved participants judging the variable luminance of the reappearing visual stimulus compared to its initial luminance at the beginning of the trial. Psychometric curves were fitted to the behavioral data of each participant and condition, and MEG recordings were analyzed using time-frequency representations obtained by wavelet convolution. To compare spectral power and ITPC estimates between conditions within frequency bands showing significant differences to the pre-stimulus baseline, we used cluster-based permutation statistics. Pearson's correlations were used to examine the relationship between ITPC or power estimates and the steepness of each participant's psychometric function.

RESULTS

ITPC analysis revealed strong increases in the delta range around stimulus disappearance and reappearance. Delta ITPC was significantly stronger during temporal prediction compared to the control condition. Only delta ITPC, but not delta power, correlated with the consistency of temporal prediction. Furthermore, temporal prediction led to increased alpha power in the dorsolateral and medial prefrontal cortex, as well as the right superior temporal sulcus and middle temporal gyrus, whereas beta power did not show differences between conditions.

CONCLUSION

Our findings suggest that increased delta ITPC is likely caused by phase resets driven by the temporal prediction process rather than evoked neural activity. Furthermore, our findings indicate that phase alignments occur during crossmodal visuo-tactile-to-visual temporal predictions, even with a combination of non-rhythmic and discrete stimulation. This highlights the broad applicability of phase resets of neural oscillations as a mechanism for predicting timing across various types of stimuli.

KEYWORDS

MEG, crossmodal temporal prediction, Inter-trial phase consistency, low-frequency oscillations, delta-band, alpha-band

1.2. INTRODUCTION

The ability to predict the timing of future events is fundamental to adaptive behavior. The brain continuously generates temporal predictions that allow for the alignment of sensory processing with expected input (Schroeder and Lakatos, 2009; Stefanics et al., 2010; Herbst et al., 2022). These predictions are thought to be particularly important when sensory input is transiently occluded or ambiguous, enabling the perceptual system to "fill in" missing information and prepare for upcoming stimuli (Summerfield and Egner, 2009). A fundamental body of research suggests that neuronal oscillations, especially in the delta-(0.5-4 Hz), alpha-(8-12 Hz), and beta-(13-30 Hz) bands, play a central role in temporal prediction (Arnal and Giraud, 2012; Arnal et al., 2015; Calderone et al., 2014; Rohenkohl and Nobre, 2011). Low-frequency oscillations are ideally suited for encoding temporal regularities due to their alignment with behaviorally relevant timescales (Schroeder and Lakatos, 2009). In particular, delta-band oscillations have been implicated in phase alignment mechanisms that support sensory anticipation and attentional entrainment (Daume et al., 2021; Burke et al., 2025b; Arnal et al., 2015; Cravo et al., 2013). In the context of rhythmic or temporally structured input, increased inter-trial phase consistency (ITPC) has been interpreted as evidence for phase resetting, whereby the brain aligns ongoing oscillations with anticipated stimulus onsets (Stefanics et al., 2010; Lakatos et al., 2008; Arnal et al., 2015). While many studies have focused on the auditory modality, there is growing evidence that visual and cross-modal temporal prediction also rely on phase-based neural dynamics (Samaha et al., 2015; van Ede et al., 2011; Daume et al., 2021; Burke et al., 2025b). However, the frequency specificity and topographical distribution of such effects remain debated. Beta-band activity is frequently associated with sensorimotor predictions and has been shown to decrease in response to temporal uncertainty (Daume et al., 2021; Fujioka et al., 2012). Some studies suggest that visual temporal predictions preferentially modulate alpha-band activity, even when

stimuli are presented at delta frequencies. Rohenkohl and Nobre (2011), for example, presented visual stimuli rhythmically at 1.25 and 2.5 Hz, yet only alpha oscillations, rather than delta, showed predictive modulation during stimulus occlusion. This raises the possibility that alpha-band power may play a dominant role in visual prediction, potentially reflecting higher-order cognitive control over sensory anticipation. The neural mechanisms of cross-modal temporal prediction, particularly involving visuo-tactile interactions, remain less well understood. Moreover, few studies have directly compared predictive versus non-predictive tasks using identical sensory stimulation, limiting our understanding of how task-specific cognitive demands shape neural oscillations. Building on the work of Daume et al. (2021), our study introduces a visuo-tactile-to-visual occlusion paradigm that probes temporal prediction across sensory modalities. Further, we employed a control condition, using the exact same sensory stimuli. This design allowed us to isolate the neural effects specific to temporal prediction, independent of sensory input. We focused on two main neural markers: spectral power and ITPC in the delta-, alpha-, and beta-bands, during the critical window of stimulus disappearance. Based on previous work (Daume et al., 2021; Burke et al., 2025b), we hypothesized that temporal prediction would be associated with (1) increased delta ITPC reflecting enhanced phase alignment, and (2) reduced beta power indicative of temporal uncertainty. We also explored alpha-band modulations as a potential signature of higher-order cognitive control (Samaha et al., 2015; Rohenkohl and Nobre, 2011). Furthermore, we tested whether individual differences in ITPC or power correlated with the steepness of the psychometric function, as a measure of temporal prediction precision (Daume et al., 2021). Our study aims to shed light on the distributed and frequency-specific oscillatory mechanisms supporting temporal prediction in a crossmodal visuo-tactile context.

1.3. MATERIALS AND METHODS

1.3.1. Participants

Twenty-three healthy adult volunteers participated in the study (9 females; mean age = 26.09 years, SD = 5.06; all right-handed). All participants reported normal or corrected-to-normal vision, no reduced tactile sensitivity, and no history of neurological or psychiatric disorders. Written informed consent was obtained in accordance with the Declaration of Helsinki and the study protocol was approved by the Ethics Committee of the Hamburg Medical Association. Participants received monetary compensation for taking part in the study.

1.3.2. Experimental procedure

The experimental paradigm comprised two tasks: a temporal prediction (temporal prediction (TP)) task involving visuo-tactile-to-visual temporal prediction, and a luminance matching (luminance matching (LM)) task as a working memory control condition. Both tasks were physically identical in terms of visual and tactile stimulation as well as timing structure but differed in cognitive demands and response criteria. Stimuli were presented on a matte back-projection screen (60 Hz refresh rate; resolution 1920 $\times$ 1080 pixels), positioned 65 cm in front of the participant. The main visual stimulus was a small oval (3.5° $\times$ 1.0° visual angle), which moved linearly across the screen towards a central white-noise occluder (7.5° $\times$ 11.3°), smoothed using a Gaussian filter. The occluder was centered on a gray background (44 cd/m^2; RGB = 115), and a red fixation dot was displayed in its center throughout each trial. Participants were instructed to maintain fixation at all times. Each trial began with 1500 ms of fixation. Then, the visual stimulus appeared in the periphery and moved toward the occluder at a speed of 6.9°/s. The onset of stimulus movement was jittered (1000-1500 ms before disappearance) to prevent temporal predictability and the initial side of stimulus onset (left or right) was counterbalanced across participants but remained constant within individuals. Importantly,

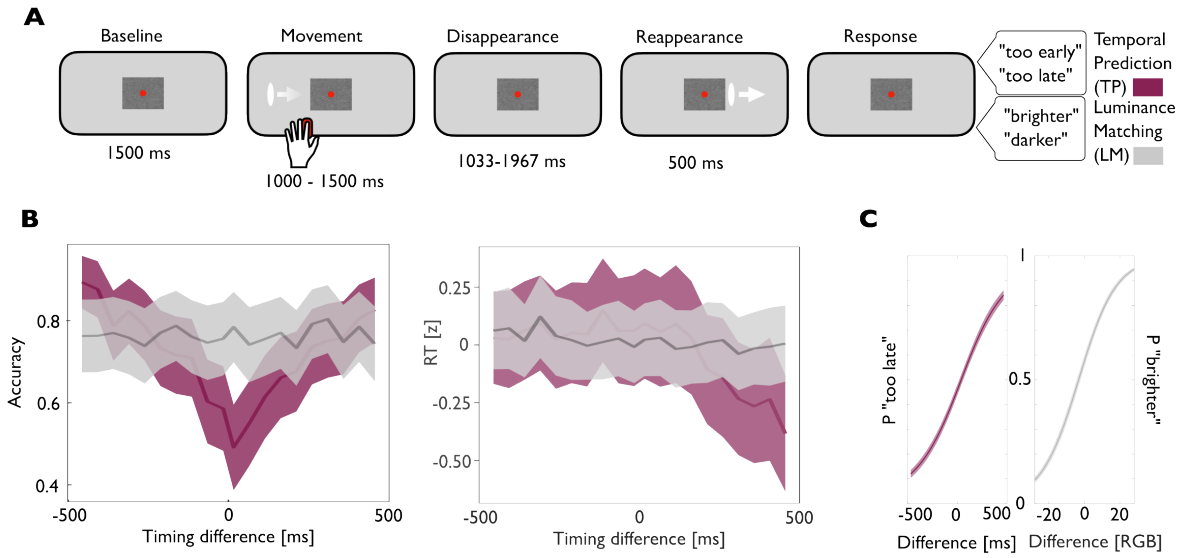

Figure 1.1: Experimental design and behavioral results. (A) Experimental paradigm. Participants viewed a white ellipse moving toward and disappearing behind an occluder. Just before disappearance, the ellipse faded in contrast to make the visual offset less informative. Instead, participants received a brief tactile cue to the ipsilateral hand at the time of disappearance. Therefore, the timing of the tactile stimulus provided an important cue needed to judge the appropriateness of the reappearance of the visual stimulus. After a variable delay, the ellipse reappeared with a slightly different luminance. In the temporal prediction (TP) task, participants judged whether the reappearance was *too early* or *too late*, based on the velocity of the stimulus but ignoring the luminance change. In the luminance matching (LM) control task, visual and tactile stimulation identical to the TP task was used, but participants judged the brightness of the reappearing stimulus, ignoring its timing. (B) Accuracy and reaction times along timing differences. The left panel shows participant accuracy across various timing differences, with time 0 ms indicating the objectively correct reappearance after 1500 ms for the TP (red) and LM (grey) condition. The right panel displays log-transformed and standardized reaction times (RT) across timing differences. (C) Psychometric curves illustrate response sensitivity and bias in the TP (red) and LM (grey) condition. Time 0 ms in the TP condition (left) refers to the objectively correct reappearance, while a luminance difference of 0 RGB values in the LM condition (right) indicates objective luminance equality upon reappearance. P=proportion, RGB=red-green-blue.

the visual stimulus decreased in luminance, thereby making the visual offset less informative. Instead, participants received a brief tactile cue (70 ms) at the time point of full disappearance to the index finger of the side where the stimulus was moving toward the occluder. The occluder size and stimulus speed were calibrated such that a constant time of 1500 ms was required to move behind the occluder. After disappearance, the stimulus reappeared at variable time points (jittered from ±17 ms to ±467 ms around the expected reappearance at 1500 ms), resulting in 20 different reappearance latencies. This temporal manipulation allowed assessment of subjective timing perception. The initial luminance of the moving stimulus changed on a trial-by-trial level. Similarly, the luminance changed after reappearance relative to the initial luminance (range: ±1 to ±40 cd/m^2; in 20 steps). These values were matched across conditions to ensure the same physical stimulus structure.

In the TP task, participants had to judge whether the reappearing stimulus appeared either *too early* or *too late*, based on the previously perceived visual motion before occlusion. The tactile stimulus was administered using a Braille piezostimulator (QuaeroSys, Stuttgart, Germany; 24 pins, 1 mm diameter, 2.5 mm spacing), activating all pins simultaneously. At the time point of tactile stimulation, no concurrent visual event occurred on the screen. Responses were given via button press using the hand contralateral to the stimulus reappearance side. Response mapping (*too early* = left key / *too late* = right key, or vice versa) was counterbalanced across participants. In the LM control task, participants were instructed to judge whether the luminance of the reappearing stimulus was *brighter* or *darker* than the pre-disappearance luminance. All other aspects of the physical stimulation and timing were identical to the TP task. This task served as a cognitive control to account for non-temporal processing demands and ensured identical visual stimulation between tasks. The experiment was conducted in a single recording session, including 12 blocks (6 per condition), resulting in 60 trials per block and a total

of 720 trials per participant (360 per condition). Each participant completed a brief initial practice of the task, including feedback after each trial. For the main experiment, participants received feedback at the end of each block in which the overall accuracy was displayed. Participants could rest as needed after each block. To mask the sound of the Braille stimulator, participants wore in-ear MEG-compatible headphones delivering continuous pink noise (85 dB, 48 kHz sampling rate) during all experimental blocks.

1.3.3. Data acquisition and preprocessing

The electrophysiological data was recorded with a 275-channel whole-head MEG system (CTF MEG International Services LP, Coquitlam, Canada) at 1200 Hz in a dim, magnetically shielded room. Electrooculogram (EOG), electromyogram (EMG), and electrocardiogram (ECG) were recorded using Ag/AgCl electrodes for artifact rejection. Head position was monitored online and realigned before each block if deviations exceeded 5 mm from the original position (Stolk et al., 2013). We used MATLAB (R2016b) (The MathWorks Inc., 2019), FieldTrip (Oostenveld et al., 2011), and custom scripts to analyze the data. Preprocessing included bandpass filtering (0.5-170 Hz), notch filters at 50, 100, and 150 Hz and downsampling the data to 400 Hz. Trials with artifacts (e.g., muscle, jumps) were excluded via a semi-automatic rejection procedure. On average, 666.6 $\pm$37.4 (92.58% $\pm$5.14%) trials remained after preprocessing. Finally, independent component analysis (ICA) was used to remove ocular, cardiac, and muscle artifacts. Approximately 25 $\pm$6.9 out of 275 components were removed per participant. Furthermore, trials deviating by $\geq$1 frame (17 ms) from the intended stimulus timing were excluded. Sensors were flipped to ensure comparability across participants who viewed stimuli from different directions (see Time-frequency analysis).

Behavioral analysis

Reaction times (RT) and accuracy were analyzed using R (R Core Team, 2024) and RStudio (RStudio Team 2020). Psychometric curves were calculated in MATLAB (The

MathWorks Inc., 2019). Trials with reaction times >3 SDs from the mean were excluded. RTs were logarithmically transformed and standardized prior to statistical modeling. Psychometric curves were fitted using binomial logistic regression (MATLAB's *glmfit.m* and *glmval.m*) to determine each participant's subjective point of right on time (ROT) in the prediction task and point of subjective equality (PSE) in the working memory control task. The steepness of the psychometric function was quantified using the inverse difference between 25% and 75% threshold points. One-sample t-tests ($\alpha = 0.025$, Bonferroni-corrected) were used for comparisons of the two tasks.

Time-frequency analysis

Time-frequency decomposition was performed via convolution with 40 complex Morlet wavelets (0.5-100 Hz). Spectral power was computed for each trial and normalized to a pre-stimulus baseline (-500 to -200 ms). Power estimates were binned into 100 ms steps and averaged per condition. Trials were segmented into four overlapping time windows: Baseline: -550 to -50 ms before stimulus motion onset; Movement: -50 to 950 ms from motion onset; Disappearance: -350 to 950 ms from full occlusion; Reappearance: -350 to 450 ms from stimulus reappearance; For statistical comparisons between tasks, we used cluster-based permutation tests (Maris and Oostenveld, 2007), correcting for multiple comparisons across time, frequency, and space. Sensor data were flipped along the sagittal axis for participants who viewed leftward motion. Our analyses focused primarily on the Disappearance window, since this is thought to be the critical time window for the temporal prediction process. Furthermore, for source localization we used Dynamic Imaging of Coherent Sources (DICS) beamforming (Gross et al., 2001) based on individual magnetic resonance images and a single-shell volume conductor model (Nolte, 2003) with a 5003 voxel grid aligned to the MNI152 template brain. Again, as for sensor-level analysis, all voxels were flipped along the sagittal axis for participants who were presented with the white ellipse moving from right to left prior to statistical calculations.

Inter-trial phase consistency (ITPC)

ITPC was computed from complex time-frequency representations obtained via wavelet convolution (see above). Phase angles were extracted at each time point and trial using MATLAB's *angle.m* function, and ITPC was calculated as:

$$ITPC_{tf} = \left| \frac{1}{N} \sum_{r=1}^{n} e^{i\phi_{r,tf}} \right|$$

where n is the number of trials and $\phi_{r,tf}$ the phase angle in trial r at time frequency point *tf*. ITPC values were averaged in 100 ms bins and pooled across channels and conditions to provide an overview of phase alignment throughout the trials. Furthermore, to focus on dynamics surrounding stimulus disappearance, we additionally computed ITPC in a -1,900 to 1,900 ms window centered on full occlusion of the white ellipse. Values were averaged within the 0.5-4 Hz delta-band and compared between conditions using cluster-based permutation statistics over time bins and sensors. At the source level, ITPC was estimated using the same beamformer filters as in the spectral power analysis. Finally, to assess neural-behavioral coupling, voxel-wise Pearson correlations were performed between ITPC (averaged 0 to 800 ms post-disappearance) and the steepness of each participant's psychometric function. Multiple comparisons were corrected via cluster-based permutation testing.

1.4. RESULTS

1.4.1. Comparable behavioral performance across conditions

To assess behavioral differences between the TP and LM conditions, we compared behavioral accuracy, reaction times, as well as the slope and bias of the psychometric curve. Accuracy was significantly lower in the TP condition (mean = 0.719, SEM = 0.060) compared to LM (mean = 0.764, SEM = 0.034) ($t(22)$ = -4.21, $p < .001$, Cohen's d = -0.88). Therefore, participants performed more accurately when judging luminance than

when making temporal predictions. However, a more sensitive measure of performance, the psychometric curve, showed no statistically significant difference in the slope of responses between the TP and LM conditions ($t(22)$ = -1.89, p = .072, Cohen's d = -0.39). Similarly, the bias did not differ significantly between conditions ($t(22)$ = -0.30, p = .764, Cohen's d = -0.06). These results show comparable response trends and discrimination sensitivity between conditions. Analysis of log-transformed and standardized reaction times showed no significant overall difference between conditions ($t(22)$ = -0.59, p = .559, Cohen's d = -0.12).

1.4.2. Alpha power significantly increased during temporal prediction

We first examined time-resolved total power across frequencies, averaged over all conditions, sensors, and participants. To characterize general oscillatory dynamics during the trial, we applied cluster-based permutation statistics to compare the TP and LM task against baseline (Figure 1.2). Relative to the pre-stimulus baseline, a significant increase in delta-band power was observed during the disappearance window, time-locked to the stimulus occlusion (all cluster-p<.001). In contrast, beta-band power showed a significant decrease following stimulus disappearance, consistent with previous reports of beta suppression during prediction processes. Similarly, we found significant alpha-band modulations during the occlusion window. To isolate condition-specific effects, cluster-based permutation statistics were applied to compare the TP and LM tasks against each other within the delta-, alpha-, and beta-band on sensor and source level (Figure 1.2B&C). While no significant clusters were found for delta or beta power, we observed a significant increase in alpha-band power during the TP task compared to the LM task in the dorsolateral and medial prefrontal cortex. A second cluster was found in the area of middle temporal gyrus and superior temporal sulcus (both cluster-p=.02).

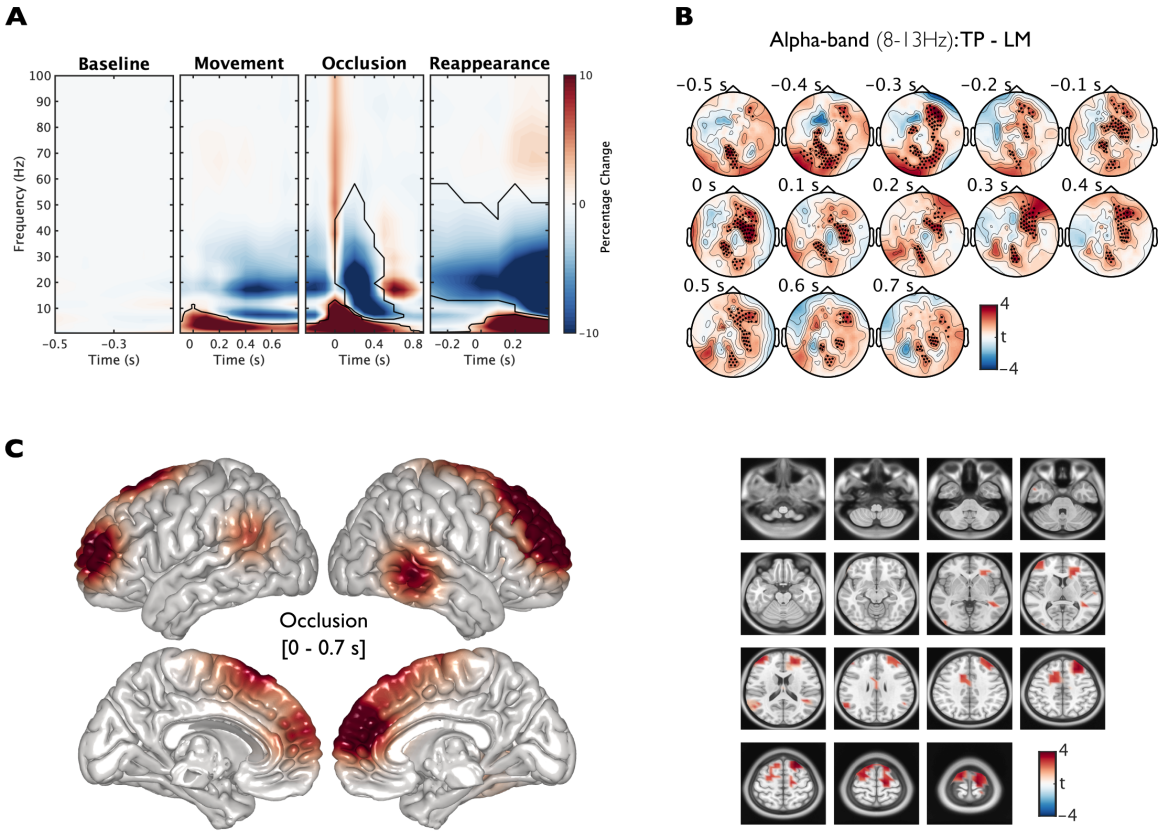

Figure 1.2: Spectral power modulations. (A) Spectral power was averaged across all sensors, conditions, and participants, with each time window aligned to key events in the taks and normalized using a pre-stimulus baseline. Time 0 s marks the onset of each event. Significant power changes relative to baseline are indicated by areas enclosed in solid lines, as determined by cluster-based permutation testing. (B, C) Comparison of alpha-band activity (8–13 Hz) between the temporal prediction and luminance matching task during time intervals surrounding stimulus occlusion. (B) On sensor level, black dots mark sensors within clusters that showed statistically significant differences between conditions. (C) At the source level, cluster-based permutation tests identified voxel clusters with significant task-related differences, visualized as colored regions in the surface and slice images averaged across the disappearance time window (0-0.7s).

1.4.3. Delta inter-trial phase consistency was increased during and correlated with temporal prediction

Similarly to our spectral power analysis, we examined time-resolved ITPC across frequencies, averaged across all conditions, sensors, and participants (Figure 1.3A). Cluster-based permutation statistics revealed a significant ITPC increase in all frequency bands at the time point of disappearance compared to pre-stimulus baseline (all cluster-p=<.001). To assess task-specific differences, we compared the TP and LM tasks using cluster-based permutation statistics. This revealed significantly stronger ITPC in the delta-band during the disappearance window for the TP task compared to the LM task (cluster-p=.02). This effect was most pronounced within the time window from 0 to 800 ms following stimulus disappearance, indicating enhanced phase alignment across trials when participants were engaged in predicting the reappearance of the visual stimulus (Figure 1.3B). Source-level analysis of this contrast revealed increased delta-band ITPC in several visual and visual-association regions, including the left and right primary and secondary visual cortices as well as the right inferotemporal cortex (cluster-p=.01). The pattern of increased phase consistency in early visual areas, particularly contralateral to the anticipated stimulus, supports the interpretation of a phase reset mechanism in response to internally generated temporal predictions. Finally, correlational analyses revealed a significant correlation between delta ITPC and the steepness of the individual psychometric function, with clusters primarily located in the bilateral primary somatosensory cortex and sensory association areas (Figure 1.4) (cluster-p=.03). No such correlation was observed for delta power, nor did alpha power correlate significantly with psychometric slope.

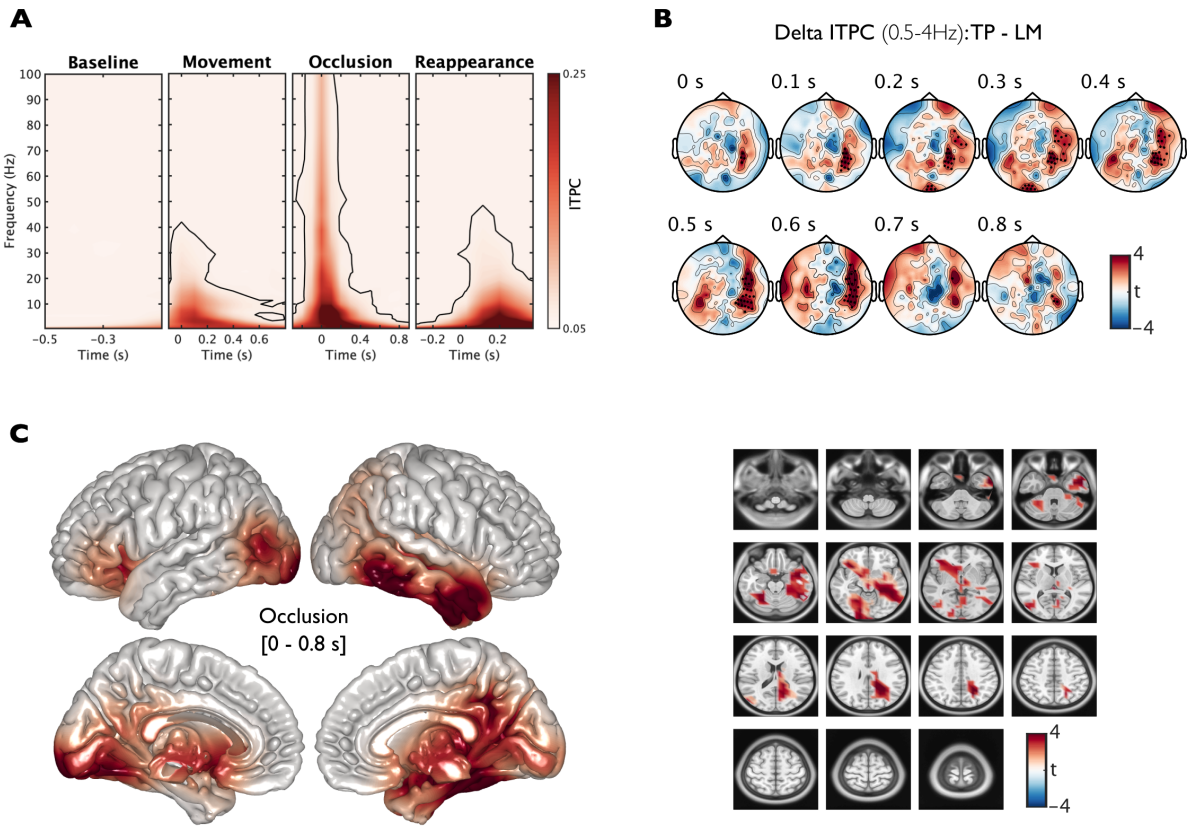

Figure 1.3: ITPC. (A) ITPC values were averaged across all sensors, conditions, and participants, with significant deviations from baseline highlighted by outlines derived from cluster-based permutation testing. (B, C) Differences in delta-band ITPC (0.5–3 Hz) between the temporal prediction task and the luminance matching control. (B) Black dots mark sensors that formed significant clusters in the group comparison on sensor level. (C) On source level, colored regions indicate voxel clusters with statistically significant differences between conditions.

1.5. DISCUSSION

The current study investigated neural oscillatory dynamics during a visuo-tactile-to-visual temporal prediction task, with a luminance matching task as a cognitive control.

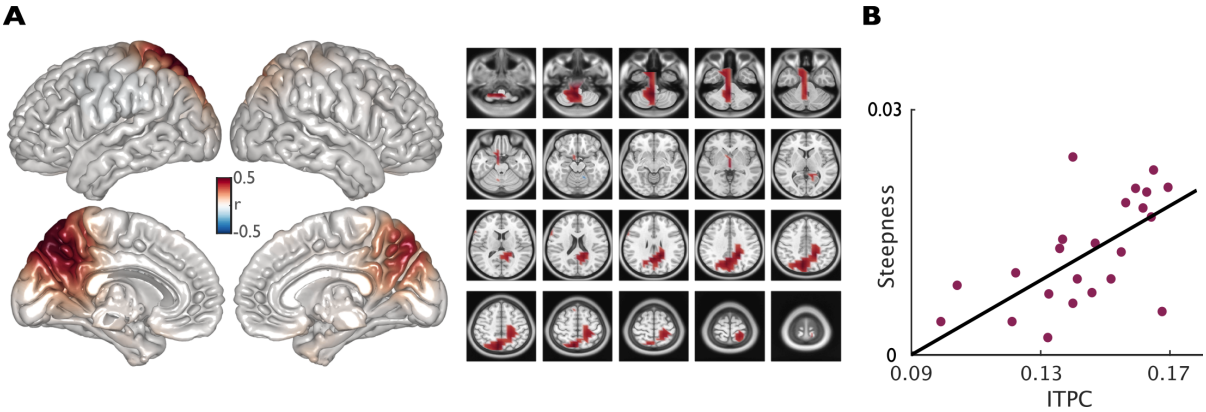

Figure 1.4: Correlation of delta ITPC and behavior. (A) Voxel-wise correlations between individual ITPC values and the steepness of participants' psychometric functions are shown for the temporal prediction task. ITPC was computed in the delta-band (0.5–4 Hz) over a time window from 0 to 800 ms following stimulus disappearance (see Figure 1.3). Colored regions highlight voxel clusters where correlations reached statistical significance using cluster-based permutation statistics. (B) The scatter plot shows this correlation, with each dot representing one participant; ITPC values were averaged across voxels within the significant clusters. No significant correlations were found for the luminance matching condition or between spectral power in the delta-, alpha-, and beta-band and behavioral measures.

Beta desynchronization during visual occlusion occurs across predictive and non-predictive tasks

In line with previous studies, we observed a significant reduction in beta-band power during the disappearance window, relative to pre-stimulus baseline. This suppression occurred in both the TP and LM conditions, and while the effect was robust, no significant task difference emerged. Beta power suppression could reflect processes engaged during both predictive and non-predictive evaluation of dynamic sensory events. Beta-band oscillations, particularly over sensorimotor and associative cortices, have been widely implicated in top-down predictive control, timing, and maintenance of the current sensorimotor set (Engel and Fries, 2010; Arnal, 2012; Fujioka et al., 2012; Kilavik et al., 2013). The transient suppression of beta power in our task is consistent with the notion that beta desynchronization facilitates adaptive updating of internal models in response to sensory transitions. In our study, this would occur due to the sudden occlusion of the visual stimulus. Importantly, beta suppression has also been linked to increased temporal uncertainty, with reduced beta power observed when stimulus timing becomes unpredictable or requires estimation (Arnal et al., 2015; Palmer et al., 2019; Todorovic et al., 2015). However, the absence of a task-specific difference in beta power between TP and LM conditions is notable. Given that both tasks involved identical sensory transitions and attentional demands, but only TP required active temporal estimation, it is possible that beta-band dynamics encode uncertainty in a modality- or context-unspecific manner. For example, beta suppression may signal increased reliance on internal models during periods of occlusion, regardless of whether a specific temporal prediction is required, thus serving as a non-specific readiness or preparatory mechanism across tasks (Palmer et al., 2019).

Increased alpha power during temporal prediction suggests top-down engagement

Alpha oscillations constitute a central component of the neural architecture underpinning temporal prediction in multisensory contexts (Keil and Senkowski, 2018). Our results are in line with this by showing that alpha-band power increased significantly during the TP compared to LM condition in a cluster of voxels in the dosolateral prefrontal cortex (DLPFC) and medial prefrontal cortex (mPFC) (BA 9), despite both tasks involving identical sensory input. A second alpha cluster emerged in middle temporal gyrus (MTG)/superior temporal sulcus (STS), regions typically implicated in timing and multisensory integration (Beauchamp et al., 2008; Noesselt et al., 2012). These regions appear to leverage dynamic modulations in alpha-band activity to implement top-down expectations. Specifically, event-related alpha power increases, are believed to transiently inhibit task-irrelevant sensory processing, in line with the gating-by-inhibition framework (Jensen and Mazaheri, 2010; Klimesch et al., 2007). In this framework, enhanced alpha power does not reflect a passive state, but an active process of internal attentional control, aimed at suppressing potentially interfering sensory input during task phases that rely on internal computation rather than external stimulation. The , specifically the DLPFC and mPFC, are repeatedly implicated in orchestrating these forms of internal control. During the occlusion phase of our task, when no sensory input is present and participants must internally maintain a dynamic temporal model to judge the timing of the stimulus reappearance, increased alpha power in frontal regions likely reflect inhibition of premature or irrelevant processing (e.g., of sensory noise or competing expectations) (Klimesch et al., 2007; Sauseng et al., 2005). Meanwhile, temporal regions including the STS and MTG have been implicated in adjudicating the temporal alignment of incoming multisensory stimuli, modulating alpha power in accordance with the temporal congruency or asynchrony of visuo-tactile inputs (Noesselt et al., 2012). In an fMRI study, Noesselt et al. (2012) examined how the brain encodes synchronous vs. asynchronous audiovisual

stimuli. They identified subregions along the STS that preferentially responded when stimuli were out of sync versus in sync. Notably, when participants perceived asynchrony, there was stronger functional coupling between the STS complex and prefrontal areas. Therefore, these regions may be inherently connected during temporal processing tasks. Although our temporal prediction task is contrasted against a working memory control condition, it is important to recognize that temporal prediction itself recruits executive processes analogous to those used in working memory, including the maintenance and updating of internal representations over time. Specifically, during the occlusion period, participants must hold in mind the velocity and trajectory of a moving stimulus and project it forward to estimate the expected time of reappearance, a process that closely parallels processes in visuospatial working memory tasks (Sauseng et al., 2005). While both tasks rely on internal processing and top-down control, the working memory task involves the maintenance of static visuospatial information, with comparatively less emphasis on internal modeling over time, which may enhance alpha synchronization due to increased task demands (Klatt et al., 2022). In summary, the observed increase in alpha power in the TP condition, relative to the LM condition, supports the view that alpha-band oscillations play a central role in implementing top-down control during internally guided temporal prediction processes. The engagement of both prefrontal and temporal regions suggests a coordinated network in which increased alpha synchronization supports the maintenance of temporal expectations by actively suppressing premature or distracting input. These findings may extend existing models of alpha-based inhibition by demonstrating that such mechanisms are not only recruited during classical working memory or attention tasks but also during anticipatory processes. Thus, alpha oscillations could reflect a dynamic control process that is flexibly deployed depending on the temporal structure and cognitive demands of a task, reinforcing their role as a fundamental neural mechanism for predictive processing in multisensory contexts.

Delta phase alignment may support crossmodal predictive timing

A central finding of our study is the enhanced delta-band ITPC during stimulus disappearance in the TP condition compared to the LM control condition. This supports the idea that delta oscillations subserve temporal prediction by providing a phase-based reference frame for aligning internal neural states with anticipated external events (Arnal and Giraud, 2012; Schroeder and Lakatos, 2009; Cravo et al., 2013). The increase in ITPC was most pronounced between 0 and 800 ms after disappearance of the stimulus, corresponding to the time window in which participants internally simulated the continuation of the visual trajectory. Our results directly replicate the findings of Daume et al. (2021), who reported increased delta-band ITPC during a unimodal visual and crossmodal visuo-tactile temporal prediction task. While our findings conceptually align with the work by Daume et al. (2021), the visuo-tactile-to-visual paradigm introduces a novel and more demanding form of crossmodal temporal prediction. The previous design assessed whether visual input could prime the somatosensory system to anticipate tactile onset. In contrast, the novel task reverses this logic: we presented a moving visual stimulus that gradually decreased in luminance prior to disappearing, thereby rendering the visual offset temporally ambiguous. Crucially, just before disappearance, a brief, tactile stimulus was delivered to the index finger. This tactile cue served as a precise temporal anchor for participants to initiate an internal prediction about the timing of a subsequent visual reappearance from behind the occluder. This subtle yet important change in task structure entails a crossmodal shift in predictive responsibility: the tactile system now supplies the timing cue, while the visual system becomes the target of temporal anticipation, necessitating participants to integrate temporally informative, non-redundant cues across modalities. Our results thus extend the phase reset framework by demonstrating that delta-band ITPC tracks crossmodal predictions in contexts where temporal structure is not visually salient, but is conveyed through a secondary modality. This supports the interpretation that delta oscillations facilitate the binding of temporally disjoint,

crossmodal cues into coherent predictive representations, even when sensory input is ambiguous or degraded. Importantly, delta ITPC was positively correlated with individual differences in temporal prediction performance, providing further evidence that phase alignment is not only a marker of neural synchronization but also reflects behaviorally meaningful anticipatory processes. Source localization revealed increased delta ITPC in bilateral early visual cortices (V1/V2), consistent with research showing that primary and secondary occipital areas exhibit phase alignment during visual anticipation (Cravo et al., 2013). Additionally, robust delta-phase synchronization was observed in right-lateralized inferotemporal cortex, a region implicated in high-level visual processing and predictive coding of object identity and motion trajectories (Summerfield and Egner, 2009). Importantly, our findings also implicate regions beyond the sensory cortices. Enhanced delta ITPC in the cerebellum aligns with extensive literature attributing to the cerebellum a key role in subsecond timing and sensorimotor prediction (Ivry and Keele, 1989; Merchant et al., 2013). This supports the view that cortico-cerebellar loops contribute to temporal anticipation by modulating the timing of cortical excitability through slow oscillatory dynamics. Notably, we also found that delta ITPC in bilateral somatosensory and sensory association cortices significantly correlated with the steepness of individual psychometric functions, indicating a direct relationship between neural phase alignment and the precision of temporal predictions. These results support earlier findings showing delta-phase consistency contributes to timing accuracy and crossmodal temporal integration (Breska and Ivry, 2018; Cravo et al., 2013). The absence of corresponding correlations with delta power underscores the specific functional relevance of phase-based measures in capturing behaviorally relevant neural dynamics (Haegens and Golumbic, 2018). Together, these results highlight delta ITPC as a robust index of temporal prediction across a distributed network encompassing sensory, associative, and subcortical structures, with functionally specific contributions to crossmodal timing precision and anticipatory behavior.

1.6. CONCLUSION

These results contribute to a growing literature, suggesting delta oscillations as a scaffold for predictive timing, especially under uncertainty. The lack of task-specific effects in beta power, and the task-dependent modulation of alpha activity in frontal and temporal regions further suggest that temporal prediction recruits a flexible hierarchy of oscillatory mechanisms at multiple timescales (Senkowski and Engel, 2024). Importantly, this data underscores the need for studies using causal manipulations, such as phase-specific tACS, to determine whether phase alignment is not only correlated with, but causally drives, enhanced temporal prediction.

Data availability statement

Data to evaluate the results will be made available upon reasonable request to the authors.

Declaration of competing interest

The authors declare that they have no known competing financial interests or personal relationships that could have appeared to influence the work reported in this paper.

CRediT authorship contribution statement

Rebecca Burke: Formal analysis, Validation, Visualization, Data curation, Writing - original draft, Writing - review & editing. **Jonathan Daume**: Conceptualization, Methodology, Investigation, Writing - review & editing. **Till R. Schneider**: Conceptualization, Methodology, Writing - review & editing, Supervision. **Andreas K. Engel**: Conceptualization, Methodology, Writing - review & editing, Funding acquisition, Project administration, Supervision.

Acknowledgements

This work was supported by grants from the Deutsche Forschungsgemeinschaft (SFB TRR 169/B1/B4 awarded to A.K.E.) and from the European Research Council (project cICMs, ERC-2022-AdG-101097402 awarded to A.K.E.). We thank Christiane Reißmann for assistance in data recording, and Alexander Maÿe, Marleen J. Schoenfeld, and Peng Wang for helpful discussions on the data. Views and opinions expressed in this paper are those of the authors only and do not necessarily reflect those of the European Union or the European Research Council. Neither the European Union nor the granting authority can be held responsible for them.

CHAPTER 2

THE ROLE OF DELTA PHASE FOR TEMPORAL PREDICTION INVESTIGATED WITH BILATERAL PARIETAL TACS

Status: *published*

R. Burke, A. Maÿe, J. Misselhorn, M. Fiene, F.J. Engelhardt, T.R. Schneider, A.K. Engel (2025). *Brain Stimulation*

2.1. ABSTRACT

BACKGROUND
Previous research has shown that temporal prediction processes are associated with phase resets of low-frequency delta oscillations in a network of parietal, sensory and frontal areas during non-rhythmic sensory stimulation. Transcranial alternating current stimulation (tACS) modulates perceptually relevant brain oscillations in a frequency and phase-specific manner, allowing the assessment of their functional qualities in certain cognitive functions like temporal prediction.

OBJECTIVE
We addressed the relation between oscillatory activity and temporal prediction by using tACS to manipulate brain activity in a sinusoidal manner. This enables the investigation of the relevance of low-frequency oscillations' phase for temporal prediction.

METHODS
Delta tACS was applied over the left and right parietal cortex in two separate unimodal and crossmodal temporal prediction experiments. Participants judged either the visual or the tactile reappearance of a uniformly moving visual stimulus, which shortly disappeared behind an occluder. tACS was applied with six different phase shifts relative to sensory stimulation in both experiments. Additionally, a computational model was developed and analysed to elucidate oscillation-based functional principles for the generation of temporal predictions.

RESULTS
Only in the unimodal experiment, the application of delta tACS resulted in a phase-dependent modulation of temporal prediction performance. By considering the effect of sustained tACS in the computational model, we demonstrate that the entrained dynamics can phase-specifically modulate temporal prediction accuracy.

CONCLUSION
Our results suggest that delta oscillatory phase contributes to unimodal temporal prediction. Crossmodal prediction may involve a broader brain network or cross-frequency interactions, extending beyond parietal delta phase and the scope of our current stimulation design.

KEYWORDS

Non-invasive brain stimulation, Transcranial alternating current stimulation, Temporal prediction, Phase-specificity

2.2. INTRODUCTION

Temporal prediction involves the brain's ability to anticipate the timing of future events. This ability contributes to numerous aspects of human behaviour, from simple sensory processing to complex decision-making. Neural underpinnings related to temporal prediction emphasise the role of phase alignment or entrainment of neural oscillations, particularly in the low-frequency delta band, as a key mechanism (Lakatos et al., 2008; Schroeder and Lakatos, 2009). Studies have shown that delta oscillations align with the temporal structure of the incoming sensory information stream and that oscillatory phase plays a crucial role in determining the accuracy of responses (Arnal et al., 2015; Stefanics et al., 2010). When events are highly temporally predictable, such as rhythmic patterns, the high-excitability phase of ongoing oscillations can be adjusted to align with the predicted onset of incoming information, enhancing neural excitability and thereby optimising behaviour. (Gulberti et al., 2015; Kayser et al., 2010; Lakatos et al., 2008). This phase alignment is strengthened when top-down resources are engaged, e.g., when expectation cues indicate the occurrence of relevant stimuli (Herbst et al., 2022; Stefanics et al., 2010). Furthermore, oscillatory phase in one modality can be modified not only by events within the same modality, but also by events from different modalities (Bauer et al., 2018; Diederich and Colonius, 2012; Fiebelkorn et al., 2011; Lakatos et al., 2008; Romei et al., 2012). Supporting this notion, Daume et al. (2021) highlight the importance of delta phase alignment across trials in supporting temporal prediction tasks within and across sensory modalities. This study investigated the role of low-frequency neural oscillations, particularly in the delta band (0.5-4 Hz), in temporal prediction tasks. The strength of delta ITPC in parietal areas was found to correlate with individual task performance, suggesting a direct link between the degree of oscillatory phase alignment and the accuracy of temporal predictions. This enhancement was observed in parietal cortices, along with other regions like sensory and frontal areas, highlighting a distributed

network for temporal prediction. This correlation was observed for both unimodal (i.e., visual) and crossmodal (i.e., visuo-tactile) task settings, indicating that this process is not modality-specific. Despite these findings, the study does not provide causal evidence for the functional role of delta phase in predicting the onset of relevant stimuli. As the correlation between delta ITPC and temporal prediction performance was strong, the direct manipulation of delta phase through transcranial stimulation could provide causal evidence for this relation. Building on this previous work (Daume et al., 2021), we set out to investigate the causal role of oscillatory phase in temporal prediction. To achieve this, precise control over both oscillatory phase and sensory stimulation is required (de Graaf and Sack, 2014; Fiene et al., 2020, 2022; Sack, 2006). Extending our previous work (Daume et al., 2021), we delivered sensory stimuli with precise timing during transcranial alternating current stimulation (tACS) with systematic phase offset. If temporal prediction performance is related to delta phase, we expect to observe a fluctuation in performance depending on the tACS phase, leading to either enhancement or deterioration of performance (Figure 2.1) in the unimodal as well as the crossmodal experiment.

2.3. MATERIAL AND METHODS

2.3.1. Participants

In the unimodal experiment, 29 naïve, right-handed participants (mean age 26.5 $\pm$ 4.35 years, 16 female; 13 male) were recruited and in the crossmodal experiment, 30 naïve, right-handed participants (mean age 25.7 $\pm$ 3.9 years, 15 female; 15 male) were recruited based on previous effect size observations in studies that investigated phase-dependent stimulation effects on sensory perception using tACS (Fiene et al., 2022, 2020). Participants had normal vision and no psychiatric or neurological history. Handedness was assessed using the short version of the Edinburgh Handedness Inventory. The experiments, approved by the Hamburg Medical Association, adhered to the Declaration of

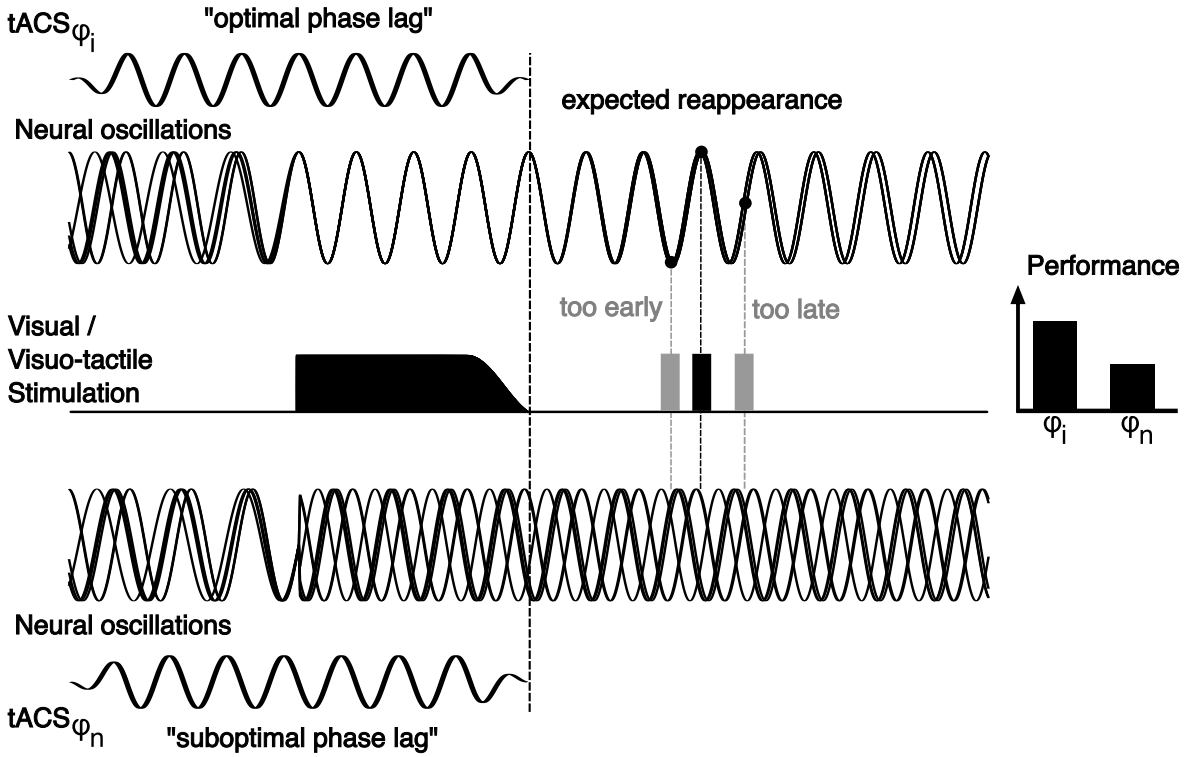

Figure 2.1: Rationale of the study. We explored how the timing of oscillatory phase affects temporal prediction by integrating sensory stimulation with transcranial alternating current stimulation (tACS). Building on Daume et al. (2021), our approach differed by using a gradually disappearing visual stimulus to reduce prominent sensory induced offset effects. Instead, the application of tACS was employed to induce phase alignment by engaging neural oscillations to synchronise with the electrical rhythm applied to the scalp. The notion of phase alignment assumes that the accuracy of predictions regarding incoming relevant information depends on the magnitude of phase alignment and that the phase encodes the expected time point of reappearance. The visual stimulus is designed to coincide with or disrupt the oscillatory phase alignment induced by tACS, thereby either maintaining the phase alignment or interfering with the ongoing oscillation. If the phase of neural oscillations constitutes an integral element for temporal prediction, we should either see an enhancement or a deterioration of performance depending on the tACS phase lag relative to the visual stimulus. Furthermore, an optimal phase lag of tACS would align the expected reappearance of the stimulus with a high-excitability phase of the neural oscillations and thereby augment temporal prediction performance.

Helsinki, with informed consent given by all participants and monetary compensation provided.

2.3.2. Experimental procedure

The experimental design of the current studies was based on Roth et al. (2013) which examined visual temporal predictions in cerebellar patients, and closely aligns with a previous MEG study that we have carried out on the neural mechanisms of temporal predictions (Daume et al., 2021). Participants sat in a dimly lit, electrically shielded and sound-attenuated chamber. The visual stimuli were projected onto a matte LCD screen at 120 Hz with a resolution of 1920 × 1080 px. A white noise occluder with a red fixation dot (visual angle: 3.5° x 4.7° (h x w), corresponding to 150 x 200 px) processed with a Gaussian filter (*imgaussfilt.m* in MATLAB) was presented centrally against a grey background (Figure 2.2). Trials began with a fixation interval of 2000 ms accompanied by the application of tACS or active control stimulation, followed by a white ellipse stimulus (size: 1.7° x 0.5° visual angle) moving at 5.6°/s from the left periphery towards the occluder, and fading out over 500 ms before disappearing. After a certain time t, the visual stimulus (i.e. white ellipse) reappeared on the right side of the occluder and continued moving for another 500 ms at the same constant velocity as before the occlusion (Figure 2A). In each trial, the reappearance time of the stimulus varied randomly between $\Delta t = \pm 17$ and ± 467 ms (± 2 to ± 60 frames; refresh rate:120 Hz) in steps of 50 ms (3 frames) relative to the objectively correct reappearance time of 1500 ms. Participants were instructed to judge whether the stimulus reappeared *too early* or *too late* via button press with their right hand (BlackBoxToolKit USB Response Pad, Black Box ToolKit Ltd) based on the stimulus' movement before the occluder and the estimated movement behind the occluder. Response mapping of the two buttons was counterbalanced across all participants. The crossmodal experiment mirrored the unimodal setup, substituting the visual reappearance with a tactile stimulus to the left index finger (Figure 2B). The tactile stimulus indicated the time point $t \pm \Delta t$ (as described in the unimodal design) at

which the disappearing visual stimulus would have reappeared on the other side of the occluder. The tactile stimulus was presented using a Braille piezo-stimulator (QuaeroSys, Stuttgart, Germany; 2 × 4 pins, each 1 mm in diameter with a spacing of 2.5 mm) by pushing all eight pins up simultaneously for 200 ms. Participants were instructed to respond as fast and as accurate as possible, once the visual or tactile stimulus reappeared after the occluder. Immediate feedback was not provided, but participants received block-wise performance summaries and could rest between blocks. Each participant took part in two sessions on two days, maintaining consistent timing of the day and response mapping. Each session comprised ten blocks of 60 trials, resulting in a total of 600 trials. Prior to the main experiment, participants carried out a training block of 30 trials to get familiar with the task and stimulus material and received immediate feedback about the correctness of their response. To mask the sound of the Braille stimulator during tactile stimulation and other background noise, participants wore ear plugs for the whole duration of the recording session in both experimental designs. At the end of the second recording day, participants filled out a questionnaire asking for a specific strategy they might have used for the temporal prediction task. We used MATLAB R2016b (MathWorks, Natick, USA; RRID: SCR_001622) and Psychophysics Toolbox (RRID: SCR_002881) (Brainard, 1997) on an MS-Windows 10 operating system for stimulus presentation.

Transcranial alternating current stimulation

Participants attended two stimulation sessions in which two high-definition tACS (HD-tACS) 2x2-montages (Figure 2.3B) were employed at a frequency of 2 Hz and a peak-to-peak current of 2 mA to target the left and right parietal cortex. The electric field $\overrightarrow{E}$ was estimated prior to the experiment by linear superposition of lead fields $\overrightarrow{L}$, weighted by

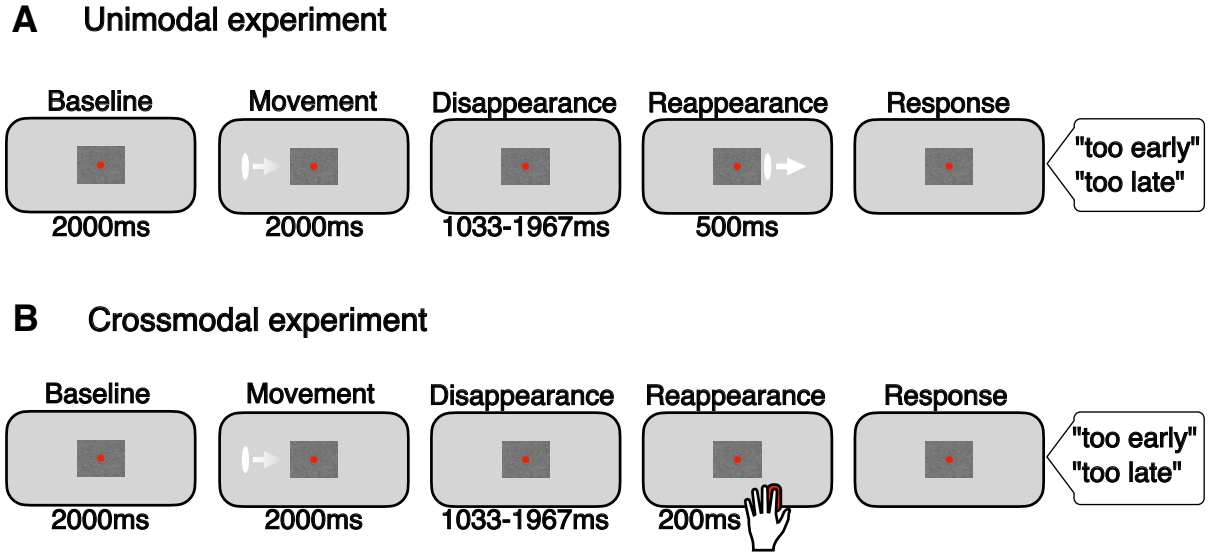

Figure 2.2: Experimental design. (A) Unimodal experiment: In the beginning of each trial, a white ellipse appeared on the screen and moves towards the occluder before disappearing. After 1500 ms ± 17 to ± 467 ms the stimulus reappears. The participants then had to decide whether the stimulus reappeared "too early" or "too late". (B) Crossmodal experiment: Like in the unimodal experiment, the participants saw a white ellipse moving towards the occluder before disappearing behind it. After time intervals of 1500 ms ± 17 to ± 467 ms, the participants received a tactile stimulus, signalling the reappearance. Again, the participant's task was to identify whether the tactile stimulus reappeared "too early" or "too late".

the injected currents α_i at stimulation electrodes $i = \{1,2,3,4\}$:

$$\overrightarrow{E}(\overrightarrow{x}) = \sum_i (\overrightarrow{L_i}\ (\overrightarrow{x})\ \alpha_i)$$

The lead field matrix $\overrightarrow{L}$ was computed by using boundary element three-shell head-models (Nolte and Dassios, 2005). The estimated electrical field intensities were comparable to those shown to effectively modulate neural activity in both non-human primates and humans (Huang et al., 2018; Johnson et al., 2020; Kasten et al., 2019) (Figure 2.3C). Additionally, the tACS montage was slightly modified between the two experiments to account for differences between unimodal and crossmodal stimulation (Daume et al., 2021). Despite this adjustment, the electrical fields remained comparable across both experiments (see supplementary material A, Figure 2.2). The stimulation was administered using 12 mm Ag/AgCl electrodes and neuroConn stimulators (direct current (DC)-Stimulator plus, neuroConn, Illmenau, Germany) with Signa electrolyte gel (Parker Laboratories Inc.) to maintain electrode impedances below 25 $k\Omega$ and ensure uniform electric fields. To minimize transcutaneous effects, EMLA cream (2.5% lidocaine, 2.5% prilocaine) was applied for local anaesthesia one hour prior to the experiment. tACS was delivered intermittently, with 4 s intervals and current ramps of 500 ms at six different phase lags (0°, 60°, 120°, 180°, 240°, 300°) relative to the visual events. A full cycle (360°) of a 2 Hz sine wave lasts 500 ms, making 60° phase differences equivalent to 83.333 ms. The phase lags were manipulated with respect to the disappearance of the visual target (i.e., white ellipse), as the tACS stimulation stopped at specific phases coinciding with the time point of disappearance of the white ellipse. By extension, the phase lags were also aligned with the motion onset, given that visual events consistently spanned 2 s within the 4 s tACS interval. In the unimodal experiment, the active control condition involved delivering short tACS pulses (1 s) at two points: 2 s prior to the appearance of the white ellipse and 1 second before its disappearance. In contrast, the

crossmodal experiment featured a single 1 s ramped tACS applied only at the beginning of the stimulation interval (Figure 2.3A). The rationale for introducing a second ramp in the unimodal control condition was to render the control condition perceptually similar to the tACS condition. In the crossmodal experiment that was designed later, we refrained from presenting the second ramp at the end of the stimulation, as it could induce a phase reset akin to that observed with continuous tACS stimulation. To mitigate this confounding factor, we revised the design of the crossmodal experiment by restricting the ramp to the interval start. Post-session, a questionnaire assessed perceived intensity and temporal evolvement of side effects like skin sensations, fatigue, and phosphene perception (see supplementary material, Figure 2.9 & 2.10). To ensure participants did not use potential rhythmic tactile sensations resulting from tACS for temporal prediction, they completed a tapping test after the second session. Participants were exposed to 4s intervals of tACS, matching the tACS rhythm used in the experiment, and were instructed to tap in rhythm with the stimulation if possible. Afterwards, having been shown the 2 Hz rhythm by the experimenter tapping on a table, they repeated the test. This test aimed to determine whether participants could perceive the stimulation while actively attending to it, ruling out the possibility that positive tACS effects were solely due to transcutaneous/somatosensory effects rather than direct neural effects (Asamoah et al., 2019). Participants, who were able to tap in the presented rhythm, were therefore excluded from further analyses. In the unimodal experiment, 2 out of 29 participants tapped correctly to the 2 Hz rhythm and in the crossmodal experiment, 4 out of 30 participants did. Notably, detailed instructions about the 2 Hz rhythm did not improve participantsábility to tap in sync.

Statistical analysis of behavioural data in relation to the tACS phase

Behavioural effects of tACS were evaluated by calculating accuracy values and signal detection measures, such as sensitivity *d'* and criterion *c*, for the six different phase bins. In signal detection theory (SDT) (Green and Swets, 1966), sensitivity *d'* measures

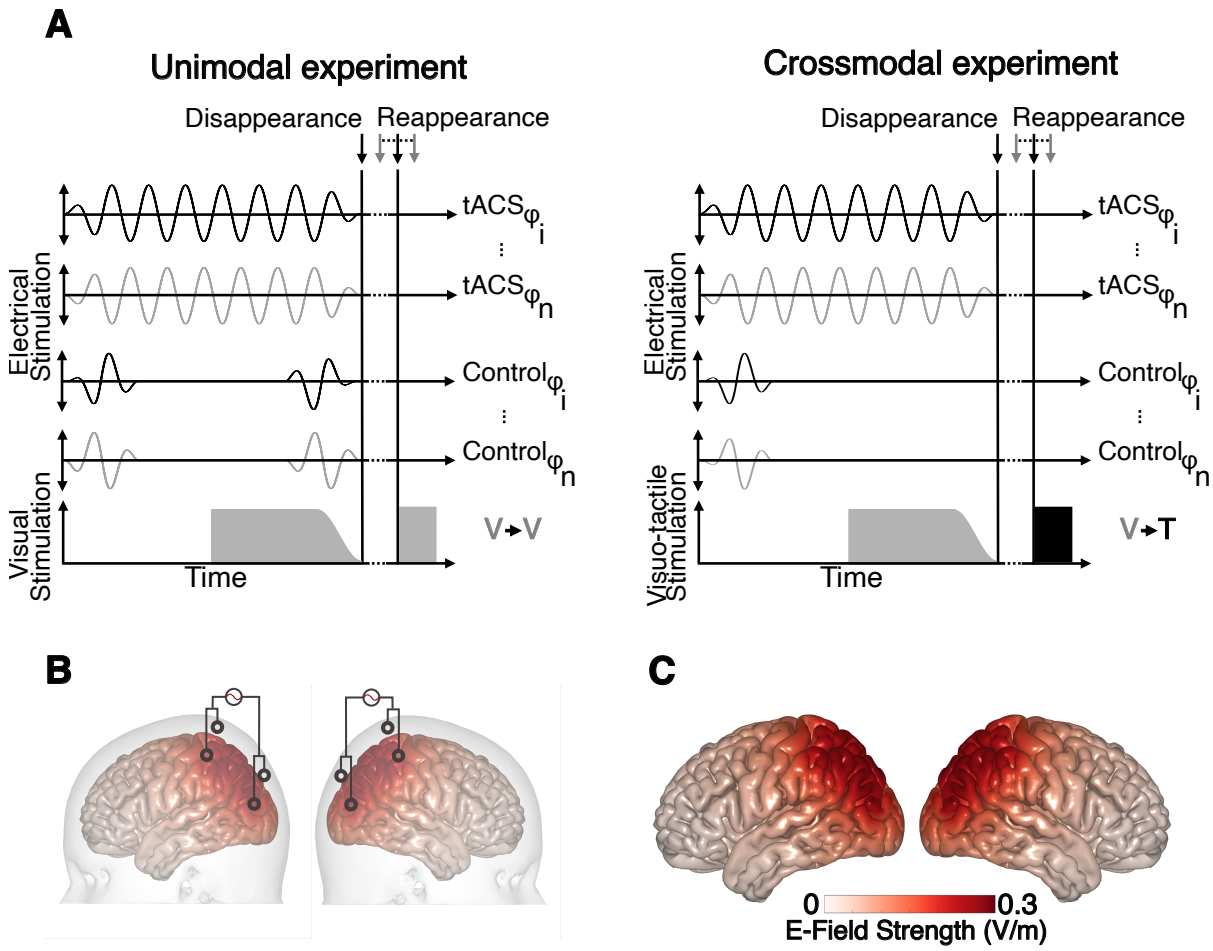

Figure 2.3: Experimental design and electrical field simulation. (A) tACS was applied at 2 Hz in a verum condition and an active control condition. In the verum condition, tACS was applied to the scalp intermittently for 4 s at six different phase lags (0°, 60°, 120°, 180°, 240°, 300°) relative to the visual stimulation. The active control condition of the unimodal experiment consisted of short ramps of tACS (1 s) in the beginning and in the end of the stimulation interval. In the crossmodal experiment, one second of ramped tACS was applied only in the beginning of the stimulation interval. The figure further depicts the amplitude of the sensory stimulation, i.e. the luminance of the white ellipse and the strength of the tactile stimulation. In each trial of both experiments, a white ellipse appeared on the screen two seconds after tACS onset. The white ellipse was moving towards an occluder, decreasing its luminance 500 ms before disappearing behind an occluder for various time intervals. The reappearing stimulus was either a visual or a tactile stimulus for the unimodal and crossmodal experiment, respectively (see Figure 1). (B) In-phase high-definition tACS montage targeting the left and right parietal cortices. (C) Simulated electrical field generated by the 2x2-montage with a peak-to-peak current of 2mA.

the ability to distinguish between signal and noise, calculated as the difference between z-transformed hit rates (HR) and false alarm rates (FAR):

$$d' = z(HR) - z(FAR)$$

Higher d' indicates better discrimination. Criterion c reflects response bias,

$$c = -\frac{1}{2}(z(HR) + z(FAR))$$

with $c = 0$ indicating no bias, $c > 0$ a conservative bias (bias towards responding *too late*), and $c < 0$ a liberal bias (bias towards responding *too early*). c is derived from the decision threshold relative to the point where signal and noise distributions intersect. Both measures assume equal variance in signal and noise responses. Sensitivity indices and response bias were normalised prior to statistical testing by subtracting the mean across the six phase bins. The tACS-phase-specific performance modulation was quantified using three measures. Firstly, the Kullback-Leibler divergence (D_{KL}) was calculated, which quantifies the deviation of the observed distribution (P) from a uniform distribution (Q) defined as

$$D_{KL}(P, Q) = \sum_{i=1}^{N} P(i)\ log\left[\frac{P(i)}{Q(i)}\right]$$

where N is the number of phase bins (Tort et al., 2010). D_{KL} values can range from 0 (indicating a strictly uniform distribution) to 1 (indicating a nonuniform distribution). Therefore, as the distance between P and Q increases, the D_{KL} value also increases. The input to this function were the accuracy values normalised by the sum of the performance values across all six phase lags. Additionally, it was examined whether the performance modulation induced by tACS over phase conditions follows a cyclic pattern, as expected due to the sinusoidal nature of tACS. A one-cycle sine function was fit to the normalised

sensitivity *d'* values of each participant using a nonlinear least-squares algorithm,

$$y_i \sim A sin\left(2\pi\varphi f_m x + \Phi_i\right) + b$$

where y_i is the observed performance. A, Φ_i, and b represent the amplitude, the phase lag of the sine fit, and the intercept, respectively. For each participant, the best sine fit function

$g_i(x) = A sin\left(2\pi f_m x + \Phi_i\right) + b$ was obtained for each condition (tACS and active control) separately by applying the nonlinear least-squares algorithm, allowing amplitude, phase lag and intercept to vary (three degrees of freedom). From this fit, the amplitude value was extracted. The goodness of fit (R^2) of the resulting best fitting function was calculated for each participant. Lastly, we applied a parametric alignment-based statistical approach (Riecke et al., 2018; Zoefel et al., 2019), aligning the phase bin with the highest normalised sensitivity index *d'* to the central bin, with the remaining bins phase-wrapped. To evaluate the contrast, we subtracted the response of the adjacent bins opposite of the central bin (ADJ) from the average response of the two bins adjacent to the central bin (MAX). This analysis was used to examine the overall effect of tACS on temporal prediction both within and between conditions. Additionally, we computed the same analysis on criterion *c* to investigate the modulation of participants' response bias. Therefore, while D_{KL} provides a general measure of temporal prediction performance modulation, the sine fit, and parametric alignment-based methods allow an assessment of systematic modulation patterns that depend on the tACS phase. Statistical significance of D_{KL}, sine fit amplitude, and MAX-ADJ value differences within conditions and between the verum and active control condition were examined. Effect sizes for one-sample and paired samples t-tests were calculated using Cohenś d and Cohen's d_z, respectively. Since traditional paired-samples t-tests are not sufficient to interpret null results, we used Bayesian hypothesis testing (de Graaf & Sack, 2018; Kass & Raftery,

1995). This approach incorporates prior beliefs and the observed data to assess the evidence for or against the null hypothesis. This analysis produces a single value known as the Bayes Factor (BF_{10}/BF_{01}). In essence, it determines which hypothesis aligns better with the data and to what degree, indicating which hypothesis provides a more accurate prediction of the observed data. For this analysis the MATLAB package Bayes Factor was used (Krekelberg, 2022).

2.3.3. Modelling temporal predictions

Oscillator ensemble model

To deepen understanding of neuronal mechanisms for temporal predictions, we developed a computational model inspired by previous lab work (Maye et al., 2019) but with a new mathematical approach focusing on temporal dynamics. The model uses Hopf oscillators, modified by Hebbian learning for frequency tuning (Righetti et al., 2006), to adapt to periodic inputs.

The Hopf oscillator is composed of an excitatory element x and an inhibitory element y:

$$\dot{x} = \left(\mu - r^2\right)\ x - \omega y + \varepsilon F \dot{y} = \left(\mu - r^2\right)\ y + \omega x,$$

where $r^2 = x^2 + y^2$, ω is the intrinsic oscillation frequency, and μ defines the radius of the limit cycle, i.e., the oscillator's amplitude. The parameter ε controls how strongly an external input F affects the intrinsic dynamics of the oscillator. This oscillator can adjust its frequency to a periodic input signal by means of the following learning rule (Righetti et al., 2006):

$$\dot{\omega} = -\varepsilon\ F\ \frac{y}{\sqrt{r}}$$

An ensemble of these adaptive-frequency oscillators (N=100) with random initial conditions learns to decompose a periodic input signal into its various components. Here, a collective behaviour was expected in which oscillators tune to one of the input compo-

nents if the frequencies are close but continue their intrinsic dynamics if they are not. The model can be linked to neurophysiological processes by considering x and y as a description of the various excitatory-inhibitory circuits that have been found in the visual cortex (Adini et al., 1997; Donner and Siegel, 2011; Xu et al., 2016). The input $F = \sin \omega_{sens}$ conceives a motion-induced oscillation that has been described in visual cortices of cats (Gray and Viana Di Prisco, 1997) and humans (Orekhova et al., 2015).

Modelling tACS

Our model assumes that tACS might modulate the coupling strength of the sensory input to the excitatory-inhibitory circuits. Formally this modulation can be modelled by a sinusoidal tACS signal and an additional coupling parameter κ which can be used to control the modulation depth:

$$\dot{x} = \left(- r^2 \right) \; x - \omega y + (\varepsilon + \kappa \sin \omega_{tACS}) F$$

The parameters were set as follows: $= 1$, $\varepsilon = 0.1$, $\kappa = 0.1$, $\omega_{tACS} = 0.2\pi$, and $\omega_{sens} = 4\pi$. The initial conditions were randomized in the intervals $x, y \in [-1, 1]$ and $\omega \epsilon [2\pi, \; 6\pi]$. The equations were numerically solved by a 4^{th} order Runge-Kutta method in the interval $t \in [0, 100]$ with $dt = 0.01$ as the temporal resolution. The input F was switched off for 2 s at the end of the stimulation period to reflect the occlusion of the stimulus during the prediction period. Over time, oscillators adjust their frequencies to match sensory inputs. Research indicates stronger ITPC during the time window of occlusion (Daume et al., 2021). In line with the idea that oscillatory phase encodes the time point of reappearance through alignment of high excitability phases to the predicted onset of reappearance, this phase consistency should persist at object reappearance. To test this hypothesis, the model sampled phase distributions at the stimulus' reappearance through multiple trials with randomised initial conditions during a training phase of the model. The average of

the phases φ_n across the oscillator ensemble was considered as the ensemble's phase Φ:

$$\Phi = arg\left(\sum_{n=1}^{N} e^{i\varphi_n}\right)$$

This distribution corresponds to subjectively correct reappearance of the stimulus. In the test phase, ensemble phases tied to the time windows corresponding to earlier or late reappearances were sampled. These phases were then compared against the learned phase distribution for right-on-time reappearances. If most phases exceeded the test phase, the model indicated that the stimulus reappeared *too late* and vice versa.

2.4. Results

2.4.1. Phase-specific modulation of unimodal temporal prediction

Averaged across phase lags, participants executed the temporal prediction task better than chance, but below ceiling $\overline{X}_{tACS} = 70.81\%$, $SEM_{tACS} = 1.34\%$; $\overline{X}_{Control} = 69.24\%$, $SEM_{Control} = 1.46\%$; $t(26) = 1.89$, $p = .070$, $d = 0.363$ $\overline{X}_{tACS} = 70.81\%$, $SEM_{tACS} = 1.34\%$; $\overline{X}_{Control} = 69.24\%$, $SEM_{Control} = 1.46\%$; $t(26) = 1.89$, $p = .070$, $d = 0.363$). Furthermore, participants showed high sensitivity ($\overline{d'}_{tACS} = 2.038$, $SEM_{tACS} = 0.252$; $\overline{d'}_{Control} = 1.651$, $SEM_{Control} = 0.207$) and a low bias ($\overline{c}_{tACS} = 0.031$, $SEM_{tACS} = 0.025$; $\overline{c}_{Control} = 0.044$, $SEM_{Control} = 0.022$) in both conditions. Importantly, mean sensitivity d' was significantly increased under tACS versus active control ($t(26) = 3.29$, $p = .003$, $d_z = 0.63$). Furthermore, sensitivity d' was significantly increased in the unimodal experiment, compared to the crossmodal experiment ($t(51) = 2.56$, $p = .007$, $d = 0.70$). To assess the phasic modulation of temporal prediction performance by tACS, we quantified the behavioural modulation strength by three measures (D_{KL}, One Cycle Sine Fit, and MAX-ADJ). The D_{KL} measure shows that the behavioural performance across phase lags is nonuniformly distributed. The strength of this modulation was significantly greater during tACS compared to the ac-

tive control condition ($t(26) = 2.829,\ p = .008,\ d_z = 0.54$) (Figure 2.4A). To check whether behavioural performance systematically fluctuated around the mean along the 2 Hz tACS phase, we fitted sinusoidal waves to the behavioural performance across tACS phase lags relative to the offset of the visual events. Figure 5A shows the behavioural data of all 27 participants for both, verum and active control tACS. Comparing the amplitude values obtained from the most suitable sinusoidal curve for both conditions revealed a significantly higher modulation strength of discrimination sensitivity in the tACS condition compared to the active control condition (one-sided paired-samples t-test: ($t(26) = 2.127,\ p = .021,\ d_z = 0.41$) (Figure 2.4B). No significant difference of tACS-modulation of response bias was evident in the data ($t(26) = 0.19,\ p = .425,\ d_z = 0.036$). Although the observed relation between tACS phase and behavioural performance was robust, there was significant variability in the optimal phase among participants. Thus, different participants reached their peak behavioural performance at different tACS phase lags. In fact, when considering the entire sample (N=27), there was no evidence of a distinct concentration of behavioural entrainment at a specific phase (Rayleigh test for nonuniform distribution: $z_{tACS} = 1.04$, $p_{tACS} = 0.36$; $z_{Control} = 0.44$, $p_{Control} = 0.65$, see Figure 2.5B). Considering this, tACS phase-dependent modulation of temporal prediction was quantified by a parametric alignment-based method ($MAX - ADJ$). Temporal prediction modulation by tACS could be distinguished from zero within condition $tACS$: $t(26) = 2.011,\ p = .031,\ d = 0.13$; $Control : t(26) = -0.944,\ p = .822,\ d = -0.09$ as well as between conditions $t(26) = 2.017,\ p = .027,\ d_z = 0.39$ (Figure 2.4B). Importantly, we observed a phase-specific modulation of sensitivity $d´$ but not the response bias criterion c $tACS :\ t(26) = -2.028,\ p = .893,\ d = -0.65$; $Control : t(26) = -1.285,\ p = .736,\ d = -0.41; t(26) = -0.70, p = .0757, d_z = -0.14$. To investigate whether phasic modulation is mediated by differences in mean performance between conditions, we computed the correlation between the differences in accuracy/sensitivity d' values and the differences in the three modulation measures across active control and tACS conditions

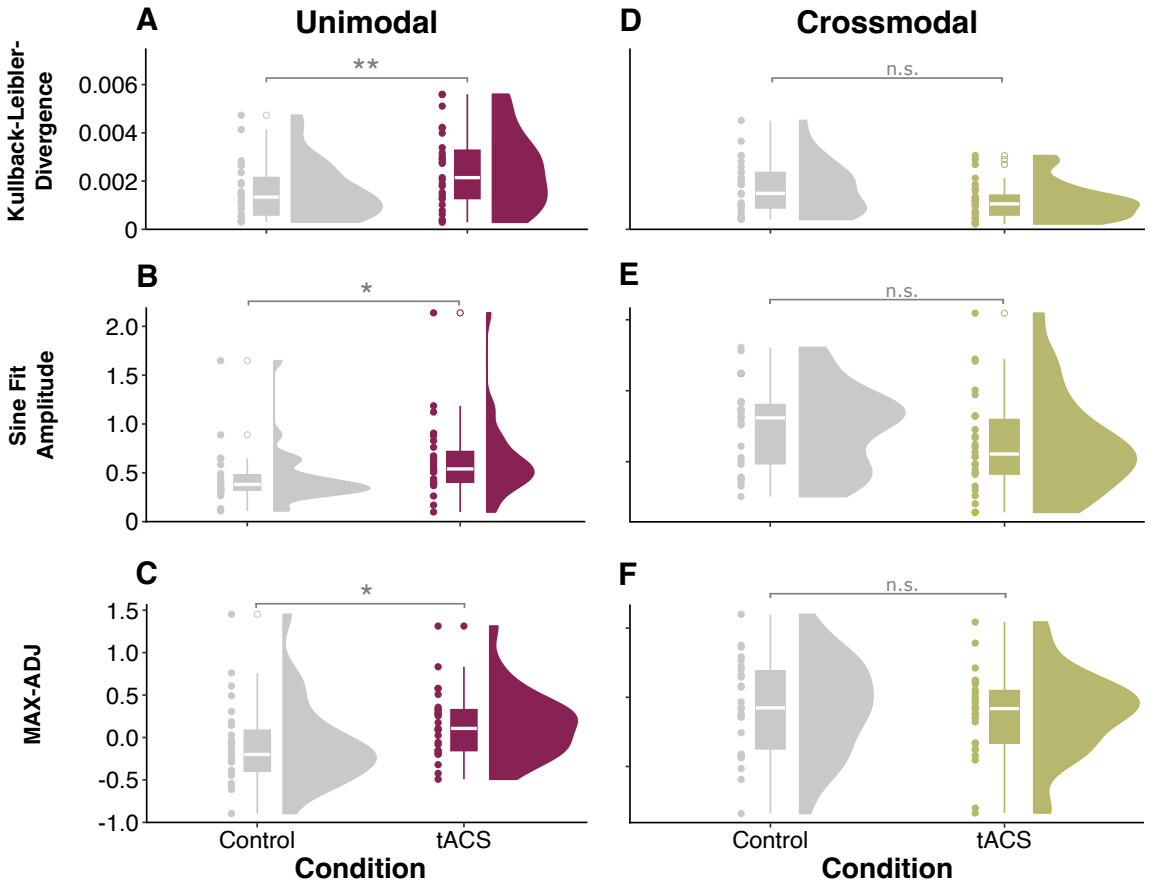

Figure 2.4: Temporal prediction performance modulation quantified via two modulation measures. (A, B, C) Significantly increased Kullback-Leibler divergence (D_{KL}, sine fit amplitudes, and MAX-ADJ values under tACS relative to active control condition in the unimodal experiment. (D, E, F) No significant difference in D_{KL} values, sine fit amplitudes, and MAX-ADJ values under tACS compared to the active control condition in the crossmodal experiment. Asterisks mark the uncorrected p-value of dependent samples t-tests; *p $<$ .05, **p$<$.01; n.s., non-significant.

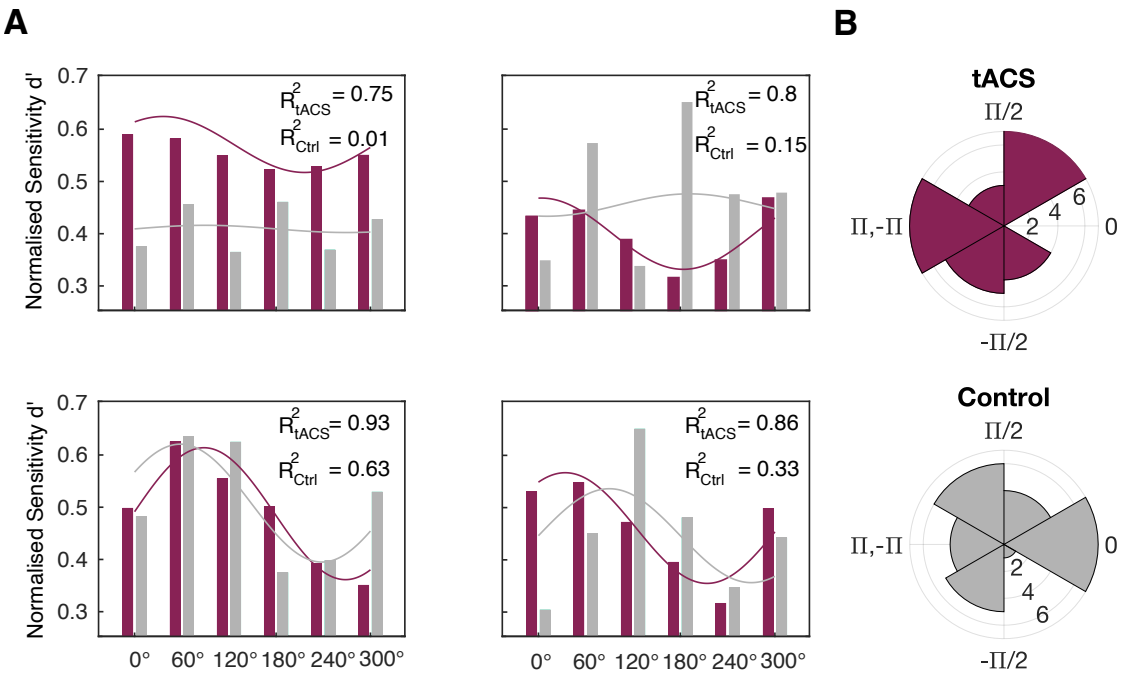

Figure 2.5: (A) Sine fits of 4 exemplary subjects for unimodal temporal prediction experiment showing the normalised discrimination sensitivity values for the six phase-lags (grey: Control, red: tACS) and (B) the distribution of the individual optimal phase lags of tACS and control condition in the unimodal experiment.

(D_{KL} : $r = 0.29$, $p = 0.133$; $Sine\ Fit$: $r = 0.26, p = 0.194$; $MAX - ADJ$: $r = 0.15, p = 0.46$). The non-significant correlations suggest that the phasic modulation is not merely driven by the mean differences in sensitivity d' between conditions.

Together, we observed a significant impact of tACS phase on temporal prediction performance in the unimodal temporal prediction task. These results suggest a substantial influence of neural low-frequency oscillatory phase on unimodal temporal prediction.

2.4.2. tACS does not phase-specifically modulate crossmodal temporal prediction

For the crossmodal temporal prediction paradigm, we could not find a similar relationship between the tACS and visuo-tactile stimulation. Participants showed no significant behavioural difference of sensitivity ($\overline{d'}_{tACS} = 1.229$, $SEM_{tACS} = 0.162$; $\overline{d'}_{Control} =$

1.307, $SEM_{Control} = 0.148$; $t(25) = -0.402$, $p = 0.69$, $d_z = 0.08$), response bias ($\overline{c}_{tACS} = 0.029$, $SEM_{tACS} = 0.023$; $\overline{c}_{Control} = 0.013$, $SEM_{Control} = 0.026$; $t(25) = 0.524$, $p = 0.605$, $d_z = 0.103$) or accuracy ($\overline{X}_{tACS} = 67,28\%$, $SEM_{tACS} = 1.66\%$; $\overline{X}_{Control} = 66.88\%$, $SEM_{Control} = 1.65\%; t(25) = 0.65$, $p = .74$, $d = 0.062$) between conditions. When statistically testing for differences between the two tACS conditions, we could neither find a significant difference in the analysis of general phasic modulation ($D_{KL}: t(25) = -0.807$, $p = .427$, $d_z = -0.149$), nor could we find a significant effect in the analysis of sinusoidal modulation of discrimination sensitivity ($t(25) = -1.342$, $p = .191$, $d_z = -0.26$) (Figure 2.4D,E) or response bias ($t(25) = 0.47$, $p = .642$, $d_z = 0.09$). Furthermore, the parametric alignment-based method revealed no phase-specific effect for sensitivity d' within $tACS: t(25) = -2.005$, $p = .97$, $d = -0.68$; $Control: t(25) = -1.033$, $p = .84$, $d = -0.39$ or between conditions $t(25) = 0.47$, $p = .642$, $d_z = 0.09$ (Figure 2.4F). Similarly, no effect was found for response bias within $tACS: t(25) = 0.532$, $p = .297$, $d = 0.171$; $Control: t(25) = -1.016$, $p = .84$, $d = -0.407$ and between conditions $t(25) = -1.08$, $p = .85$, $d_z = -0.212$. To assess the evidence for the null hypothesis and, therefore, allowing an interpretation of the null results, the Bayes Factor was calculated ($D_{KL}: BF_{01}(25) = 3.76; MAX-ADJ: BF_{01}(25) = 4.05$). This value indicates that the current data is 3.76 times more likely to be observed if the null hypothesis was true (i.e., no phasic modulation through tACS compared to the active control condition), than if the alternative hypothesis is true. According to recommended guidelines, this provides "moderate" evidence in support of the null hypothesis (BF>3, but <10). Furthermore, in the analysis of sinusoidal modulation of temporal prediction performance ($Sine\ Fit: BF_{01}(25) = 2.16$), the Bayes Factor can be descriptively interpreted as providing merely anecdotal evidence for the null hypothesis to be true (BF<3).

2.4.3. tACS-entrainment in the computational model

Under the influence of the motion-induced oscillatory input to the model, the initially random phase distribution of the ensemble developed towards a predominant phase of approximately π at the time point of the actual reappearance of the moving object (Figure 2.6A, top). This shift towards a predominant phase corresponds to the subject-specific optimal phase in the behavioral data of our experiment. In addition, oscillators with initial frequencies close to the input frequency also adjusted their frequencies to the input (Figure 2.6A, bottom). The parameter ε was adjusted to match the overall accuracy of the model's temporal prediction accuracy approximately to the results from the behavioral study. The simulation of different tACS phase offsets relative to the motion-induced input resulted in the same characteristic sinusoidal modulation of temporal prediction accuracies like in the participants (Figure 2.6B).

2.5. DISCUSSION

The present studies aimed to investigate the causal role of oscillatory phase in temporal prediction. We employed an intermittent electrical stimulation design in which we systematically combined rhythmic electrical with continuous visual or visuo-tactile stimulation. We hypothesized that applying tACS at six different phase lags relative to the disappearance of a continuously moving visual stimulus would result in a phase-dependent modulation of temporal prediction performance of the visual stimulus' reappearance. Our results confirm that unimodal visual temporal prediction performance was modulated in a tACS phase-dependent manner, leading to both enhancement and deterioration of performance. Importantly, our results implicate that tACS phase-specifically influences the ability to distinguish timing differences rather than introducing a response bias in a unimodal context. Under the assumption that neural oscillations were entrained by tACS, our data suggests a functional role of parietal low-frequency neural oscillations for temporal prediction. The computational model showcases that neural oscillations influ-

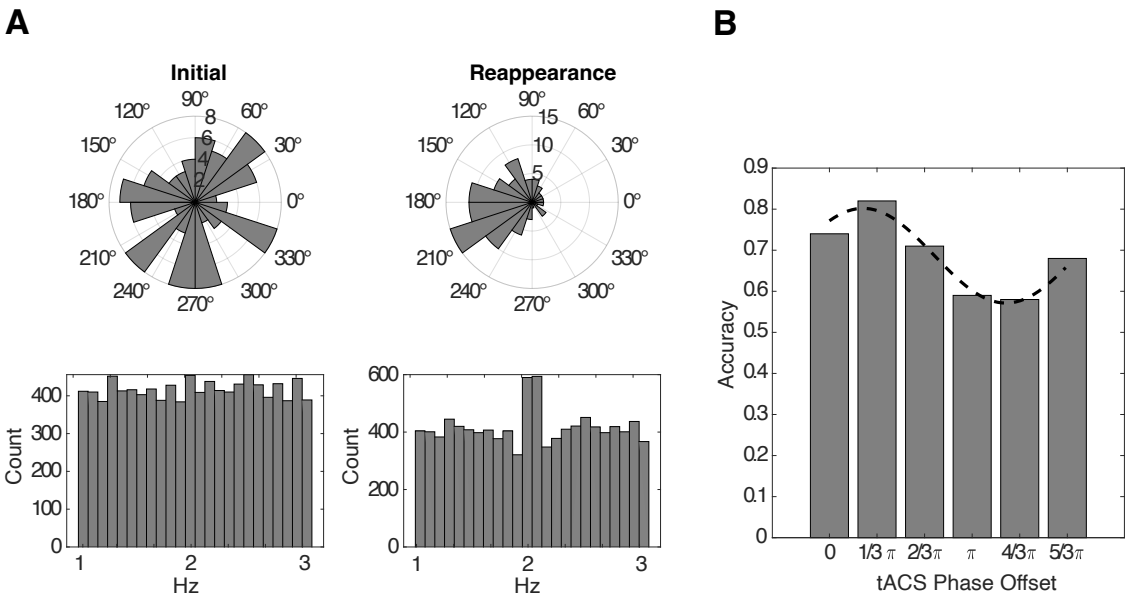

Figure 2.6: (A) Shows exemplary model data without tACS input. Histograms of phases (top) and distribution of intrinsic oscillation frequencies ω (bottom) of the ensemble oscillators at t=0 (left) and at the reappearance (right) of the moving object. Data are from 100 repetitions of an ensemble of 100 oscillators. (B) Exemplary temporal prediction accuracy of the model for different tACS phase offsets. The dashed line shows a fitted sine wave.

enced by visual motion causes the initially random phase distribution to converge toward a predominant phase, thereby essentially increasing ITPC. Additionally, incorporating phase-specific tACS parameters into the model allowed us to show that motion-induced neural oscillations, in relation to the tACS phase, either preserves or disrupts the phase alignment induced by tACS and thereby effectively enhances or deteriorates the temporal prediction accuracy of the model. Our model suggests a stronger coupling between the sensory input and the oscillator dynamics as a potential entrainment mechanism.

Implications for understanding the neural mechanisms of temporal prediction

tACS offers a distinctive approach to explore and confirm hypotheses on targeted brain regions, frequency bands and oscillatory phase. Although the sources of oscillatory activity may vary by temporal prediction task, the parietal cortex has been implicated in regulating temporal prediction across various tasks (Adini et al., 1997; Bueti et al., 2010; Bueti and Walsh, 2009; Cotti et al., 2011; Daume et al., 2021; Davranche et al., 2011; Gontier et al., 2013; Lewis and Miall, 2006; Mioni et al., 2020; Rao et al., 2001). Hence, the parietal cortex has been a popular target for non-invasive brain stimulation when investigating temporal processing (Alexander et al., 2005; Javadi et al., 2014; Mioni et al., 2020; Rao et al., 2001). In Alexander et al. (2005), the application of low frequency (1 Hz) repetitive transcranial magnetic stimulation (rTMS) to the parietal cortex led to a deterioration of performance in a temporal judgement task. Studies have revealed a hemispheric lateralisation for temporal versus spatial orienting in left and right parietal cortices, respectively (Coull and Nobre, 1998). Consistent with these findings, Javadi et al. (2014) observed that left cathodal transcranial direct current stimulation (tDCS) of the parietal cortex improved performance in duration judgment, aligning with findings by Rao et al. (2001) that the parietal cortex is crucial for encoding or maintaining temporal intervals. Here, we were able to demonstrate the significance of parietal low-frequency oscillatory phase for visual temporal prediction. Previous research has highlighted the significance

of neural oscillations in the delta range (0.5-3 Hz) for temporal prediction (Arnal and Giraud, 2012; Ng et al., 2013). Entrainment through alignment of low-frequency delta oscillations with external cues is acknowledged as an important and flexible mechanism for improving sensory processing (Besle et al., 2011; Cravo et al., 2013; Lakatos et al., 2008, 2009). Moreover, it has been suggested that the functional role of low-frequency delta oscillations in human anticipatory mechanisms involves the modulation of synchronized rhythmic fluctuations in the excitability of neuronal populations. When additional top-down resources are employed, this synchronisation through phase reset is enhanced (Herbst et al., 2022; Stefanics et al., 2010). The phase of low-frequency delta oscillations has further been linked to accuracy in temporal judgment tasks (Arnal et al., 2015) and to precise behavioural adjustments made subsequent to temporal errors (Barne et al., 2017). Here, we extend the findings of Daume et al. (2021) by causally inferring with tACS that the phase of aligned low frequency delta oscillations to the external stimulus encodes the onset of upcoming information through alignment of high-excitability phases of the oscillation with the time window of expected reappearance. This alignment allows optimal sampling of incoming information, considering top-down expectations regarding the occurrence and timing of stimuli (Oever et al., 2015). Notably, the temporal structure (i.e., the velocity of the moving stimulus and the time window of disappearance) in our experiments has been restricted to the delta frequency range. This aligns with the frequency range of endogenous brain oscillations expected to be functionally relevant for temporal prediction (Lakatos et al., 2008). It remains to be explored whether the observed sinusoidal modulations of behavioural performance in the unimodal task can occur outside of this frequency range. This could be investigated with different velocities of the fading visual stimulus and different temporal scales of the disappearance window to gain a comprehensive understanding of how oscillatory frequency and phase influences temporal prediction. Temporal prediction is not solely reliant on delta phase but involves the interplay of other frequency bands, such as the beta band (Daume et al., 2021; de Lange et al.,

2013; Fujioka et al., 2012; Gulberti et al., 2015). Delta oscillations are thought to provide a framework for aligning neural excitability with anticipated sensory events, while beta oscillations refine these predictions and modulate responses to expected stimuli. This interaction facilitates synchronization with external rhythms, enhancing perceptual and motor accuracy in tasks like speech parsing and rhythmic activities (Arnal et al., 2015). Delta phase appears to influence beta bursts, aligning neural excitability with expected events to ensure precise timing in auditory attention tasks (Morillon and Baillet, 2017). Overall, delta-beta coupling across sensory and motor systems reflects the coordination between low-frequency temporal expectations and high-frequency attentional modulation. Specifically, the functional roles of delta phase have been linked to oscillatory temporal expectations, beta power to temporal attention (Chang et al., 2018). Each participant reached their peak performance at different phase lags, suggesting individual differences in the effects of tACS. The heterogeneity could be attributed to varying levels of neuronal entrainment to the 2 Hz tACS rhythm due to interindividual differences in intrinsic delta rhythms as well as to variability in anatomical connectivity and cortical morphology, leading to different neural phase lags (Bauer et al., 2018; Besle et al., 2011; Henry and Obleser, 2012; Kösem et al., 2014). Furthermore, the variable effects of tACS may be due to different field orientation and variability in electrical current intensity concerning the target area. A prospective approach could involve not only considering individual stimulation location but also optimising individual current intensities to optimise tACS efficacy (Radecke et al., 2020). Finally, the application of tACS at a fixed frequency suggests that entrainment effects might be comparatively weaker and tailoring the stimulation to the individual frequency may enhance tACS effects (Lorenz et al., 2019).

Comparison of unimodal visual and crossmodal visuo-tactile temporal prediction

The crossmodal experiment revealed no significant impact of tACS on temporal prediction. Our Bayesian analysis provided weak to moderate support for this null effect, suggesting that our non-significant findings, in fact, might be merely coincidental (Ronconi et al., 2022). Crossmodal sensory integration for shaping temporal predictions may have increased task difficulty, resulting in a greater variability in performance and thereby potentially diminishing small tACS effects, as indicated by significantly higher sensitivity indices d' in the unimodal experiment. It was shown that assessing the duration of empty time intervals between different sensory modalities is harder than within the same modality, leading to decreased performance. This diminished performance was attributed to a suggested attentional bias induced by the cognitive load and the requirement to switch between modalities (Gontier et al., 2013). Moreover, the electrical field of the tACS montage, although slightly adjusted, did not differ significantly between the crossmodal and unimodal experiment. However, the crossmodal experiment is likely to involve at least partially different cortical areas and, thus, more specific optimization might be required to achieve phase-specific effects in the crossmodal experiment. For example, in addition to the parietal cortex, frontal cortices have been shown to play a functional role in managing fixed versus evolving temporal probabilities, emphasizing the dynamic contributions of frontal areas in updating predictions (Coull et al., 2016). Another study supports the notion that crossmodal temporal prediction engages a distributed network with bilateral fronto-parietal activation (Binder, 2015). Furthermore, crossmodal temporal prediction might also involve frequency bands beyond the scope of our study. Several studies noted that building temporal predictions of upcoming events can be attributed to alpha-band desynchronisation and/or beta-band modulation (Arnal and Giraud, 2012; Daume et al., 2021; van Ede et al., 2011). Desynchronisation of the respective frequency-band activity in these studies was suggested to serve as an active inhibitory mechanism that gates sensory information processing as a function of cognitive relevance. Furthermore, crossmodal integration, particularly in the context of temporal prediction of moving visual

objects, has been shown to depend on theta oscillations (Ronconi et al., 2023). This shows that the task demands, and multisensory integration scenarios might determine the involvement of certain frequency bands. Therefore, the current study design cannot discern whether the noted disparities between the results of the unimodal and crossmodal experiment originate from variations in how oscillatory activity affects temporal prediction across different sensory modalities or are a result of discrepancies inherent in the two experimental designs. Future research on crossmodal entrainments may shed light on the underlying mechanisms by incorporating both unimodal and crossmodal temporal prediction tasks within a single study and by recording neurophysiological data to address the issue of neural efficacy (de Graaf and Sack, 2018).

2.6. CONCLUSION

In the present experiments, we used tACS over bilateral parietal cortex to examine the causal relevance of delta oscillations for temporal prediction. In the unimodal task, we found a significant behavioural modulation of prediction accuracy in line with a phasic modulation of prediction-related neural activity. These behavioural results were replicated in a computational model which suggests that phase alignment sinusoidally fluctuates under the influence of phase-specific tACS. Accordingly, predictions about relevant future events can be implemented by phase adjustments to enhance sensory processing at the predicted time, leading to effective 'gating' of sensory inputs. The notion of a simple, generic mechanism of parietal delta phase for temporal prediction is challenged by our results from the crossmodal study in which phasic behavioural modulation by tACS was absent. We propose that future experiments should address this disparity in findings by exploring possible effects of task difficulty and oscillatory frequency on temporal prediction.

CRediT authorship contribution statement

Rebecca Burke: Conceptualisation, Methodology, Investigation, Software, Formal analysis, Validation, Visualisation, Data curation, Writing - original draft, Writing - review & editing. **Alexander Maÿe:** Methodology – Computational Modelling, Writing – review & editing. **Jonas Misselhorn:** Conceptualisation, Methodology, Writing - review & editing. **Marina Fiene:** Conceptualisation, Methodology, Writing - review & editing. **Felix J. Engelhardt:** Conceptualisation, Investigation, Writing – review & editing. **Till R. Schneider:** Conceptualisation, Methodology, Writing - review & editing, Supervision. **Andreas K. Engel:** Conceptualisation, Methodology, Writing - review & editing, Funding acquisition, Project administration, Supervision.

Declaration of competing interest

The authors declare that they have no known competing financial interests or personal relationships that could have appeared to influence the work reported in this paper.

Acknowledgements

This work was supported by grants from the Deutsche Forschungsgemeinschaft (SFB TRR 169/B1/B4 awarded to A.K.E.) and from the European Union (project cICMs, ERC-2022-AdG-101097402 awarded to A.K.E.). We thank Karin Reimann for assistance in data recording, and Marleen J. Schoenfeld and Peng Wang for helpful discussions on the data. Views and opinions expressed in this paper are those of the authors only and do not necessarily reflect those of the European Union or the European Research Council. Neither the European Union nor the granting authority can be held responsible for them.

A

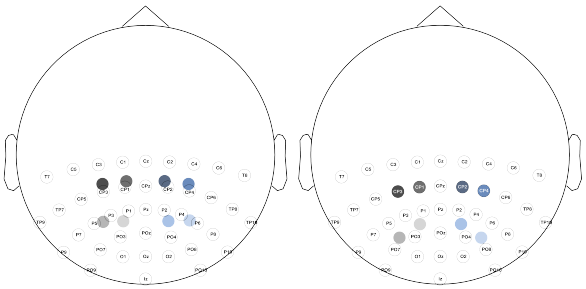

B

Electrode	unimodal			crossmodal		
	X	Y	Z	X	Y	Z
E1	-6.685	-4.350	6.650	-6.356	-4.701	6.562
E2	-3.400	-4.500	9.350	-3.551	-4.729	9.132
E3	-5.850	-8.900	2.800	-5.287	-9.156	2.278
E4	-3.450	-9.900	4.650	-2.977	-9.394	4.791
E5	3.400	-4.500	9.400	3.838	-4.707	9.070
E6	6.685	-4.350	6.650	6.661	-4.664	6.558
E7	3.550	-9.875	4.650	3.089	-9.386	4.786
E8	6.100	-8.700	2.800	5.345	-9.146	2.241

Supplementary Figure 2.7.1. Stimulation electrode montages of unimodal and crossmodal experiments. (A, left) In the unimodal experiment, stimulation electrodes (depicted as grey and blue circles) were arranged using a 64-channel equidistant layout, with additional electrodes placed equidistantly between existing ones. The electrode montage is presented here in relation to the 10-10 system. (A, right) Stimulation electrode arrangement for the crossmodal experiment referenced to the standard 10-10 system. (B) MNI coordinates of stimulation electrodes for the unimodal and crossmodal experiment. E1-E4 correspond to the left hemisphere and E5-E8 correspond to the right hemisphere.

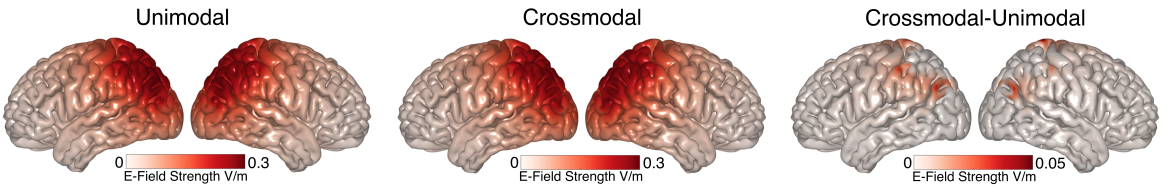

Supplementary Figure 2.7.2. Electrical field simulations of unimodal and crossmodal experiment as well as their difference. The electrical field was generated by two in-phase 2x2-montages with a peak-to-peak current of 2mA. Note the difference in the scales of the e-field strengths of 0.3V/m for the uni- and crossmodal experiments and 0.05V/m for their condition difference.

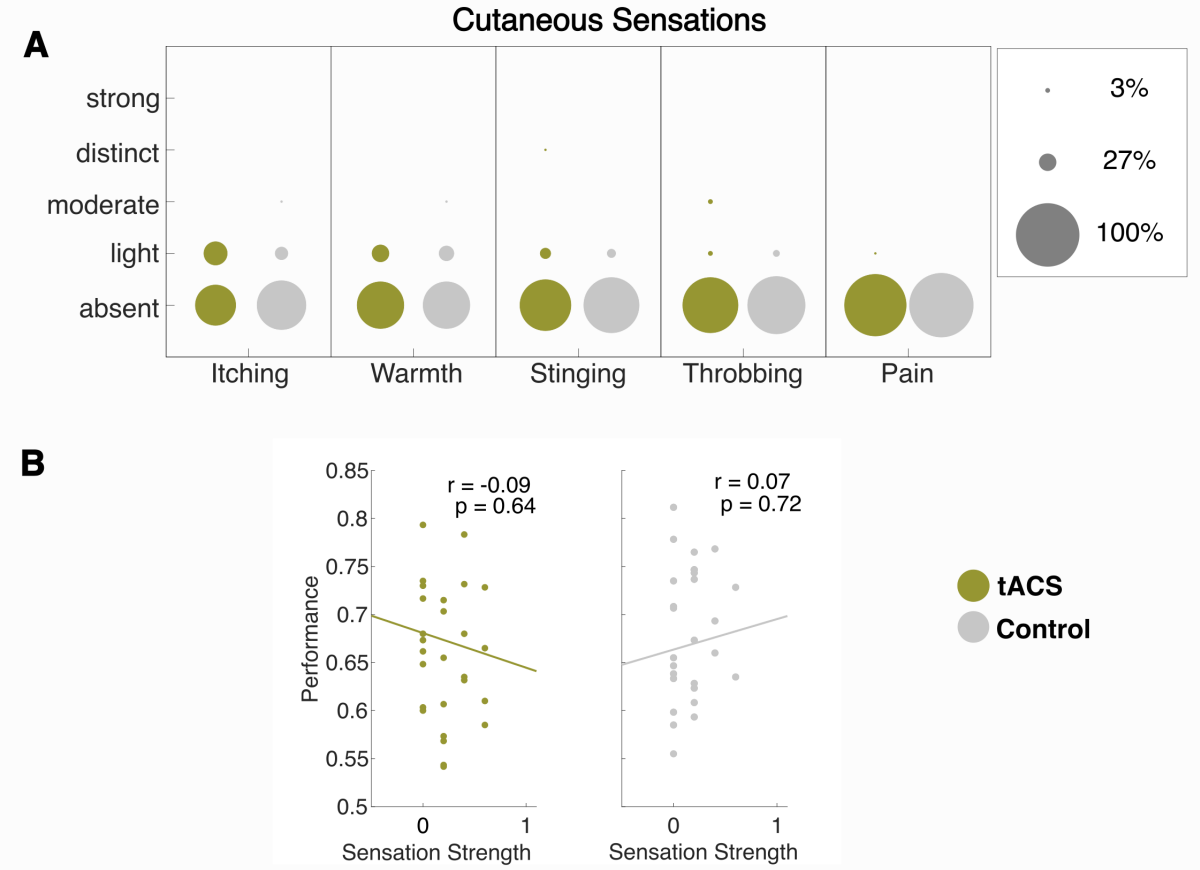

Supplementary Figure 2.7.3. Unimodal experiment (red: tACS, grey: Control). (A) Somatosensory artefacts of active tACS and active control condition, with no significant difference observed between conditions. Around 90% or more of the participant reported no cutaneous sensations. (B) Low correlation between cutaneous sensations and performance, further supporting the notion that tactile sensations did not significantly impact performance.

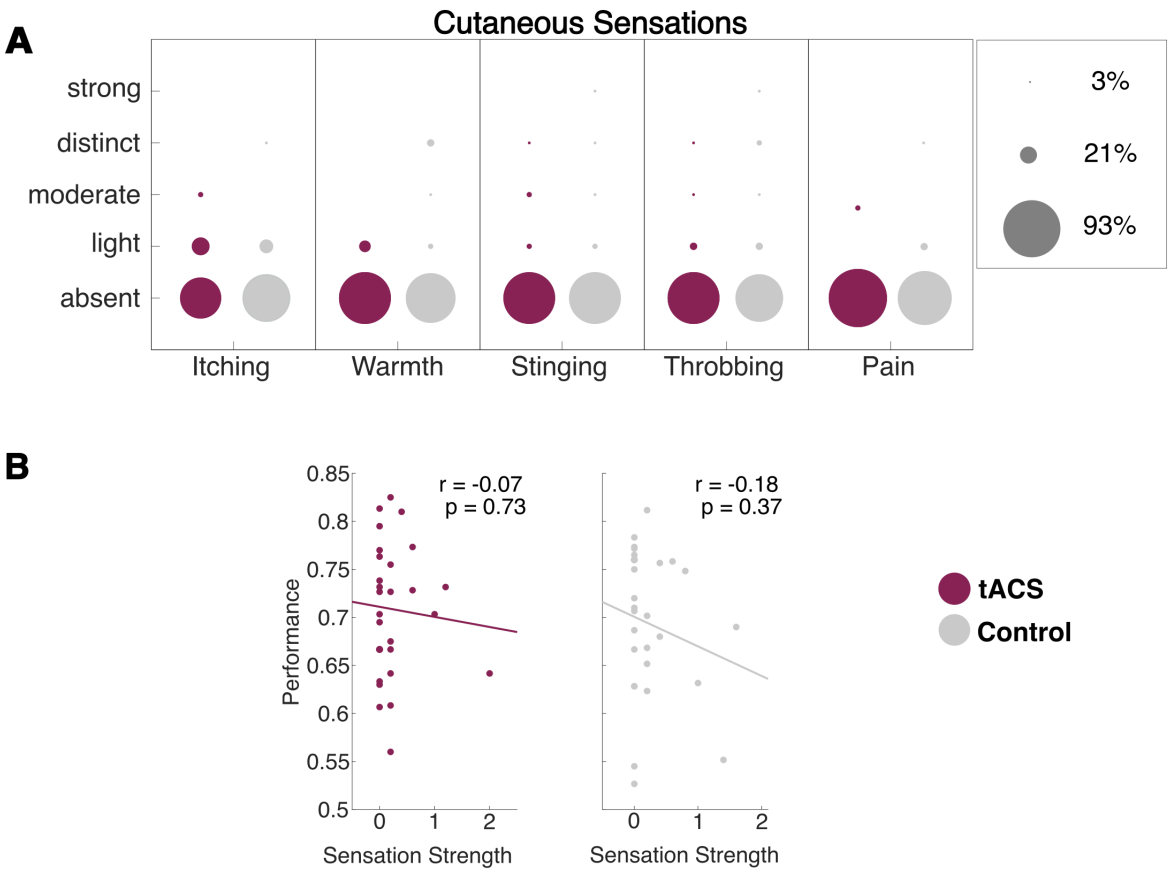

Supplementary Figure 2.7.4. Crossmodal experiment (green: tACS, grey: Control). (A) Somatosensory artefacts of active stimulation and active control condition. No significant difference between conditions. Around 90% or more of the participant reported no cutaneous sensations. (B) Low correlation of cutaneous sensations and performance suggest no influence of tactile sensations on performance.

CHAPTER 3

MODULATION OF TEMPORAL PREDICTION BY STN-DBS IN PARKINSON'S DISEASE: LINKS BETWEEN BEHAVIOR AND CORTICAL OSCILLATIONS

Status: *preprint*

R. Burke, M.J. Schoenfeld, C.K.E. Moll, A. Gulberti, M. Pötter-Nerger, A.K. Engel (2025). *bioRxiv*

3.1. ABSTRACT

BACKGROUND
Accurate temporal prediction is essential for adaptive behavior and relies on coordinated neural activity within cortico-basal ganglia circuits. PD, with the main hallmark of dopaminergic depletion and abnormal neural synchrony, impairs this ability. Deep brain stimulation DBS of the STN is a widely used treatment for reducing motor symptoms in PD, but its effects on temporal prediction remain not fully understood.

OBJECTIVES
This study aimed to investigate how STN-DBS influences temporal prediction performance and its underlying oscillatory dynamics in PD patients, with a particular focus on beta-band power and delta-band ITPC.

METHODS
13 PD patients (5 female, age: 64 $\pm$ 5.7 years; disease duration: 11.8 $\pm$ 1.8 years) with STN-DBS performed a temporal prediction task with (DBS ON) and without (DBS OFF) stimulation, while 64-channel-EEG was recorded. 20 age-matched healthy controls completed the same task. Behavioral performance was assessed using psychometric function slopes. Time-frequency analyses and source-level EEG measures examined beta power and delta ITPC.

RESULTS
PD patients showed impaired temporal prediction performance compared to controls, reflected in shallower psychometric slopes. DBS significantly improved performance to a level comparable to those of controls. EEG revealed reduced beta suppression in PD patients during DBS OFF, while beta suppression in DBS ON was comparable to controls. Both DBS OFF and ON exhibited reduced delta ITPC compared to controls. In DBS ON, source-level delta ITPC was positively correlated with temporal prediction accuracy.

CONCLUSION
STN-DBS improves temporal prediction performance in PD, likely through modulation of beta and delta oscillatory activity. While beta power suppression is partially restored, deficits in delta phase alignment persist, suggesting frequency-specific DBS effects on temporal prediction processes.

KEYWORDS

Parkinson's disease, Deep brain stimulation, Cognitive symptoms, Temporal prediction

3.2. INTRODUCTION

Accurate perception and prediction of time are fundamental for adaptive behavior, enabling humans to anticipate and respond to events in their environment. This ability involves estimating durations in the seconds-to-minutes (Coull and Nobre, 1998; Meck, 1996) and sub-seconds range (Smith et al., 2007) and is central to cognitive and motor processes. A key neural substrate underlying interval timing is the basal ganglia, a complex network of structures involved in motor, cognitive, and associative functions. Parkinson's disease (PD), a neurodegenerative disorder characterized primarily by the progressive loss of dopaminergic neurons in the substantia nigra pars compacta, frequently disrupts these functions (Brown, 2003; Oswal et al., 2013). The resulting dopamine deficiency slows the pace of the internal clock, leading to impairments in time perception and interval timing tasks (Meck, 1996; Rammsayer and Classen, 1997; Perbal et al., 2005). Dopaminergic medication has been shown to ameliorate these deficits by modulating the internal clock and enhancing attentional control of temporal information (Jones et al., 2008). However, despite medication, timing performance in PD remains heterogeneous, suggesting the involvement of additional neural mechanisms (Merchant et al., 2008). Next to standard dopaminergic medication, deep brain stimulation (DBS) of the subthalamic nucleus (STN) is an established treatment for PD, primarily used to alleviate motor symptoms by reducing excessive beta synchronization within the cortico-basal ganglia loops (Oswal et al., 2013). Beyond motor improvements, DBS has been shown to have heterogeneous effects on non-motor functions, including executive processes, working memory, and cognitive flexibility (Jahanshahi et al., 2000; Witt et al., 2004; Gülke et al., 2022; Yamanaka et al., 2012). Specifically, DBS appears to mitigate PD-associated impairments in time interval memory retrieval (Wojtecki et al., 2011). By modulating STN activity, DBS provides a unique opportunity to investigate the contribution of the basal ganglia in temporal prediction. In this study, we sought to examine

how anticipatory neural dynamics associated with temporal prediction are influenced by DBS in PD. Using electroencephalography (EEG) and a well-established temporal prediction task (Burke et al., 2025b; Daume et al., 2021), we compared oscillatory markers of anticipation in PD patients in one session with bilateral therapeutic STN-DBS turned on (DBS ON), and in another session with the device switched off (DBS OFF) to those in healthy age-matched controls. Our findings aim to bridge gaps in understanding the role of the basal ganglia in temporal processing and extend previous work on the cognitive effects of DBS (Jahanshahi et al., 2000; Pillon et al., 2000). We expected that individuals with PD would show impairments in temporal prediction relative to age-matched healthy controls, reflected in greater variability in their timing judgments. This deficit was expected to appear as a shallower slope in psychometric function. Additionally, we hypothesized that these behavioral differences between patients and healthy controls can be linked to altered beta-band modulation, in line with previous findings (Gulberti et al., 2015, 2024), as well as reduced phase consistency of delta oscillations in the parietal and frontal cortices following stimulus offset. We further presumed that DBS might influence temporal judgments in PD patients, resulting in systematic changes in the psychometric function, either by shifting the perceived timing or by modifying the slope.

3.3. MATERIALS AND METHODS

3.3.1. Participants

13 patients (5 female, mean age: 64 ± 5.7 years) with a diagnosis of advanced idiopathic PD (mean disease duration: 11.8 ± 1.8 years) and 20 healthy age-matched controls (13 female, mean age: 60.3 ± 3.9 years) took part in the study. The experiment was conducted in accordance with the Declaration of Helsinki and approved by the ethics committee of the Hamburg Medical Association. All participants gave written informed consent and received monetary compensation. Handedness was assessed using the short version of the Edinburgh Handedness Inventory (Oldfield, 1971). All participants reported normal

or corrected-to-normal vision and no history of psychiatric diseases. Participants were excluded if they showed indications of dementia based on a global dementia screening battery (Mini-Mental State Exam score <25) or psychiatric diseases (per DSM-IV) or neurological conditions other than PD or were receiving medication for depression. PD patients underwent therapeutical bilateral implantation of DBS electrodes in the STN prior to the experiment (months since surgery: 23.1 ± 15.4) and their levodopa-equivalent daily dose (LEDD, conversion factors as described by Jost et al. (2023)) was 786.6 ± 547.4 mg at the time of participation (see Table 3.1). To demonstrate patients' disease progression and severity, we derived the motor-subscore (III) of the -Unified Parkinson's Disease Rating Scale (UPDRS) (Goetz et al., 2008) and the Hoehn & Yahr scale (H&Y) (Hoehn and Yahr, 1967) from patients' medical history. Controls reported no history of neurological or psychiatric disorders. Both patients (for both sessions in DBS OFF and ON) and controls completed the Trail Making Test A and B (Reitan, 1956), as well as the digital version of Berg's Card Sorting Test (Grant and Berg, 1948), to assess their executive functions, specifically cognitive flexibility and logical reasoning. Patients and controls were excluded if they could not perform these tests. Since our focus in the present study was on effects of STN-DBS on temporal prediction, all patients were on their regular medication for all recordings. This also ensured patients' physical comfort during the measurement. While the present manuscript focuses on the comparison between PD patients and age-matched healthy controls, the control data will also be included in a separate publication examining age-related differences between younger and older adults.

Case Gender Age	Disease duration (years)	Pre-op H&Y	Pre-op medication (LEDD)	Pre-op UPDRS DOPA-OFF	Pre-op UPDRS DOPA-ON	DBS device	DBS parameters for: Left electrode (1. row) Right electrode (2. row)	Post-op H&Y	Post-op medication (LEDD)	Post-op UPDRS DOPA-OFF DBS-ON	Post-op UPDRS DOPA-ON DBS-ON
1, M, 72	5	2	300mg	21	12	ME	130Hz, 1-, 2.0V, 60μs 130Hz, 9-, 2.0V,60 μs	2	100mg	26	20
2, M, 65	12	2	1646mg	42	11	ME	130Hz, 1-, 2-, 6.0V, 60μs 130Hz, 9-, 5.5V, 60μs	2	713mg	19	13
3, F, 59	12	3	1413mg	29	13	BS	130Hz, 2-, 1.5V, 60μs 130Hz, 2-, 1.7V, 60μs	1	963mg	6	5
4, F, 63	11	2	1449mg	21	13	ME	140Hz, 1-, 7.5V, 60μs 140Hz, 9-, 6.6V, 60μs	2	255mg	15	10
5, M, 60	10	2	1875mg	23	17	BS	130Hz, 2-, 1.1V, 60μs 130Hz, 2-, 2.0V, 60μs	2	630mg	12	11
6, M, 72	15	2	1150mg	41	17	BS	130Hz, 1-, 4.3V, 60μs 130Hz, 1-, 5.7V, 60μs	2	1253mg	33	12
7, M, 58	11	2	924mg	18	9	BS	130Hz, 2-, 1.8V, 60μs 130Hz, 2-, 1.4V, 60μs	1	1862mg	15	7
8, F, 58	10	2.5	1121mg	24	9	BS	128Hz, 1-,2-, 6.7V, 60μs 128Hz, 2-, 1.4V, 60μs	2	350mg	16	12
9, M, 66	11	1	1442mg	24	14	BS	130Hz, 2-, 4.8V, 80μs 135Hz, 2-, 4.5V, 80μs	2	1692mg	17	9
10, F, 71	13	2	1325mg	35	11	BS	130Hz, 3-, 2.5V, 60μs 130Hz, 2-, 2.3V, 60μs	0	507mg	25	9
11, M, 70	15	2.5	1181mg	22	17	BS	130Hz, 3-, 2.0V, 60μs 130Hz, 3-, 2.3V, 60μs	2	971mg	20	11
12, F, 63	10	3	1000mg	46	12	BS	130Hz, 3-, 4.0V, 60μs 130Hz, 2-,4-, 1.7V, 60μs	2	405mg	34	19
13, M, 59	12	3	1782mg	31	11	ME	125Hz, 1-, 5.4V, 60μs 125Hz, 9-, 3.9V, 60μs	2	525mg	9	5

Case Gender Age	Disease duration (years)	Pre-op H&Y	Pre-op medication (LEDD)	Pre-op UPDRS DOPA-OFF	Pre-op UPDRS DOPA-ON	DBS device	DBS parameters for: Left electrode (1. row) Right electrode (2. row)	Post-op H&Y	Post-op medication (LEDD)	Post-op UPDRS DOPA-OFF DBS-ON	Post-op UPDRS DOPA-ON DBS-ON

Table 3.1: Clinical and demographic characteristics of PD patients. In column "DBS parameters" values reported are: stimulation frequency in Hz, active contacts, impulse amplitude in volts and impulse width in μs for the left and right electrode, respectively. For the left Medtronic (ME) electrode, contact 0 was the most ventral and contact 3 was the most dorsal. For the right ME electrode, contact 8 was the most ventral and contact 11 was the most dorsal. For the left Boston Scientific (BS) electrode, contact 1 was the most ventral and contact 8 was the most dorsal. For the right BS electrode, contact 9 was the most ventral and contact 16 was the most dorsal. Abbreviations: H&Y = Hoehn & Yahr scale. Op = operation for DBS electrodes implantation. UPDRS-III = Unified Parkinson's Disease Rating Scale of the Movement Disorder Society, motor-subscore (part III). LEDD = levodopa equivalent daily doses.

3.3.2. Experimental Paradigm

The study was conducted in two sessions (two different recording days within one week), maintaining consistent timing of the day and response mapping. In each session, participants performed the neuropsychological tests followed by the temporal prediction task (see Figure 1A; for details on experimental parameters see Daume et al. (2021) and Burke et al. (2025b). Participants were seated in a dimly lit chamber that was both electrically shielded, and sound attenuated. Visual stimuli were presented on a matte LCD screen (1920 $\times$ 1080 px, 120 Hz refresh rate). Throughout the experiment, participants were asked to fixate a red fixation dot surrounded by a white noise occluder. Each trial began with a fixation period lasting 1500 ms. Following this, a white ellipse appeared in the left periphery of the screen and moved towards the occluder at a constant velocity. The starting position of the ellipse varied, resulting in movement intervals lasting between 1000 and 1500 ms. After a delay t, it reemerged on the right side and continued moving for 500 ms. Reappearance times varied randomly by Δt ($\pm$34 to $\pm$934 ms, in 100 ms steps), relative to the objectively correct 1500 ms interval. Participants judged whether the reappearance was *too early* or *too late* via right-hand button press, based on motion perception. Response-button mapping was counterbalanced across participants and recorded using a BlackBoxToolKit USB Response Pad (Black Box ToolKit Ltd). Controls performed the task in two sessions, interleaved with a more difficult condition (data from both conditions will be reported in a separate publication). Each condition was conducted in blocks of 60 trials, with 8 blocks (4 per condition) presented per session. This setup resulted in 480 trials per session per condition, totaling 960 trials across both sessions. The order of conditions was pseudo-randomized across participants and sessions, ensuring that both conditions were equally presented within each session. PD patients performed the task as described above in one session with bilateral therapeutic stimulation switched off (DBS OFF) or with their stimulation turned on (DBS ON). EEG recordings commenced no earlier than 60 minutes after the DBS device was turned off.

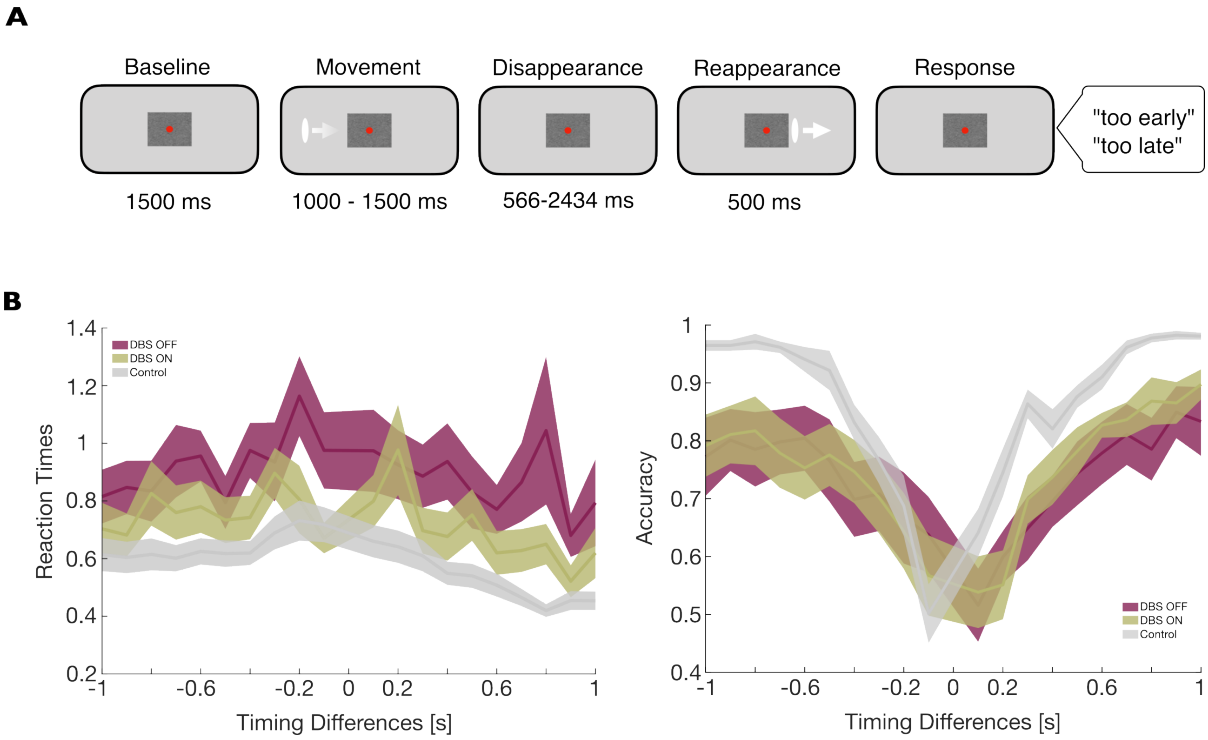

Figure 3.1: (A) Experimental design of the temporal prediction task is shown. In the beginning of each trial, a white ellipse appeared on the screen and moved towards the occluder before disappearing. After 1500 ms ± 34 to ± 934 ms the stimulus reappeared. Participants had to decide whether the stimulus reappeared *too early* or *too late* by responding with a keypress. (B) Reaction times, as well as accuracy values for all timing differences are presented as mean and shaded regions represent the standard error of the mean (SEM).

Each session contained 480 trials. At the end of each block, all participants received feedback on their performance using an average accuracy score. The start of each block was self-paced, allowing participants to decide when to proceed. Additionally, each session began with 30 practice trials to help participants familiarize themselves with the task. To further minimize the impact of background noise, participants wore earplugs. Stimulus presentation was carried out using MATLAB R2016b (MathWorks, Natick, USA; RRID: SCR_001622) in combination with the Psychophysics Toolbox (RRID: SCR_002881) (Brainard, 1997), running on a Windows 10 operating system.

3.3.3. Data acquisition and pre-processing

EEG activity was recorded using a 64-channel actiCAP snap electrode system (Brain Products GmbH, Gilching, Germany) with active Ag/AgCl electrodes embedded in an elastic cap. Each electrode was equipped with an integrated impedance converter to minimize noise from the environment and movement artifacts, which was particularly crucial for recordings in PD patients experiencing resting tremor. The data was digitized at a sampling rate of 1000 Hz using BrainAmp amplifiers (Brain Products GmbH, Gilching, Germany). Analysis was performed using MATLAB R2019b (The MathWorks Inc., 2019) and two open-source toolboxes: EEGLAB (Delorme and Makeig, 2004) (RRID:SCR_007292) and FieldTrip (Oostenveld et al., 2011) (RRID:SCR_004849), as well as the MEG and EEG Toolbox Hamburg (METH, Guido Nolte; RRID:SCR_016104) or custom-made scripts.

3.3.4. EEG preprocessing/artefact removal

Initially, EEGLAB was used to extract data from the experimental blocks. Each of these blocks was filtered with a high-pass filter at 0.5 Hz to reduce slow drifts, a low-pass filter at 95 Hz to eliminate high-frequency DBS artefacts and a band-stop filter at 49.5-50.5 Hz for line noise removal. Additionally, the DBSFilt toolbox was employed to remove artefacts in the harmonics and subharmonics of the stimulation frequency. All blocks from each session were subsequently merged. The merged data were segmented into epochs of variable lengths using FieldTrip. Each trial was cut from 1240 ms before the stimulus movement onset to 1240 ms after the offset of the reappeared stimulus, resulting in trial durations ranging between 4546 ms and 6914 ms. To remove artifacts from eye movements, muscle activity, and cardiac signals, an ICA was performed using the infomax algorithm. Components were identified and rejected based on their time course, variance, power spectrum, and topography through visual inspection. On average, 19 $\pm$ 3 out of 64 components were removed per participant per session. After ICA, all trials were

visually inspected, and those containing residual artifacts not detected in earlier steps were excluded. On average, 470 ± 5 trials per session remained after preprocessing, out of a total of 480 trials.

3.3.5. Quantification and statistical analysis

Our primary focus for statistical analyses was to compare data from patients across DBS OFF and DBS ON conditions, as well as to contrast patient data with control group data. To examine differences between DBS OFF and DBS ON conditions within patients, we conducted paired-samples t-tests. For comparisons between the patient and control group, we utilized independent-samples t-tests. We accounted for multiple comparisons by adjusting the alpha level (α=0.025).

3.3.6. Behavioral data analysis

Participants were not provided with feedback regarding the correctness of their responses. As a result, they made judgments based on their subjective interpretation of what constituted a "correct" reappearance timing. To determine these individual points of subjective equality (PSE), we fitted a psychometric curve to the behavioral data of each participant across all trials in each condition. For each timing difference, we first calculated the proportion of *too late* responses for each participant. A binomial logistic regression (psychometric curve) was then fitted to the data using the *glmfit.m* and *glmval.m* functions in MATLAB. The timing difference corresponding to a 50% *too late* response rate was identified as the PSE for each participant. To evaluate whether there was a significant bias in the PSE values, we compared them to zero using one-sample t-tests. The steepness of the psychometric function was quantified as the reciprocal of the difference between the timing differences at 75% and 25% *too late* response rates, providing a measure of the slope of the curve.

3.3.7. EEG analysis

We decomposed EEG recordings into time-frequency representations using complex Morlet wavelets (Cohen, 2014). Each trial and channel were convolved with 40 wavelets logarithmically spaced between 0.5-100 Hz, with cycles increasing logarithmically from 2 to 10. Only trials labeled as correct based on individual PSEs (see 2.6) were analyzed. After the wavelet convolution, we estimated spectral power modulations by dividing trials into four overlapping windows: baseline (-550 to -50 ms), movement (-50 to 950 ms), disappearance (-350 to 950 ms), and reappearance (-350 to 450 ms), all aligned relative to their respective events. Spectral power estimates were averaged across trials, binned into 100 ms intervals, and normalized using a pre-stimulus baseline (-500 to -200 ms prior to movement onset). Grand averages across channels were tested against baseline using paired-sample t-tests with cluster-based permutation statistics for multiple comparison correction (cluster-α=0.05, 1000 randomizations). For source-space analysis, leadfields were computed using a single-shell volume conductor model (Nolte, 2003) aligned to a Montreal Neurological Institute (MNI) template with a 5003-voxel grid. Cross-spectral density (CSD) matrices were derived from wavelet-convolved data in 100 ms steps and used to compute common adaptive linear spatial filters (DICS beamformer; (Gross et al., 2001). Normalized source power was analyzed using cluster-based permutation tests to identify significant power differences between groups (two-sample t-tests: DBS OFF vs. Controls and DBS ON vs. Controls) and within conditions (paired-sample t-tests: DBS OFF vs. DBS ON). To quantify phase alignment, we computed ITPC from wavelet-convolved complex time-frequency data by extracting phase angles per trial and time point (using MATLAB-function *angle.m*). ITPC values (ranging from 0 to 1) were calculated for all subjectively correct trials and averaged in 100 ms bins across the four time windows (see above). Statistical comparisons between the movement, disappearance, and reappearance windows and a pre-stimulus baseline were conducted using cluster-based permutation tests for each condition and group. For source level analyses, we used the

same procedure applied to spectral power (see above) and extracted ITPC estimates for each voxel. Our analyses focused on group and condition differences in the disappearance window, specifically in the delta-band (0.5-4 Hz). In all statistical comparisions, we used cluster-based permutation tests to identify significant ITPC differences between groups (independent-sample t-tests: DBS OFF vs. Controls and DBS ON vs. Controls) and within conditions (paired-sample t-tests: DBS OFF vs. DBS ON). Finally, Pearson correlations between delta ITPC and the slope of the psychometric function were computed, again, correcting for multiple comparisons through cluster-based permutation statistics.

3.4. RESULTS

3.4.1. DBS improved temporal prediction performance

To assess the effects of DBS on temporal prediction performance, we compared the slopes of the psychometric functions between and within groups. Significant differences were observed between conditions of DBS OFF and DBS ON (*t(12)=-1.68, p=.007, Cohen's d=-1.7*), as well as between DBS OFF and Controls (*t(32)=-5.04, p<.001, Cohen's d=-1.79*), but not between DBS ON and Controls (*t(32)=-1.68, p=.10, Cohen's d=-0.60*) (Figure 2). This suggests that DBS ON improved performance in the temporal prediction task compared to DBS OFF, while performance in DBS ON was comparable to controls.

3.4.2. DBS restored cortical beta suppression during temporal prediction

The effects of DBS on task performance were associated with specific cortical activity modulation as measured by EEG. Based on previous findings (Daume et al., 2021; Gulberti et al., 2015), indicating the relevance of beta-band activity in temporal prediction, we were mostly interested in the beta frequency range after stimulus disappearance, i.e., the onset of the temporal prediction process. In controls, we observed suppression of cortical beta activity during temporal prediction compared to baseline (Figure 3.3A). In PD patients, this beta-band suppression was generally less pronounced in both DBS

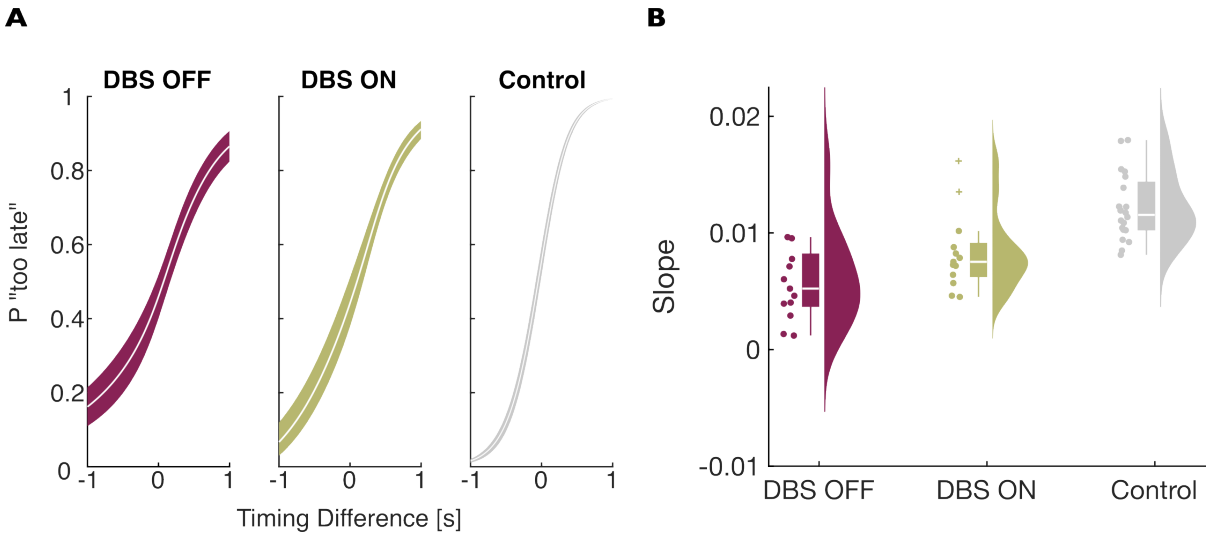

Figure 3.2: Behavioral results of the temporal prediction task. (A) Fitted psychometric curves of patients in the DBS OFF (red) and DBS ON (green) condition and healthy controls (grey). The timing difference of 0 refers to the objectively correct reappearance of the stimulus after 1500 ms. Colored areas depict standard errors of the mean (SEM) (B) Distribution of slope differences of psychometric functions between conditions and groups are shown as individual data points, boxplots and distributions. *p $<$ .05, **p$<$.01, ***p$<$.001; n.s., non-significant.

OFF and DBS ON conditions compared to controls. When observing oscillatory activity changes across DBS conditions in patients, beta power appeared to be stronger during DBS OFF than during DBS ON. This observation was supported by the results of cluster-based permutation statistics, which revealed significant clusters of voxels across bilateral medial prefrontal areas and the left temporal cortex (cluster-p=.019; Figure 3.3B). Notably, the present analysis reveals a significant decrease in beta power within the medial frontal and left temporal regions in patients with PD during the DBS OFF condition when compared to controls. However, no significant differences in beta power were observed between the DBS ON condition and the controls.

3.4.3. Delta ITPC was stronger in controls compared to DBS OFF or ON

For the ITPC analysis, a similar approach to the one above was used. First, we examined ITPC differences relative to baseline within three different time windows by averaging across all sensors, using cluster-based permutation statistics. The results showed a significant increase in ITPC across various frequency ranges in time bins corresponding to movement onset, occlusion, and stimulus reappearance, respectively (all cluster-p <0.001; Figure 3.4A). The most pronounced ITPC increases for the time window centered around stimulus disappearance, i.e., the time window relevant for the temporal prediction process, were found in the delta range in patients as well as controls. Therefore, our group comparisons were focused on frequencies between 0.5 and 4 Hz in a time window of -200 to 900 ms around stimulus disappearance. When comparing delta ITPC of patients with DBS OFF or DBS ON to controls, we identified negative clusters of sensors located in frontal and occipital regions showing significant differences (all cluster-p<.001; Figure 3.4B). At source level, analysis of the -200 to 900ms time window revealed the strongest ITPC differences between patients (either DBS OFF or DBS ON condition) and controls in voxels spanning across the occipital, temporal, parietal and right frontal lobes (all cluster-p<0.01; Figure 3.4C). No significant difference of delta ITPC was found for the comparison of patients with DBS OFF vs. DBS ON condition.

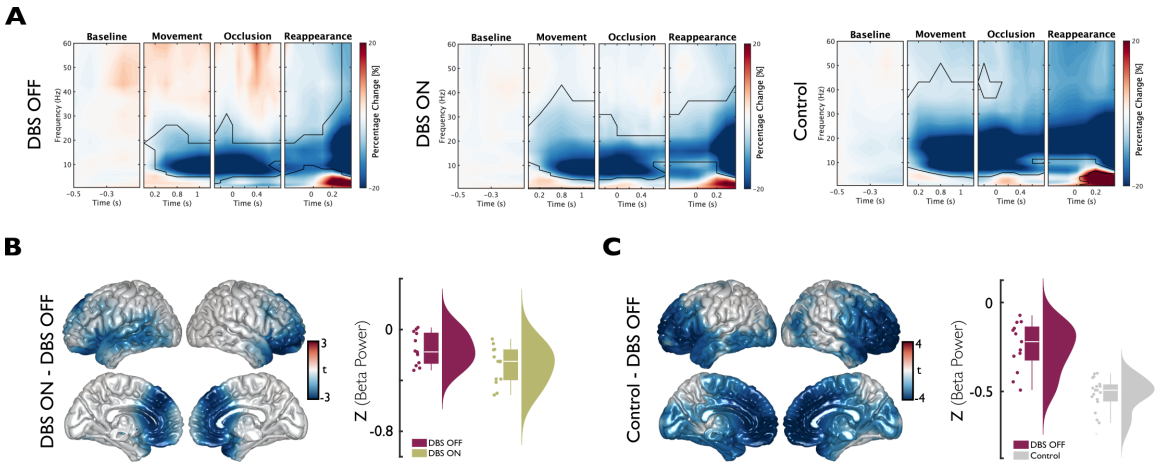

Figure 3.3: Spectral power modulations across conditions and groups. (A) Spectral power estimates compared to baseline. The panels show time-frequency plots of spectral power, averaged across sensors and participants. Each window is centered on their respective event within the paradigm and normalized to the pre-stimulus baseline. Time 0 s marks the onset of each event. Cluster-based permutation statistics revealed significant power modulations relative to baseline (indicated by regions enclosed with continuous lines). (B) Source-level comparison of beta power between DBS ON and DBS OFF conditions during the disappearance window (-0.2 to 0.6 s). Left: Surface plots of spectral beta power differences. Clusters of voxels with significant differences are highlighted in color. Right: Distribution of z-scored beta power averaged across voxels showing significant differences between conditions for the time window of disappearance. (C) Left: Source level data of beta power differences between Control and DBS OFF for the time window of disappearance (-0.2s to 0.6 s). Clusters of voxels with significant differences are highlighted in color. Right: Distribution of z-scored beta power averaged across voxels showing significant differences between groups for the time window of disappearance.

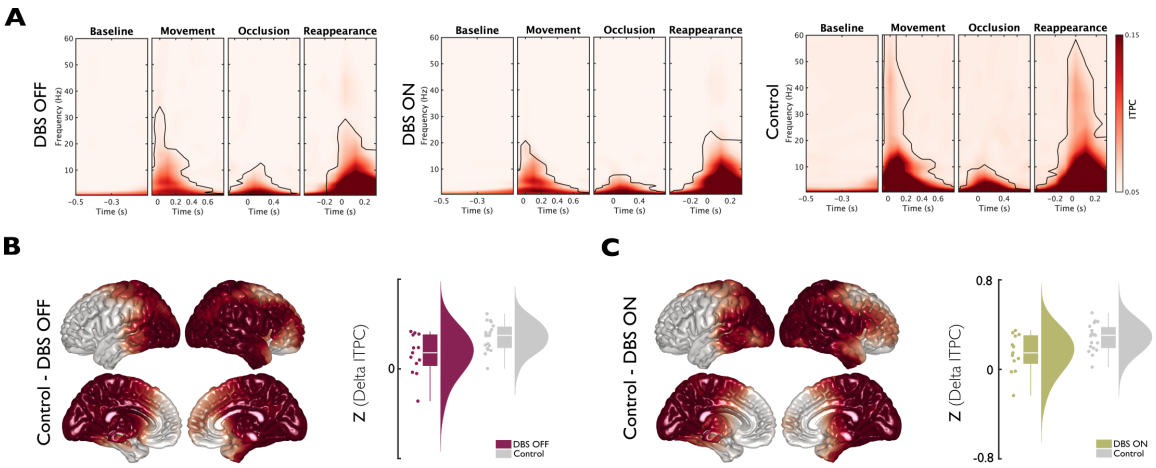

Figure 3.4: ITPC during temporal prediction in patients and controls. (A) The panels show time-frequency plots of ITPC, averaged across sensors, and participants. Each window is centered on different events within the experiment. Time 0 s marks the onset of each event. Cluster-based permutation statistics revealed significant ITPC modulations relative to baseline (indicated by regions enclosed with continuous lines). (B) Source level data of differences between Control and DBS OFF within the delta-band (0.5-4 Hz) for the time window of disappearance (-0.2 s to 0.9 s). Left: Surface plots of ITPC differences. Clusters of voxels showing significant differences between groups are highlighted in color. Right: Distribution of z-scored delta ITPC averaged across voxels showing significant differences between groups for the time window of disappearance. (C) Left: Source level comparison of ITPC data of Control and DBS ON within the delta-band (0.5-4 Hz) for the time window of disappearance (-0.2 s to 0.9 s). Clusters of voxels showing significant differences between groups are highlighted in color. Right: Distribution of z-scored delta ITPC averaged across voxels showing significant differences between groups for the time window of disappearance.

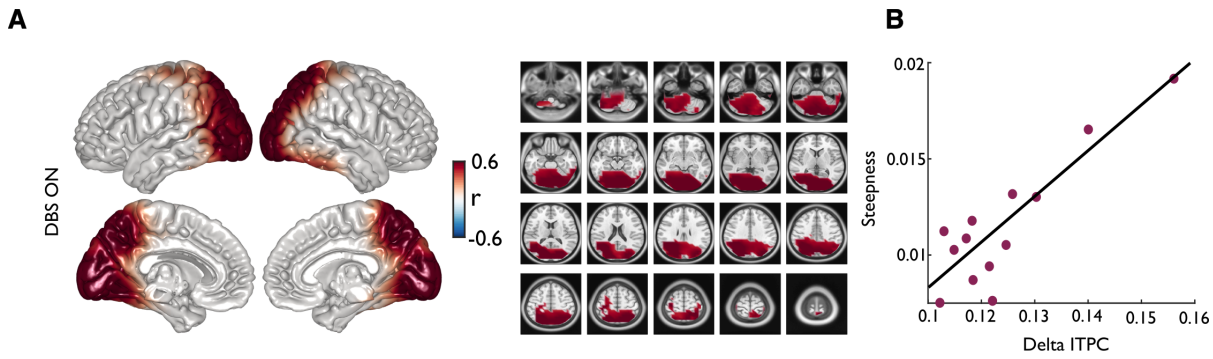

Figure 3.5: Relationship of delta ITPC and behavior. (A) Correlation of individual delta ITPC and the slope of the psychometric function within all voxels. ITPC was averaged across the delta-band (0.5-4 Hz) and time windows of -0.2 to 0.9 s around the disappearance of the stimulus. Only the clusters of voxels with significant correlations are colored. (B) Significant correlation of individual delta ITPC and steepness of the psychometric function (r=0.75, p=.003). Each dot of the scatter plot represents one participant. ITPC was averaged across all voxels within the clusters of significant correlations.

3.4.4. Delta ITPC in patients with DBS ON was correlated with performance

To investigate whether the phase alignment of neural oscillations was associated with temporal predictions in patients and controls, we computed Pearson correlations of source level delta ITPC with the steepness of the psychometric function. We found a significantly positive correlation only in patients in the DBS ON condition (cluster-p=.012; Figure 3.5B). Strongest correlations were found in the cerebellum and occipital as well as parietal areas (Figure 3.5A). No significant correlation was found for either patients in the DBS OFF condition or controls.

3.5. DISCUSSION

The present study provides novel insights for the modulatory effects of DBS on temporal prediction in PD, offering a new perspective on how basal ganglia dysfunction impacts anticipatory cognitive processes. Consistent with our hypothesis and previous studies,

PD patients showed impairments in temporal prediction relative to controls, as indicated by a shallower psychometric slope. Importantly, DBS improved performance to levels comparable to controls in the DBS ON condition. Beta suppression was less pronounced in PD patients in the DBS OFF compared to DBS ON condition and comparable between DBS ON condition and controls. In contrast, delta ITPC, was reduced in both DBS ON and OFF conditions compared to controls. For the DBS ON condition, source-level delta ITPC was positively correlated with temporal prediction accuracy. Our findings underscore that the basal ganglia play a significant role in interval timing and highlight that DBS is able to modulate higher-order cognitive functions.

DBS and temporal prediction performance

Our behavioral results align with earlier studies showing that PD patients exhibit increased variability in timing judgments due to a slowing or disruption of the internal clock mechanism (Jones et al., 2008; Meck, 1996; Merchant et al., 2008). These impairments have been linked to dopamine depletion in the basal ganglia, particularly the nigrostriatal pathway, which plays a central role in interval timing and temporal processing (Buhusi and Meck, 2005; Coull et al., 2011). Within this framework, the basal ganglia are thought to modulate temporal prediction by integrating sensory and motor information across time, a process that becomes dysfunctional in PD. The restoration of temporal prediction performance in the DBS ON condition of our study suggests that STN stimulation may partially compensate for disrupted timing mechanisms. This effect may arise through the modulation of pathological oscillatory activity and partial normalization of dopaminergic transmission within the cortex-basal ganglia loop (Paulo et al., 2023). The observed behavioral improvement of temporal prediction in our study is consistent with prior findings from studies showing that STN-DBS can enhance time perception and time reproduction tasks (Koch et al., 2004; Wojtecki et al., 2011). Notably, our results extend these findings by demonstrating that DBS improves not only retrospective time

estimation but also predictive timing, which is crucial for anticipating and responding to future events. Predictive timing is essential for a wide range of adaptive behaviors, including speech processing, motor coordination, and action planning (Arnal and Giraud, 2012; Coull et al., 2008). Its disruption in PD may contribute not only to motor symptoms like bradykinesia but also to non-motor deficits in attention, working memory, and executive control (Allman and Meck, 2012; Buhusi and Meck, 2009). By showing that DBS improves predictive timing, our findings suggest that the therapeutic effects of STN-DBS extend into the cognitive domain, potentially by enhancing the temporal structure of cortical processing. This has important implications for understanding the full spectrum of DBS benefits and for refining stimulation protocols aimed at cognitive enhancement in PD (Herz et al., 2018; Witt et al., 2004).

Beta oscillations and the role of the basal ganglia

Beta oscillations have been widely associated with sensorimotor processing, typically emerging during postural stability and diminishing during active states such as movement preparation and execution (Barone and Rossiter, 2021; Kilavik et al., 2013; Pfurtscheller et al., 2003). Furthermore, previous research has linked beta suppression to cognitive flexibility and motor readiness (Engel and Fries, 2010). Consistent with this notion and in line with prior work (Daume et al., 2021), we observed pronounced beta power suppression in both healthy controls and patients during the temporal prediction task. However, this suppression was significantly less pronounced in patients during the DBS OFF condition, particularly in medial prefrontal and left temporal regions, compared to both patients during the DBS ON condition and healthy control participants. The reduced beta suppression in the DBS OFF condition in our study may reflect the characteristic change in cortical dynamics in PD, where excessive beta activity is associated with impaired movement initiation and reduced cognitive adaptability (Brown, 2003). This is in line with research by Paulo et al. (2023) which highlights that cognitive impairments

in PD are associated with altered beta oscillatory activity in cortex-basal ganglia circuits, specifically involving the dorsolateral prefrontal cortex and caudate nucleus. In their study, reduced beta suppression during a working memory task was associated with poorer cognitive performance in PD, suggesting a mechanistic link between beta desynchronization and cognitive function. These findings underscore the role of beta oscillations not only in motor control but also in cognitive processes, including temporal prediction. In the DBS ON condition, patients exhibited levels of beta power suppression comparable to those of healthy controls. This recovery supports the notion that STN-DBS disrupts pathological beta synchronization, thereby restoring a more flexible and responsive network state (Kühn et al., 2008; Little and Brown, 2014). The relationship between subcortical and cortical beta is central to this dynamic. Beta activity in the STN is tightly coupled to cortical regions via the cortex-basal ganglia loop and in PD, this loop exhibits pathological synchronization and elevated beta cortico-subthalamic coherence (Brown, 2003; Lalo et al., 2008; Litvak et al., 2011; Oswal et al., 2016; Sharott et al., 2005). Subthalamic DBS as well as administration of therapeutic doses of dopaminergic medication have been shown to attenuate beta power within the STN of PD patients (Barone and Rossiter, 2021; Kühn et al., 2009; Ray et al., 2008; Weinberger et al., 2006; Whitmer et al., 2012). Thus, when STN-DBS reduces subcortical beta activity, it may also decouple pathological cortico-subcortical coherence (Oswal et al., 2016), enabling cortical regions, particularly motor and prefrontal areas, to re-engage in task-relevant beta desynchronization (Hemptinne et al., 2015; Whitmer et al., 2012). The restoration of cortical beta suppression in patients during DBS ON observed in our study is consistent with this notion. Although stimulation is delivered locally to the STN, its broader therapeutic impact likely stems from the normalization of aberrant beta synchronization across interconnected cortico-subcortical pathways, thereby enabling greater functional flexibility across the system. This restoration of neural flexibility is essential for dynamic cognitive functions such as temporal anticipation, and may underlie the observed

enhancements in predictive processing under DBS in individuals with PD.

3.5.1. Delta-band ITPC and temporal prediction

Beyond power changes, we also examined ITPC in the delta-band, which is associated with the phase alignment of neural oscillations to expected stimuli (Arnal et al., 2015; Schroeder and Lakatos, 2009; Daume et al., 2021). Both PD patients and healthy controls exhibited increases in delta ITPC during stimulus occlusion and reappearance, consistent with the notion that low-frequency phase alignment supports the temporal prediction of sensory input. However, both DBS OFF and DBS ON conditions in patients showed reduced delta ITPC compared to healthy controls. This might indicate that DBS did not fully restore phase alignment mechanisms. At sensor level, significant differences in delta ITPC were found in frontal and occipital regions. Source-level analyses revealed that the largest discrepancies in delta phase consistency were located in occipital, temporal, parietal, and right frontal cortices, areas involved in attentional and predictive timing (Arnal et al., 2015; Coull et al., 2008). These findings suggest that while DBS may help recover power dynamics, it may not sufficiently restore the phase consistency necessary for optimal temporal prediction. Interestingly, the correlation between delta ITPC and psychometric function slope was only significant in the DBS ON condition, particularly in the cerebellum, occipital, and parietal regions. These are structures known to support sensorimotor timing and predictive processing (Ivry and Spencer, 2004). This indicates that despite reduced ITPC in absolute terms, individual differences in residual phase alignment under DBS ON may still support more accurate temporal judgments. The absence of a similar relationship in DBS OFF and control groups might underscore a potentially unique, compensatory role of DBS in facilitating phase-behavior coupling.

Overall, our findings contribute to a growing literature emphasizing the role of oscillatory dynamics in cognitive processes such as temporal prediction. Specifically, our results support the view that beta and delta oscillations are key signatures of temporal

prediction, and that PD disrupts both power and phase-based mechanisms. While DBS appears effective in modulating beta power and improving behavioral performance, its impact on phase-based delta coherence seems limited, warranting further investigation. Future studies could assess whether different DBS parameters (e.g., frequency, pulse width, or stimulation pattern) differentially affect beta and delta-band dynamics, respectively. For instance, applying low-frequency stimulation protocols may more effectively engage slower rhythms like delta, and could be used to causally investigate the role of low frequency phase alignment in temporal prediction.

3.6. CONCLUSION

In summary, our study demonstrates that DBS enhances temporal prediction performance in PD by modulating key oscillatory mechanisms, particularly through beta power suppression. This is consistent with a broader body of work suggesting that beta desynchronization facilitates adaptive cognitive processes, including attention and anticipation (Engel and Fries, 2010). However, both DBS ON and OFF conditions showed diminished delta phase alignment compared to controls, indicating that DBS may only partially restore predictive processing mechanisms. Our findings underscore the importance of integrating both power and phase-based measures when evaluating DBS effects and highlight the potential of oscillatory biomarkers to refine therapeutic strategies for cognitive dysfunction in PD. Future work combining DBS with targeted cognitive or neuromodulatory interventions may offer new avenues for restoring both the timing and precision of neural dynamics supporting temporal prediction.

Declaration of competing interest

The authors declare that they have no known competing financial interests or personal relationships that could have appeared to influence the work reported in this paper.

CRediT authorship contribution statement

Rebecca Burke: Conceptualization, Methodology, Investigation, Software, Formal analysis, Validation, Visualization, Data curation, Writing - original draft, Writing - review & editing. **Marleen J. Schönfeld**: Conceptualization, Methodology, Investigation, Formal analysis, Writing - review & editing. **Alessandro Gulberti**: Writing - review & editing. **Christian K.E. Moll**: Writing - review & editing**. Monika Pötter-Nerger**: Investigation - Assisted in patient recruitment. Writing - Review & Editing. **Andreas K. Engel**: Conceptualization, Methodology, Writing - review & editing, Funding acquisition, Project administration, Supervision.

Acknowledgements

This work was supported by grants from the Deutsche Forschungsgemeinschaft (SFB TRR 169/B1/B4 261402652 awarded to A.K.E.). We thank Karin Reimann for assistance in data recording, and Till R. Schneider, Alexander Maÿe, and Peng Wang for helpful discussions on the data.

3.7. SUPPLEMENTARY MATERIAL

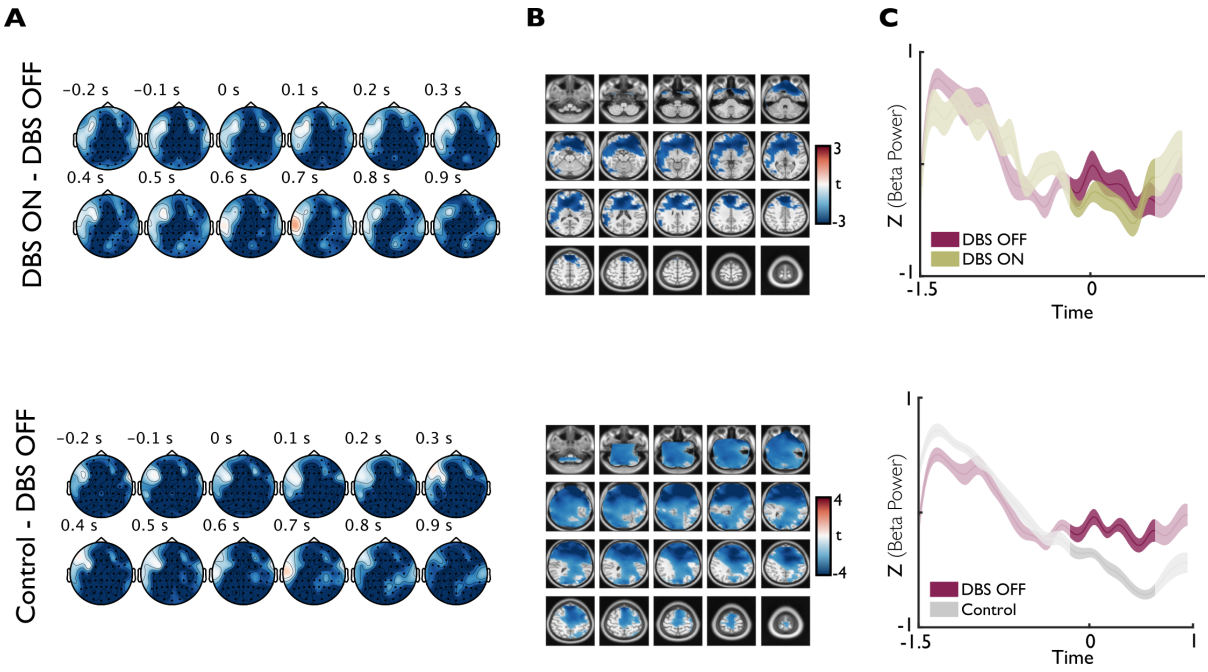

Supplementary Figure 3.7.1. Beta power differences between conditions (DBS ON & DBS OFF) and groups (Control & DBS OFF). (A) Sensor level data of beta power differences between DBS ON and DBS OFF (top) and Control and DBS OFF (bottom) for the time window of disappearance (-0.2s to 0.6 s). Clusters of sensors with significant differences indicated by black dots. (B) MRI slices of beta power differences between DBS ON and DBS OFF for the time window of disappearance (-0.2 s to 0.6 s). Clusters of voxels with significant differences are highlighted in color. (C) Time course of beta power (± SEM) averaged across voxels of significant clusters for the difference between conditions and groups. Time 0 s marks the onset of disappearance.

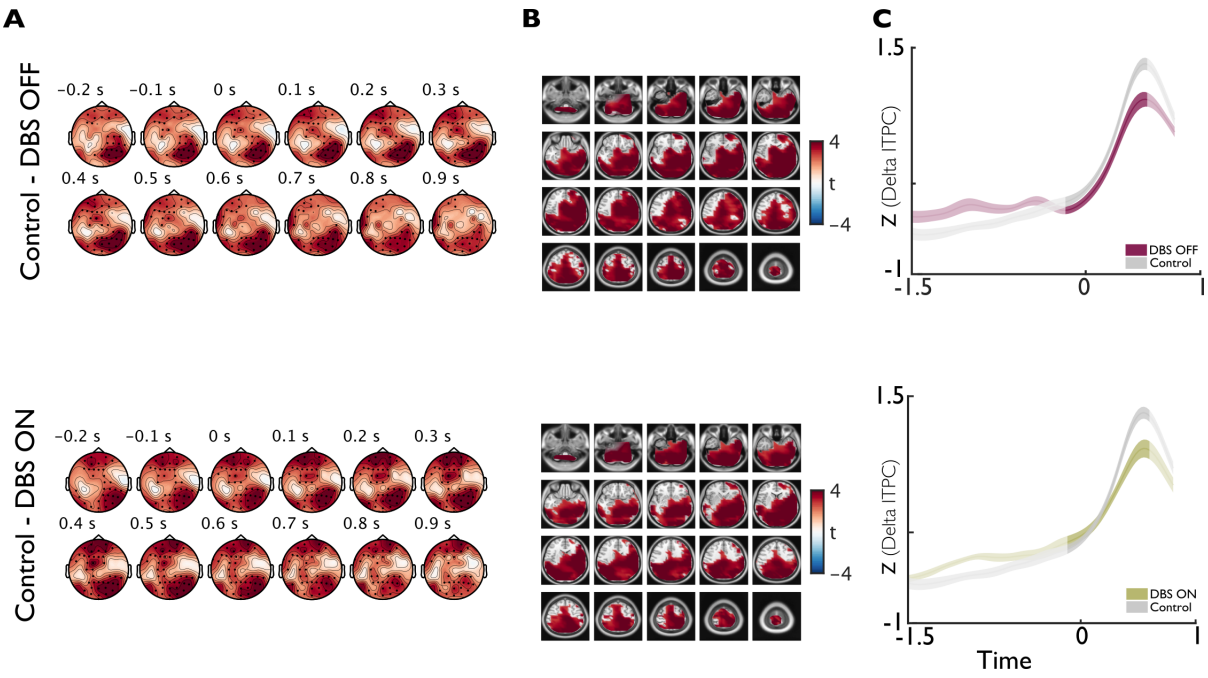

Supplementary Figure 3.7.2. Delta ITPC differences between groups. (A) Sensor level data of ITPC differences between Control and DBS OFF (top) and Control and DBS ON (bottom) for the time window of disappearance (-0.2s to 0.9 s). Clusters of sensors with significant differences indicated by black dots. (B) MRI slices of delta ITPC differences between DBS ON and DBS OFF for the time window of disappearance (-0.2 s to 0.9 s). Clusters of voxels with significant differences are highlighted in color. (C) Time course of ITPC (± SEM) averaged across voxels of significant clusters for the difference between groups. Time 0s marks the onset of disappearance.

DISCUSSION

While there may be no dedicated sensory organ for time, temporal information is nonetheless a pervasive and essential dimension of perception. Rather than being isolated from the senses, time is embedded within and arises through our sensory experiences, whether vision, audition or touch. This is not confined to individual modalities: it often spans them. Crossmodal temporal prediction, for instance, involves using cues in one sensory modality to anticipate the timing of an event in another. This process likely recruits integrative neural mechanisms beyond those engaged during unimodal temporal prediction, where expectations are formed within a single sensory modality. Understanding how the brain predicts *when* events will occur thus offers a window into how time itself is constructed from and shared across perceptual systems. Therefore, the lack of a sensory organ for time is an opportunity, not a limitation, to understand perception more broadly (Singhal, 2021). A large body of work suggests that neural oscillations, specifically, phase alignment of neural oscillations, play a crucial role in supporting temporal prediction (Daume et al., 2021; Arnal et al., 2015; Arabkheradmand et al., 2020; Burke et al., 2025b; Herbst and Obleser, 2019; Wilsch et al., 2015). However, the mechanism by which these oscillations contribute to unimodal and crossmodal non-rhythmic temporal prediction, and how the mechanisms are distributed across cortical and subcortical structures, remain to be fully understood. By combining correlational, causal, and clinical approaches targeting distinct neural substrates, I aimed to build a layered account of how temporal prediction operates across sensory contexts. In this thesis, I presented three studies that investigate temporal prediction across distinct methodological and mechanistic levels. First, I presented magnetencephalographic evidence showing that enhanced delta-band phase alignment over trials during a crossmodal (visuo-tactile-to-visual) temporal prediction task correlates with behavioral performance, pointing towards a contributing role for oscillatory phase alignment in temporal prediction. Second, I introduced a tACS study that causally probes the role of delta phase alignment in temporal prediction. Using a 2-Hz stimulation aligned to the prediction window, we found phase-specific modulation

of unimodal visual prediction performance, but not crossmodal prediction. This suggests that cortical delta oscillations do not merely reflect but can shape anticipatory processes in a unimodal context. The lack of an effect in the crossmodal condition, however, hints at the involvement of more distributed or hierarchically higher systems. Third, I presented a study with PD patients with therapeutical STN-DBS. This study deepened the perspective that a distributed network underlies temporal prediction by revealing the critical role of basal ganglia in temporal prediction. Given that STN stimulation affects spike output directly, this study implicates subcortical loops as effectors or modulators of predictive timing, likely interacting with cortical phase-based processes. This cortical–subcortical interplay may be particularly important in the precision and adaptability of temporal mechanisms, with basal ganglia circuits orchestrating sensorimotor and attentional resources in line with temporal expectations. A striking theme across these studies is the differential vulnerability of unimodal and crossmodal prediction to perturbation. While unimodal prediction appears to be tightly governed by local cortical oscillatory phase, crossmodal prediction may rely on broader network coordination or higher-order associative systems that are more robust to localized cortical perturbation (e.g., tACS) but sensitive to subcortical dysfunction and stimulation. These findings support a multi-level framework in which oscillatory phase consistency, cortical modulation, and subcortical spike output each contribute to temporal prediction in distinct but interactive ways. Understanding these contributions offers a pathway toward both more refined models of perception and potential clinical interventions for disorders of timing.

Delta oscillations as a core mechanism of temporal prediction

A unifying theme across all studies presented in this thesis is the central role of delta-band phase alignment in facilitating temporal prediction. In the MEG study, increased delta ITPC was associated with higher temporal prediction accuracy, more specifically, in a crossmodal task where a combination of a visuo-tactile cue predicted visual stimulus

reappearance. This underscores delta oscillations as a supramodal reference frame for aligning internal neural states with anticipated events. Crucially, delta ITPC was source-localized not only to sensory areas (V1/V2, somatosensory cortex) but also to the cerebellum, consistent with theories positing distributed cortical-subcortical involvement in temporal prediction processes (Breska and Ivry, 2018). These findings support a model in which delta phase acts as a unifying clock signal, aligning separate sensory higher-order regions around shared temporal expectations. It adds weight to frameworks positing that delta rhythms are foundational for active sensing and crossmodal binding (Keil and Senkowski, 2018; Bauer et al., 2020). In the tACS study, causal evidence was added to this correlation. Applying 2 Hz tACS over the parietal cortex modulated unimodal visual prediction performance in a phase-dependent manner, establishing a functional role for delta phase in unimodal temporal prediction (Burke et al., 2025b). Notably, performance effects followed a sinusoidal pattern, supporting the idea that delta oscillations modulate perceptual sensitivity by aligning high-excitability phases with expected stimuli. Although temporal prediction was not modulated by tACS in the crossmodal condition, we argued that this may reflect increased cognitive demands, the recruitment of additional frequency bands, and/or cortical and subcortical areas not targeted by our distinct stimulation protocol. In the DBS study, delta ITPC was disrupted in PD patients, with only partial restoration under STN stimulation. While DBS normalized beta power and improved behavioral performance, delta phase alignment remained impaired. Therefore, delta phase dysregulation persisted in cortical regions even when motor symptoms were alleviated. However, in the DBS ON condition, individual differences in delta ITPC correlated with behavioral precision, suggesting that even partial preservation or restoration of phase alignment may support temporal prediction under therapeutic stimulation. Extensive research has highlighted the role of delta-band oscillations as a potential intrinsic mechanism for temporal prediction (Herbst and Obleser, 2019; Wilsch et al., 2015; van Wassenhove, 2016; Daume et al., 2021; Arnal et al., 2015). The slow periodicity of

delta oscillations aligns well with the temporal structure of various behavioral rhythms, including speech syllables rates (Arnal and Giraud, 2012; Giraud and Poeppel, 2012) or musical beats (Schroeder and Lakatos, 2009). Delta oscillations can entrain to the temporal structure of sensory input, by aligning the phase of a slow wave to anticipated stimuli. Therefore, the brain effectively modulates neuronal excitability in sensory areas at the expected moment to input. In other words, neural firing is optimized when an incoming event arrives at a high-excitability phase of an ongoing delta cycle (Lakatos et al., 2005, 2008; Schroeder and Lakatos, 2009). This principle, known as neural entrainment, has been demonstrated in non-human primates (Lakatos et al., 2013) and in humans as a mechanism for temporal attention (Besle et al., 2011; Obleser and Kayser, 2019). This forms the neural basis of the dynamic attending theory, a notion that our attention rhythmically oscillates in sync with environmental rhythms to enhance processing at expected moments (Jones, 1976; Jones and Boltz, 1989). Therefore, in line with previous research, the evidence from the three studies presented in this thesis suggest delta phase alignment as a potential unifying mechanism underlying non-rhythmic unimodal and crossmodal temporal prediction. However, temporal prediction does not solely rely on cortical delta oscillations in isolation. Computational models like the striatal beat-frequency model (Matell and Meck, 2000; Miall, 1989) propose that interval timing arises from the coincidence detection of oscillatory processes in thalamo-cortico-striatal loops (Buhusi and Meck, 2005). In addition to delta-band phase alignment, beta-band activity has emerged as a key substrate of temporal prediction (Arnal et al., 2015; Morillon and Baillet, 2017).

Beta oscillations: generalized predictive modulation and network flexibility

Overall, beta-band dynamics in our studies were less task-specific than delta band oscillations but nonetheless crucial. In both, MEG and DBS studies, beta power suppression

was consistently observed during periods of temporal uncertainty and sensory occlusion. Our DBS study showed that beta suppression in DBS OFF compared to DBS ON and controls was diminished during temporal prediction, which is consistent with evidence of reduced abnormal beta synchronization in the cortico-basal ganglia loops through STN stimulation (Oswal et al., 2016). While beta-band activity is classically associated with the sensorimotor system, showing characteristic suppression during movement and rebounds at movement cessation (Fujioka et al., 2012; Arnal, 2012), it is also linked to higher-order timing functions: They synchronize across cortical and subcortical networks during tasks that require anticipating upcoming stimuli in time (Biau and Kotz, 2018; Chang et al., 2018; de Lange et al., 2013; van Ede et al., 2011; Gulberti et al., 2015; Lewis et al., 2016). Beta power in auditory and motor areas aligns with the tempo of rhythmic sounds and increase just before expected beats. When a beat is unexpectedly omitted, beta activity remains elevated instead of rebounding, suggesting that beta rhythms help encode temporal predictions (Fujioka et al., 2009, 2012). Clinical observations reinforce beta's importance in timing. Parkinson's disease, a movement disorder primarily marked by excessive beta synchrony in cortico-basal ganglia circuits (Brown, 2003), often features impaired timing and rhythm processing (Beudel et al., 2019). PD patients have particular difficulty with internally timed or rhythmic tasks, despite relatively preserved perception of single intervals (Breska and Ivry, 2018; Beudel et al., 2008). This aligns with the idea that beta oscillations serve a predictive function: beta modulation prepares upcoming actions or sensory events, whereas in PD this prospective control is deficient, leading to more reactive, stimulus-driven timing (te Woerd et al., 2014). Notably, treatments that suppress pathological beta in PD (dopaminergic medication or DBS) tend to improve motor timing performance and restores pathological beta dynamics (Gulberti et al., 2015). In the MEG study, the beta suppression occurred irrespective of whether the task involved explicit temporal prediction or a working memory task, suggesting a broader role for beta desynchronization in modulating internal models during sensory

transition periods. Rather than encoding prediction per se, beta suppression may signal increased reliance on internal representations or readiness for sensory change. This preparatory mechanism is consistent with the *status quo* framework of beta oscillations (Engel and Fries, 2010). When the status quo should be maintained, beta stays elevated; when a shift or new event is imminent, beta transiently dips, allowing new information to be processed or new actions to commence (Lewis et al., 2016). This principle may explain why excessive beta (as in PD patients) has adverse effects: the brain is locked in maintenance mode and has difficulty shifting at the appropriate time, leading to delayed or frozen reactions. These findings support a dual role of beta: facilitating sensorimotor flexibility and supporting internal representation during prediction tasks. Despite allowing for more sensorimotor and cognitive flexibility, the adaptability to temporal contingencies could be further improved by using closed-loop or adaptive DBS. The severity of Parkinsonian symptoms fluctuates due to dopaminergic medication (Nutt, 2001) or fatigue (Storch et al., 2013; Santos-García et al., 2022). Therefore, DBS may be most effective in PD when delivered contingent upon the presence of pathological neural activity and overt symptom expression (Brittain et al., 2014). Conventional stimulation strategies that globally suppress beta activity may offer only a partial solution, since they lack the necessary volatility of beta modulation to process essential temporal information (Beudel et al., 2019). A more physiologically grounded therapeutic goal would be to preserve the dynamic, event-related nature of beta oscillations that allows them to occur transiently and adaptively in response to behavioral demands, rather than being chronically attenuated as a form of nonspecific background noise (Tinkhauser et al., 2017). Therefore, in order to establish a direct, causal link between pathological neural activity in PD and temporal prediction, adaptive DBS may allow to target distinct pathophysiological parameters and its behavioral effects (Beudel et al., 2019).

Alpha Oscillations and top-down control

The MEG study of this thesis identified increased alpha power in prefrontal and temporal regions during temporal prediction. This aligns with theories that alpha synchronization reflects active inhibition of irrelevant input to protect ongoing internal computations (Jensen and Mazaheri, 2010), particularly in the absence of external sensory information. The involvement of dorsolateral and medial prefrontal cortex suggests executive modulation (Sauseng et al., 2005), while superior temporal sulcus and medial temporal gyrus engagement highlights alpha's role in multisensory temporal alignment (Beauchamp et al., 2008; Noesselt et al., 2012; Nath and Beauchamp, 2011). These findings complement the broader literature by extending gating-by-inhibition models to anticipatory timing. The gating-by-inhibition framework posits that alpha-band oscillations serve to rhythmically inhibit task-irrelevant regions, thereby controlling the flow of information and enhancing signal-to-noise ratios in behaviorally relevant circuits (Jensen and Mazaheri, 2010). In the context of temporal prediction, this suggests that alpha activity may help suppress competing sensory or cognitive input while internal timing mechanisms operate, especially under conditions of uncertainty or sensory sparsity. Although alpha dynamics were not targeted in the tACS and DBS studies, the findings from our MEG study suggest they play a complementary role, likely interacting with delta and beta rhythms to orchestrate temporal prediction via hierarchical and context-dependent oscillatory control. In the context of PD, alpha-band abnormalities are associated with cognitive dysfunction (Oswal et al., 2013; Zhao et al., 2025). A globally reduced peak alpha frequency has been shown to indicate dopaminergic deficits (Morita et al., 2011), while parieto-occipital alpha power reductions are particularly evident in PD patients with cognitive impairment (Jaramillo-Jimenez et al., 2021). Furthermore, reduced parietal alpha power predicts executive deficits, and posterior temporal alpha power decreases are associated with memory impairment (Rea et al., 2021; Polverino et al., 2022). Therefore, in order

to investigate alpha's distinct role in temporal prediction, future studies could contrast predictive and non-predictive timing tasks with matched sensory input in clinical studies with patients with PD, isolating anticipatory alpha dynamics from general attentional demands.

Limitations

While the three studies presented here offer a multi-method perspective on the neural mechanisms underlying temporal prediction, several limitations should be acknowledged.

The MEG study provides important correlational evidence linking ITPC to crossmodal temporal prediction performance. However, the nature of MEG inherently limits causal interpretation. Although enhanced ITPC in the delta-band was associated with improved performance, this relationship does not establish whether oscillatory phase alignment plays a driving role in temporal prediction, or merely reflects a downstream correlate of attentional or integrative processes. Furthermore, the crossmodal nature of the task may have engaged broader attentional or associative networks, complicating attribution to specific frequency bands or neural generators.

While tACS allows for causally probing the role of low-frequency oscillatory phase in temporal prediction, it is paradoxically constrained by its vast parameter space. Fixed-frequency protocols, trade-offs between electric field strength and focality, and standard electrode montages impose limitations on the specificity and interpretability of results. For instance, conventional montages may not optimally target functionally relevant networks, since they are not tailored to individual differences in brain structure or functional organization. However, personalization based on individual anatomy or endogenous rhythms typically require time-consuming neuroimaging, modeling, and calibration procedures, making them less feasible. Moreover, while the phase-specific modulation of unimodal prediction supported the role of delta phase in temporal prediction, the absence

of an effect in the crossmodal condition raised interpretational ambiguities: it remains unclear whether this reflects a true mechanistic dissociation or a limitation of tACS sensitivity in more distributed, integrative circuits. The fixed-frequency stimulation may also have failed to align optimally with each participant's endogenous delta rhythm.

The STN-DBS study provided valuable causal evidence implicating basal ganglia output in visual temporal prediction. However, the reliance on clinical populations also may have introduced several confounds. Motor and cognitive deficits (and its fluctuations) intrinsic to the disease, and potential medication effects, could have influenced performance independently of stimulation state. While the within-subjects DBS ON/OFF design partially controls for this, the stimulation effects are not restricted to temporal prediction. Additionally, we did not change the stimulation parameters of DBS, thus neural firing patterns were modulated broadly and did not permit frequency- or phase-specific inferences.

Although the three studies differed in sensory modality (unimodal vs. crossmodal), they all shared a common temporal prediction task structure, which offers a valuable opportunity to explore how prediction mechanisms may vary across perceptual domains. However, this shared experimental design also introduced a further limitation: the velocity of the white ellipse was held constant in all three studies. Consequently, future research is required to determine whether the role delta phase alignment for temporal prediction generalizes beyond this specific temporal parameter. Furthermore, the differential sensitivity of unimodal and crossmodal temporal prediction to experimental cortical and subcortical stimulation raised important but unresolved questions about whether these forms of temporal prediction are governed by fundamentally distinct neural mechanisms or differ in their susceptibility to experimental perturbation. Nevertheless, the integration of correlational, causal, and clinical perspectives across studies provides a complementary perspective, enabling a richer understanding of how oscillatory phase alignment, cortical excitability, and subcortical output might interact to support temporal prediction.

Although each method captures different facets of the underlying mechanisms, their convergence lays the groundwork for more comprehensive, multi-level models of temporal prediction.

CONCLUSION

Integration and broader implications

Taken together, the results from the three studies converge on a dynamic and multiscale model of temporal prediction that operates through distinct but possibly interacting neural oscillations. Within this framework, delta oscillations serve as a core mechanism for encoding when an event is expected to occur. These slow rhythms provide a temporal reference frame that aligns neural excitability with anticipated sensory input, especially under conditions of temporal uncertainty or in the absence of rhythmic cues. Beta oscillations, on the other hand, reflect the dynamic modulation of internal models, with beta suppression marking periods of heightened flexibility and adaptive control. This desynchronization may signal a release from the maintenance of the status quo, allowing for the updating of temporal expectations in response to changing sensory contingencies. Alpha rhythms appear to subserve a complementary role, supporting the maintenance of attentional focus and the suppression of irrelevant or distracting input during periods that rely on internally guided prediction rather than external stimulation. Crucially, these frequency bands are not isolated in their function. Rather, they interact across a distributed network of cortical and subcortical structures, including sensory cortices, prefrontal and parietal areas, the cerebellum, and basal ganglia, whose engagement is shaped by task demands and modality. This aligns closely with hierarchical predictive coding theories (**?**Friston, 2010), in which different oscillatory timescales implement specific computational roles (Senkowski and Engel, 2024). Slower rhythms such as delta might carry temporal priors, while faster rhythms like beta and alpha coordinate the timing of information flow, prediction error signaling, and sensory gating. Moreover, emerging evidence suggests that cross-frequency coupling, particularly between delta and beta bands, orchestrate the fine-tuning of anticipatory processing (Arnal et al., 2015), linking phase-based expectations with power-based attentional mechanisms.

Future directions

Moving forward, several avenues of research are warranted to refine and extend our understanding of neural mechanisms underlying non-rhythmic unimodal and crossmodal temporal prediction. First, future studies should investigate whether the observed delta phase alignment generalizes across different temporal parameters. In the present studies, the velocity of the white ellipse was held constant across all experiments, representing a limitation that constrains conclusions about the flexibility of delta phase mechanisms. Varying stimulus velocity or temporal intervals systematically would help determine whether oscillatory delta phase alignment reflects a more general mechanism of timing or is specific to our particular setup. Second, neuromodulation approaches, varying non-invasive brain stimulation protocols targeting delta, beta, and alpha frequencies, could help delineate the specific contributions and interactions of these oscillatory systems in shaping temporal prediction. Such approaches would allow researchers to test the hypothesis that low-frequency phase alignment provides a reference frame for higher-frequency modulation, and that performance is optimized when excitability and attention are aligned in time. Third, individualized stimulation paradigms represent a promising step toward effective neuromodulation. Tailoring stimulation frequency, phase, and intensity based on each individual's intrinsic oscillatory dynamics and cortical architecture could enhance entrainment efficacy and explain some of the variability observed in stimulation outcomes (Bauer et al., 2018; Radecke et al., 2020). Personalized stimulation strategies may be particularly important in crossmodal tasks, where the timing of sensory integration is more variable and may depend on the specific neuroanatomical configuration of multimodal networks. Fourth, further work is needed to optimize crossmodal stimulation protocols, potentially by targeting not only parietal regions but also the fronto-temporo-parietal networks known to support audiovisual and sensorimotor prediction (Binder, 2015; Coull et al., 2016). Given that crossmodal prediction may involve multiple oscilla-

tory frequencies, including alpha and beta ranges depending on the modalities involved, future tACS and MEG studies should systematically investigate how different rhythms interact across sensory systems during temporally guided behavior. Fourth, DBS and LFP recordings could provide a direct, causal link to how distinct modulation of subcortical structures like the STN (i.e., by varying stimulation parameters) influences not only motor outcomes but also cognitive functions such as temporal anticipation. Finally, further research should move beyond tightly constrained laboratory tasks and toward more naturalistic paradigms that capture the temporal complexities of everyday life. Tasks involving conversational turn-taking, audiovisual speech comprehension, or dynamic sensorimotor interactions can reveal how oscillatory dynamics support temporal prediction in ecologically valid settings. Such designs will be critical for bridging the gap between basic research and real-world application, especially in clinical populations where deficits in timing and anticipation are widespread.

In conclusion, the findings of this thesis extend our understanding of how the brain generates and maintains temporal expectations. Overall, the three studies unifyingly revealed that low-frequency delta phase alignment is a core mechanism of temporal prediction, with complementary roles of alpha- and beta-power. These findings support a multiscale oscillatory model in which delta rhythms encode temporal expectations, beta oscillations contribute to dynamic updating, and alpha activity regulates internal attention and sensory gating. Importantly, the results show that this oscillatory architecture is not fixed but sensitive to sensory modality and task demands, and can be selectively modulated by non-invasive and invasive brain stimulation. This potentially opens translational pathways for using neuromodulation to treat disorders characterized by impaired timing and anticipatory control, such as Parkinson's disease, ADHD, or schizophrenia.

BIBLIOGRAPHY

BIBLIOGRAPHY

Adini, Y., Sagi, D., and Tsodyks, M. (1997). Excitatory-inhibitory network in the visual cortex: Psychophysical evidence. *Proceedings of the National Academy of Sciences of the United States of America*, 94(19):10426–10431.

Alexander, I., Cowey, A., and Walsh, V. (2005). The right parietal cortex and time perception: Back to critchley and the zeitraffer phenomenon. *Cogn Neuropsychol*, 22(3):306–15.

Allman, M. J. and Meck, W. H. (2012). Pathophysiological distortions in time perception and timed performance. *Brain*, 135:656–677.

Arabkheradmand, G., Zhou, G., Noto, T., Yang, Q., Schuele, S. U., Parvizi, J., Gottfried, J. A., Wu, S., Rosenow, J. M., Koubeissi, M. Z., Lane, G., and Zelano, C. (2020). Anticipation-induced delta phase reset improves human olfactory perception. *PLOS Biology*, 18:e3000724.

Arnal, L. H. (2012). Predicting "when" using the motor system's beta-band oscillations. *Frontiers in Human Neuroscience*, 6:29638.

Arnal, L. H., Doelling, K. B., and Poeppel, D. (2015). Delta-beta coupled oscillations underlie temporal prediction accuracy. *Cerebral Cortex*, 25(9):3077–85.

Arnal, L. H. and Giraud, A. L. (2012). Cortical oscillations and sensory predictions. *Trends in Cognitive Sciences*, 16:390–398.

Asamoah, B., Khatoun, A., and Mc Laughlin, M. (2019). tacs motor system effects can be caused by transcutaneous stimulation of peripheral nerves. *Nature Communications*, 10(1):266.

Barne, L. C., Claessens, P. M. E., Reyes, M. B., Caetano, M. S., and Cravo, A. M. (2017). Low-frequency cortical oscillations are modulated by temporal prediction and temporal error coding. *NeuroImage*, 146:40–46.

Barone, J. and Rossiter, H. E. (2021). Understanding the role of sensorimotor beta oscillations. *Frontiers in Systems Neuroscience*, 15:655886.

Bauer, A. R., Bleichner, M. G., Jaeger, M., Thorne, J. D., and Debener, S. (2018). Dy-

namic phase alignment of ongoing auditory cortex oscillations. *Neuroimage*, 167:396–407.

Bauer, A. R., Debener, S., and Nobre, A. C. (2020). Synchronisation of neural oscillations and cross-modal influences. *Trends Cogn Sci*, 24(6):481–495.

Beauchamp, M. S., Yasar, N. E., Frye, R. E., and Ro, T. (2008). Touch, sound and vision in human superior temporal sulcus. *NeuroImage*, 41:1011–1020.

Bendixen, A., Schröger, E., and Winkler, I. (2009). I heard that coming: Event-related potential evidence for stimulus-driven prediction in the auditory system. *Journal of Neuroscience*, 29:8447–8451.

Besle, J., Schevon, C. A., Mehta, A. D., Lakatos, P., Goodman, R. R., McKhann, G. M., Emerson, R. G., and Schroeder, C. E. (2011). Tuning of the human neocortex to the temporal dynamics of attended events. *The Journal of Neuroscience*, 31(9):3176–3185.

Beudel, M., Galama, S., Leenders, K. L., and Jong, B. M. D. (2008). Time estimation in parkinson's disease and degenerative cerebellar disease. *NeuroReport*, 19:1055–1059.

Beudel, M., Sadnicka, A., Edwards, M., and Jong, B. M. D. (2019). Linking pathological oscillations with altered temporal processing in parkinsons disease: Neurophysiological mechanisms and implications for neuromodulation. *Frontiers in Neurology*, 10:451052.

Biau, E. and Kotz, S. A. (2018). Lower beta: A central coordinator of temporal prediction in multimodal speech. *Frontiers in Human Neuroscience*, 12:394357.

Binder, M. (2015). Neural correlates of audiovisual temporal processing - comparison of temporal order and simultaneity judgments. *Neuroscience*, 300:432–447.

Brainard, D. H. (1997). The psychophysics toolbox. *Spatial Vision*, 10:433–436.

Breska, A. and Ivry, R. B. (2018). Double dissociation of single-interval and rhythmic temporal prediction in cerebellar degeneration and parkinson's disease. *Proceedings of the National Academy of Sciences of the United States of America*, 115:12283–12288.

Brittain, J. S., Sharott, A., and Brown, P. (2014). The highs and lows of beta activity in cortico-basal ganglia loops. *European Journal of Neuroscience*, 39:1951–1959.

Brown, P. (2003). Oscillatory nature of human basal ganglia activity: Relationship to

the pathophysiology of parkinson's disease. *Movement Disorders*, 18:357–363.

Bueti, D., Bahrami, B., Walsh, V., and Rees, G. (2010). Encoding of temporal probabilities in the human brain. *Journal of Neuroscience*, 30(12):4343–52.

Bueti, D. and Walsh, V. (2009). The parietal cortex and the representation of time, space, number and other magnitudes. *Philos Trans R Soc Lond B Biol Sci*, 364(1525):1831–40.

Buhusi, C. V. and Meck, W. H. (2005). What makes us tick? functional and neural mechanisms of interval timing. *Nature Reviews Neuroscience*, 6:755–765.

Buhusi, C. V. and Meck, W. H. (2009). Relative time sharing: new findings and an extension of the resource allocation model of temporal processing. *Philosophical Transactions of the Royal Society B: Biological Sciences*, 364:1875.

Burke, R., Daume, J., Schneider, T. R., and Engel, A. K. (2025a). Differential contributions of low-frequency phase and power in crossmodal temporal prediction: A meg study. *bioRxiv*.

Burke, R., Maÿe, A., Misselhorn, J., Fiene, M., Engelhardt, F. J., Schneider, T. R., and Engel, A. K. (2025b). The role of delta phase for temporal predictions investigated with bilateral parietal tacs. *Brain Stimulation*, 18:103–113. doi: 10.1016/j.brs.2024.12.1476.

Burke, R., Schoenfeld, M. J., Moll, C. K., Gulberti, A., Poetter-Nerger, M., and Engel, A. K. (2025c). Modulation of temporal prediction by stn-dbs in parkinson's disease: Links between behavior and cortical oscillations. *bioRxiv*.

Busch, N. A., Dubois, J., and VanRullen, R. (2009). The phase of ongoing eeg oscillations predicts visual perception. *Journal of Neuroscience*, 29(24):7869–76.

Calderone, D. J., Lakatos, P., Butler, P. D., and Castellanos, F. X. (2014). Entrainment of neural oscillations as a modifiable substrate of attention. *Trends Cogn Sci*, 18(6):300–9.

Capizzi, M., Sanabria, D., and Ángel Correa (2012). Dissociating controlled from automatic processing in temporal preparation. *Cognition*, 123:293–302.

Chang, A., Bosnyak, D. J., and Trainor, L. J. (2018). Beta oscillatory power modulation reflects the predictability of pitch change. *Cortex*, 106:248–260.

Cohen, M. X. (2014). *Analyzing neural time series data: Theory and practice*. The MIT Press.

Cotti, J., Rohenkohl, G., Stokes, M., Nobre, A. C., and Coull, J. T. (2011). Functionally dissociating temporal and motor components of response preparation in left intraparietal sulcus. *NeuroImage*, 54(2):1221–1230.

Coull, J. T., Cheng, R. K., and Meck, W. H. (2011). Neuroanatomical and neurochemical substrates of timing. *Neuropsychopharmacology*, 36:3–25.

Coull, J. T., Cotti, J., and Vidal, F. (2016). Differential roles for parietal and frontal cortices in fixed versus evolving temporal expectations: Dissociating prior from posterior temporal probabilities with fmri. *NeuroImage*, 141:40–51.

Coull, J. T. and Nobre, A. K. (1998). Where and when to pay attention: The neural systems for directing attention to spatial locations and to time intervals as revealed by both pet and fmri. *Journal of Neuroscience*, 18:7426–7435.

Coull, J. T., Vidal, F., Goulon, C., Nazarian, B., and Craig, C. (2008). Using time-to-contact information to assess potential collision modulates both visual and temporal prediction networks. *Frontiers in Human Neuroscience*, 2:10.

Cravo, A. M., Rohenkohl, G., Wyart, V., and Nobre, A. C. (2013). Temporal expectation enhances contrast sensitivity by phase entrainment of low-frequency oscillations in visual cortex. *Journal of Neuroscience*, 33(9):4002–10.

Daume, J., Wang, P., Maÿe, A., Zhang, D., and Engel, A. K. (2021). Non-rhythmic temporal prediction involves phase resets of low-frequency delta oscillations. *NeuroImage*, 224.

Davranche, K., Nazarian, B., Vidal, F., and Coull, J. T. (2011). Orienting attention in time activates left intraparietal sulcus for both perceptual and motor task goals. *Journal of Cognitive Neuroscience*, 23(11):3318–3330.

de Graaf, T. A. and Sack, A. T. (2014). Using brain stimulation to disentangle neural correlates of conscious vision. *Front Psychol*, 5:1019.

de Graaf, T. A. and Sack, A. T. (2018). When and how to interpret null results in nibs: A taxonomy based on prior expectations and experimental design. *Front Neurosci*, 12:915.

de la Rosa, M. D., Sanabria, D., Capizzi, M., and Correa, A. (2012). Temporal preparation driven by rhythms is resistant to working memory interference. *Frontiers in Psychology*, 3.

de Lange, F. P., Rahnev, D. A., Donner, T. H., and Lau, H. (2013). Prestimulus oscillatory activity over motor cortex reflects perceptual expectations. *Journal of Neuroscience*, 33:1400–1410.

Delorme, A. and Makeig, S. (2004). Eeglab: an open source toolbox for analysis of single-trial eeg dynamics including independent component analysis. *Journal of Neuroscience Methods*, 134:9–21.

Deuschl, G., Schade-Brittinger, C., Krack, P., Volkmann, J., Schäfer, H., Bötzel, K., Daniels, C., Deutschländer, A., Dillmann, U., Eisner, W., Gruber, D., Hamel, W., Herzog, J., Hilker, R., Klebe, S., Kloß, M., Koy, J., Krause, M., Kupsch, A., Lorenz, D., Lorenzl, S., Mehdorn, H. M., Moringlane, J. R., Oertel, W., Pinsker, M. O., Reichmann, H., Reuß, A., Schneider, G.-H., Schnitzler, A., Steude, U., Sturm, V., Timmermann, L., Tronnier, V., Trottenberg, T., Wojtecki, L., Wolf, E., Poewe, W., and Voges, J. (2006). A randomized trial of deep-brain stimulation for parkinson's disease. *The New England journal of medicine*, 355:896–908.

Diederich, A. and Colonius, H. (2012). *Modeling multisensory processes in saccadic responses: Time-window-of-integration model.* Frontiers in Neuroscience. CRC Press/Taylor Francis, Boca Raton (FL).

Doelling, K. B., Assaneo, M. F., Bevilacqua, D., Pesaran, B., and Poeppel, D. (2019). An oscillator model better predicts cortical entrainment to music. *Proceedings of the National Academy of Sciences of the United States of America*, 116:10113–10121.

Donner, T. H. and Siegel, M. (2011). A framework for local cortical oscillation patterns. *Trends Cogn Sci*, 15(5):191–9.

Droit-Volet, S. and Gil, S. (2009). The time-emotion paradox. *Philos. Trans. R Soc. B Biol. Sci.*, 364:1943–1953.

Engel, A. K. and Fries, P. (2010). Beta-band oscillations-signalling the status quo? *Current Opinion in Neurobiology*, 20:156–165.

Engel, A. K., Fries, P., and Singer, W. (2001). Dynamic predictions: Oscillations and synchrony in top-down processing. *Nat Rev Neurosci*, 2(10):704–16.

Fiebelkorn, I. C., Foxe, J. J., Butler, J. S., Mercier, M. R., Snyder, A. C., and Molholm, S. (2011). Ready, set, reset: Stimulus-locked periodicity in behavioral performance demonstrates the consequences of cross-sensory phase reset. *Journal of Neuroscience*, 31(27):9971–81.

Fiene, M., Radecke, J. O., Misselhorn, J., Sengelmann, M., Herrmann, C. S., Schneider, T. R., Schwab, B. C., and Engel, A. K. (2022). tacs phase-specifically biases brightness perception of flickering light. *Brain Stimul*, 15(1):244–253.

Fiene, M., Schwab, B. C., Misselhorn, J., Herrmann, C. S., Schneider, T. R., and Engel, A. K. (2020). Phase-specific manipulation of rhythmic brain activity by transcranial alternating current stimulation. *Brain Stimul*, 13(5):1254–1262.

Friston, K. (2010). The free-energy principle: a unified brain theory? *Nature Reviews Neuroscience 2010 11:2*, 11:127–138.

Fujioka, T., Ross, B., and Trainor, L. J. (2015). Beta-band oscillations represent auditory beat and its metrical hierarchy in perception and imagery. *Journal of Neuroscience*, 35:15187–15198.

Fujioka, T., Trainor, L. J., Large, E. W., and Ross, B. (2009). Beta and gamma rhythms in human auditory cortex during musical beat processing. *Annals of the New York Academy of Sciences*, 1169:89–92.

Fujioka, T., Trainor, L. J., Large, E. W., and Ross, B. (2012). Internalized timing of isochronous sounds is represented in neuromagnetic beta oscillations. *Journal of Neuroscience*, 32:1791–1802.

Giraud, A. L. and Poeppel, D. (2012). Cortical oscillations and speech processing: emerging computational principles and operations. *Nature Neuroscience*, 15(4):511–7.

Goetz, C. G., Tilley, B. C., Shaftman, S. R., Stebbins, G. T., Fahn, S., Martinez-Martin, P., Poewe, W., Sampaio, C., Stern, M. B., Dodel, R., Dubois, B., Holloway, R., Jankovic, J., Kulisevsky, J., Lang, A. E., Lees, A., Leurgans, S., LeWitt, P. A., Nyenhuis, D., Olanow, C. W., Rascol, O., Schrag, A., Teresi, J. A., van Hilten, J. J., LaPelle, N., Agarwal, P., Athar, S., Bordelan, Y., Bronte-Sewart, H. M., Camicioli, R., Chou, K., Cole, W., Dalvi, A., Delgado, H., Diamond, A., Dick, J. P., Duda, J., Elble, R. J., Evans, C., Evidente, V. G., Fernandez, H. H., Fox, S., Friedman, J. H., Fross, R. D., Gallagher, D., Goetz, C. G., Hall, D., Hermanowicz, N., Hinson, V., Horn, S., Hurtig, H., Kang, U. J., Kleiner-Fisman, G., Klepitskaya, O., Kompoliti, K., Lai,

E. C., Leehey, M. L., Leroi, I., Lyons, K. E., McClain, T., Metzer, S. W., Miyasaki, J., Morgan, J. C., Nance, M., Nemeth, J., Pahwa, R., Parashos, S. A., Schneider, J. S., Sethi, K., Shulman, L. M., Siderowf, A., .Silverdale, M., Simuni, T., Stacy, M., Stern, M. B., Stewart, R. M., Sullivan, K., Swope, D. M., Wadia, P. M., Walker, R. W., Walker, R., Weiner, W. J., Wiener, J., Wilkinson, J., Wojcieszek, J. M., Wolfrath, S., Wooten, F., Wu, A., Zesiewicz, T. A., and Zweig, R. M. (2008). Movement disorder society-sponsored revision of the unified parkinson's disease rating scale (mds-updrs): Scale presentation and clinimetric testing results. *Movement Disorders*, 23:2129–2170.

Gontier, E., Hasuo, E., Mitsudo, T., and Grondin, S. (2013). Eeg investigations of duration discrimination: The intermodal effect is induced by an attentional bias. *PLoS One*, 8(8):e74073.

Gouvêa, T. S., Monteiro, T., Motiwala, A., Soares, S., Machens, C., and Paton, J. J. (2015). Striatal dynamics explain duration judgments. *eLife*, 4:e11386.

Grant, D. A. and Berg, E. (1948). A behavioral analysis of degree of reinforcement and ease of shifting to new responses in a weigl-type card-sorting problem. *Journal of Experimental Psychology*, 38:404–411.

Gray, C. M. and Viana Di Prisco, G. (1997). Stimulus-dependent neuronal oscillations and local synchronization in striate cortex of the alert cat. *Journal of Neuroscience*, 17(9):3239–53.

Green, D. M. and Swets, J. A. (1966). *Signal detection theory and psychophysics.* John Wiley.

Gross, J., Kujala, J., Hämäläinen, M., Timmermann, L., Schnitzler, A., and Salmelin, R. (2001). Dynamic imaging of coherent sources: Studying neural interactions in the human brain. *Proceedings of the National Academy of Sciences of the United States of America*, 98:694–699.

Gulberti, A., Moll, C. K., Hamel, W., Buhmann, C., Koeppen, J. A., Boelmans, K., Zittel, S., Gerloff, C., Westphal, M., Schneider, T. R., and Engel, A. K. (2015). Predictive timing functions of cortical beta oscillations are impaired in parkinson's disease and influenced by l-dopa and deep brain stimulation of the subthalamic nucleus. *Neuroimage Clin*, 9:436–49.

Gulberti, A., Schneider, T., Galindo-Leon, E. E., Heise, M., Pino, A., Westphal, M., Hamel, W., Buhmann, C., Zittel, S., Gerloff, C., Pötter-Nerger, M., Engel, A. K.,

and Moll, C. (2024). Premotor cortical beta synchronization and the network neuromodulation of externally paced finger tapping in parkinson's disease. *Neurobiology of Disease*, 197.

Gülke, E., Alsalem, M., Kirsten, M., Vettorazzi, E., Choe, C. U., Hidding, U., Zittel-Dirks, S., Buhmann, C., Schaper, M., Gulberti, A., Moll, C., Hamel, W., Koeppen, J., Gerloff, C., and Pötter-Nerger, M. (2022). Comparison of montreal cognitive assessment and mattis dementia rating scale in the preoperative evaluation of subthalamic stimulation in parkinson's disease. *PLOS ONE*, 17:e0265314.

Haegens, S. and Golumbic, E. Z. (2018). Rhythmic facilitation of sensory processing: A critical review. *Neuroscience & Biobehavioral Reviews*, 86:150–165.

Hemptinne, C. D., Swann, N. C., Ostrem, J. L., Ryapolova-Webb, E. S., Luciano, M. S., Galifianakis, N. B., and Starr, P. A. (2015). Therapeutic deep brain stimulation reduces cortical phase-amplitude coupling in parkinson's disease. *Nature Neuroscience*, 18:779–786.

Henry, M. J., Herrmann, B., and Obleser, J. (2014). Entrained neural oscillations in multiple frequency bands comodulate behavior. *Proceedings of the National Academy of Sciences of the United States of America*, 111:14935–14940.

Henry, M. J. and Obleser, J. (2012). Frequency modulation entrains slow neural oscillations and optimizes human listening behavior. *Proceedings of the National Academy of Sciences*, 109(49):20095–100.

Herbst, S. K. and Obleser, J. (2019). Implicit temporal predictability enhances pitch discrimination sensitivity and biases the phase of delta oscillations in auditory cortex. *NeuroImage*, 203.

Herbst, S. K., Stefanics, G., and Obleser, J. (2022). Endogenous modulation of delta phase by expectation - a replication of stefanics et al., 2010. *Cortex*, 149:226–245.

Herz, D. M., Little, S., Pedrosa, D. J., Tinkhauser, G., Cheeran, B., Foltynie, T., Bogacz, R., and Brown, P. (2018). Mechanisms underlying decision-making as revealed by deep brain stimulation in patients with parkinson's disease. *Current biology*, 28:1169–1178.e6.

Hoehn, M. and Yahr, M. D. (1967). Parkinsonism: Onset, progression, and mortality. *Neurology*, 17:427–442.

Huang, Y., Liu, A. A., Lafon, B., Friedman, D., Dayan, M., Wang, X., Bikson, M., Doyle, W. K., Devinsky, O., and Parra, L. C. (2018). Correction: Measurements and models of electric fields in the in vivo human brain during transcranial electric stimulation. *eLife*, 7.

Ivry, R. B. and Keele, S. W. (1989). Timing functions of the cerebellum. *Journal of Cognitive Neuroscience*, 1:136–152.

Ivry, R. B. and Schlerf, J. E. (2008). Dedicated and intrinsic models of time perception. *Trends in Cognitive Sciences*, 12:273–280.

Ivry, R. B. and Spencer, R. M. (2004). The neural representation of time. *Current Opinion in Neurobiology*, 14:225–232.

Jahanshahi, M., Ardouin, C. M., Brown, R. G., Rothwell, J. C., Obeso, J., Albanese, A., Rodriguez-Oroz, M. C., Moro, E., Benabid, A. L., Pollak, P., and Limousin-Dowsey, P. (2000). The impact of deep brain stimulation on executive function in parkinson's disease. *Brain*, 123 (Pt 6):1142–1154.

Jaramillo-Jimenez, A., Suarez-Revelo, J. X., Ochoa-Gomez, J. F., Arroyave, J. A. C., Bocanegra, Y., Lopera, F., Buriticá, O., Pineda-Salazar, D. A., Gómez, L. M., Quintero, C. A. T., Borda, M. G., Bonanni, L., Ffytche, D. H., Brønnick, K., and Aarsland, D. (2021). Resting-state eeg alpha/theta ratio related to neuropsychological test performance in parkinson's disease. *Clinical Neurophysiology*, 132:756–764.

Javadi, A. H., Brunec, I. K., Walsh, V., Penny, W. D., and Spiers, H. J. (2014). Transcranial electrical brain stimulation modulates neuronal tuning curves in perception of numerosity and duration. *NeuroImage*, 102:451–457.

Jensen, O. and Mazaheri, A. (2010). Shaping functional architecture by oscillatory alpha activity: Gating by inhibition. *Frontiers in Human Neuroscience*, 4:186.

Johnson, L., Alekseichuk, I., Krieg, J., Doyle, A., Yu, Y., Vitek, J., Johnson, M., and Opitz, A. (2020). Dose-dependent effects of transcranial alternating current stimulation on spike timing in awake nonhuman primates. *Science Advances*, 6(36).

Jones, C. R., Malone, T., Dirnberger, G., Edwards, M., and Jahanshahi, M. (2008). Basal ganglia, dopamine and temporal processing: Performance on three timing tasks on and off medication in parkinson's disease. *Brain and Cognition*, 68:30–41.

Jones, M. R. (1976). Time, our lost dimension: Toward a new theory of perception, attention, and memory. *Psychological Review*, 83:323–355.

Jones, M. R. and Boltz, M. (1989). Dynamic attending and responses to time. *Psychological Review*, 96:459–491.

Jones, M. R., Johnston, H. M., and Puente, J. (2006). Effects of auditory pattern structure on anticipatory and reactive attending. *Cognitive Psychology*, 53:59–96.

Jost, S. T., Kaldenbach, M., Antonini, A., Martinez-Martin, P., Timmermann, L., Odin, P., Katzenschlager, R., Borgohain, R., Fasano, A., Stocchi, F., Hattori, N., Kukkle, P. L., Rodríguez-Violante, M., Falup-Pecurariu, C., Schade, S., Petry-Schmelzer, J., Metta, V., Weintraub, D., Deuschl, G., Espay, A. J., Tan, E. K., Bhidayasiri, R., Fung, V. S., Cardoso, F., Trenkwalder, C., Jenner, P., Chaudhuri, K., and Dafsari, H. S. (2023). Levodopa dose equivalency in parkinson's disease: Updated systematic review and proposals. *Movement Disorders*, 38:1236–1252.

Kasten, F. H., Duecker, K., Maack, M. C., Meiser, A., and Herrmann, C. S. (2019). Integrating electric field modeling and neuroimaging to explain inter-individual variability of tacs effects. *Nature Communications*, 10(1):5427.

Kayser, C. and Logothetis, N. K. (2007). Do early sensory cortices integrate cross-modal information? *Brain Structure and Function*, 212:121–132.

Kayser, C., Logothetis, N. K., and Panzeri, S. (2010). Millisecond encoding precision of auditory cortex neurons. *Proceedings of the National Academy of Sciences*, 107(39):16976–81.

Keil, J. and Senkowski, D. (2018). Neural oscillations orchestrate multisensory processing. *The Neuroscientist*, 24(6):609–626.

Kilavik, B., Zaepffel, M., Brovelli, A., MacKay, W. A., and Riehle, A. (2013). The ups and downs of beta oscillations in sensorimotor cortex. *Experimental Neurology*, 245:15–26.

Klatt, L. I., Getzmann, S., and Schneider, D. (2022). Attentional modulations of alpha power are sensitive to the task-relevance of auditory spatial information. *Cortex*, 153:1–20.

Klimesch, W., Sauseng, P., and Hanslmayr, S. (2007). Eeg alpha oscillations: The

inhibition-timing hypothesis. *Brain Research Reviews*, 53:63–88.

Koch, G., Oliveri, M., Brusa, L., Stanzione, P., Torriero, S., and Caltagirone, C. (2004). High-frequency rtms improves time perception in parkinson disease. *Neurology*, 63:2405–2406.

Krekelberg, B. (2022). Bayes factor. https://github.com/klabhub/bayesFactor.git.

Kösem, A., Bosker, H. R., Takashima, A., Meyer, A., Jensen, O., and Hagoort, P. (2018). Neural entrainment determines the words we hear. *Current Biology*, 28:2867–2875.e3.

Kösem, A., Gramfort, A., and Wassenhove, V. V. (2014). Encoding of event timing in the phase of neural oscillations. *NeuroImage*, 92:274–284.

Kösem, A. and van Wassenhove, V. (2012). Temporal structure in audiovisual sensory selection. *PLoS ONE*, 7.

Kühn, A., Tsui, A., Aziz, T., Ray, N., Brücke, C., Kupsch, A., Schneider, G. H., and Brown, P. (2009). Pathological synchronisation in the subthalamic nucleus of patients with parkinson's disease relates to both bradykinesia and rigidity. *Experimental Neurology*, 215:380–387.

Kühn, A. A., Kempf, F., Brücke, C., Doyle, L. G., Martinez-Torres, I., Pogosyan, A., Trottenberg, T., Kupsch, A., Schneider, G. H., Hariz, M. I., Vandenberghe, W., Nuttin, B., and Brown, P. (2008). High-frequency stimulation of the subthalamic nucleus suppresses oscillatory beta activity in patients with parkinson's disease in parallel with improvement in motor performance. *Journal of Neuroscience*, 28:6165–6173.

Lakatos, P., Chen, C. M., O'Connell, M. N., Mills, A., and Schroeder, C. E. (2007). Neuronal oscillations and multisensory interaction in primary auditory cortex. *Neuron*, 53:279–292.

Lakatos, P., Karmos, G., Mehta, A. D., Ulbert, I., and Schroeder, C. E. (2008). Entrainment of neuronal oscillations as a mechanism of attentional selection. *Science*, 320(5872):110–3.

Lakatos, P., O'Connell, M. N., Barczak, A., Mills, A., Javitt, D. C., and Schroeder, C. E. (2009). The leading sense: Supramodal control of neurophysiological context by attention. *Neuron*, 64(3):419–430.

Lakatos, P., Schroeder, C. E., Leitman, D. I., and Javitt, D. C. (2013). Predictive suppression of cortical excitability and its deficit in schizophrenia. *Journal of Neuroscience*, 33:11692–11702.

Lakatos, P., Shah, A. S., Knuth, K. H., Ulbert, I., Karmos, G., and Schroeder, C. E. (2005). An oscillatory hierarchy controlling neuronal excitability and stimulus processing in the auditory cortex. *Journal of Neurophysiology*, 94(3):1904–11.

Lalo, E., Thobois, S., Sharott, A., Polo, G., Mertens, P., Pogosyan, A., and Brown, P. (2008). Patterns of bidirectional communication between cortex and basal ganglia during movement in patients with parkinson's disease. *Journal of Neuroscience*, 28:3008–3016.

Lewis, A. G., Schoffelen, J. M., Schriefers, H., and Bastlaansen, M. (2016). A predictive coding perspective on beta oscillations during sentence-level language comprehension. *Frontiers in Human Neuroscience*, 10:175739.

Lewis, P. A. and Miall, R. C. (2006). A right hemispheric prefrontal system for cognitive time measurement. *Behavioural Processes*, 71(2-3):226–34.

Little, S. and Brown, P. (2014). The functional role of beta oscillations in parkinson's disease. *Parkinsonism & Related Disorders*, 20.

Litvak, V., Jha, A., Eusebio, A., Oostenveld, R., Foltynie, T., Limousin, P., Zrinzo, L., Hariz, M. I., Friston, K., and Brown, P. (2011). Resting oscillatory cortico-subthalamic connectivity in patients with parkinson's disease. *Brain*, 134:359–374.

Lorenz, R., Simmons, L. E., Monti, R. P., Arthur, J. L., Limal, S., Laakso, I., Leech, R., and Violante, I. R. (2019). Efficiently searching through large tacs parameter spaces using closed-loop bayesian optimization. *Brain Stimulation*, 12(6):1484–1489.

Maris, E. and Oostenveld, R. (2007). Nonparametric statistical testing of eeg- and meg-data. *Journal of Neuroscience Methods*, 164:177–190.

Matell, M. S. and Meck, W. H. (2000). Neuropsychological mechanisms of interval timing behavior. *BioEssays*, 22:94–103.

Maye, A., Wang, P., Daume, J., Hu, X., and Engel, A. K. (2019). An oscillator ensemble model of sequence learning. *Frontiers in Integrative Neuroscience*, 13:43.

Meck, W. H. (1996). Neuropharmacology of timing and time perception. *Cognitive Brain Research*, 3:227–242.

Merchant, H., Harrington, D. L., and Meck, W. H. (2013). Neural basis of the perception and estimation of time. *Annual Review of Neuroscience*, 36:313–336.

Merchant, H., Luciana, M., Hooper, C., Majestic, S., and Tuite, P. (2008). Interval timing and parkinson's disease: heterogeneity in temporal performance. *Experimental Brain Research*, 184:233–248.

Miall, C. (1989). The storage of time intervals using oscillating neurons. *Neural Computation*, 1(3):359–371.

Mioni, G., Shelp, A., Stanfield-Wiswell, C. T., Gladhill, K. A., Bader, F., and Wiener, M. (2020). Modulation of individual alpha frequency with tacs shifts time perception. *Cerebral Cortex Communications*, 1(1):tgaa064.

Morillon, B. and Baillet, S. (2017). Motor origin of temporal predictions in auditory attention. *Proceedings of the National Academy of Sciences of the United States of America*, 114:E8913–E8921.

Morillon, B., Schroeder, C. E., and Wyart, V. (2014). Motor contributions to the temporal precision of auditory attention. *Nature Communications*, 5.

Morita, A., Kamei, S., and Mizutani, T. (2011). Relationship between slowing of the eeg and cognitive impairment in parkinson disease. *Journal of Clinical Neurophysiology*, 28:384–387.

Nath, A. R. and Beauchamp, M. S. (2011). Dynamic changes in superior temporal sulcus connectivity during perception of noisy audiovisual speech. *Journal of Neuroscience*, 31:1704–1714.

Ng, B. S., Logothetis, N. K., and Kayser, C. (2013). Eeg phase patterns reflect the selectivity of neural firing. *Cerebral Cortex*, 23(2):389–98.

Nobre, A. C. and Ede, F. V. (2018). Anticipated moments: temporal structure in attention. *Nature Reviews Neuroscience*, 19:34–48.

Noesselt, T., Bergmann, D., Heinze, H. J., Münte, T., and Spence, C. (2012). Coding of multisensory temporal patterns in human superior temporal sulcus. *Frontiers in*

Integrative Neuroscience, 6:30900.

Nolte, G. (2003). The magnetic lead field theorem in the quasi-static approximation and its use for magnetoencephalography forward calculation in realistic volume conductors. *Physics in Medicine & Biology*, 48:3637.

Nolte, G. and Dassios, G. (2005). Analytic expansion of the eeg lead field for realistic volume conductors. *Physics in Medicine & Biology*, 50(16):3807–23.

Nutt, J. G. (2001). Motor fluctuations and dyskinesia in parkinson's disease. *Parkinsonism & Related Disorders*, 8(2):101–108.

Obleser, J. and Kayser, C. (2019). Neural entrainment and attentional selection in the listening brain. *Trends in Cognitive Sciences*, 23(11):913–926.

Oever, S. T., Atteveldt, N. V., and Sack, A. T. (2015). Increased stimulus expectancy triggers low-frequency phase reset during restricted vigilance. *Journal of Cognitive Neuroscience*, 27:1811–1822.

Oldfield, R. C. (1971). The assessment and analysis of handedness: the edinburgh inventory. *Neuropsychologia*, 9:97–113.

Oostenveld, R., Fries, P., Maris, E., and Schoffelen, J. M. (2011). Fieldtrip: Open source software for advanced analysis of meg, eeg, and invasive electrophysiological data. *Computational Intelligence and Neuroscience*, 156869:9.

Orekhova, E. V., Butorina, A. V., Sysoeva, O. V., Prokofyev, A. O., Nikolaeva, A. Y., and Stroganova, T. A. (2015). Frequency of gamma oscillations in humans is modulated by velocity of visual motion. *Journal of Neurophysiology*, 114(1):244–255.

Oswal, A., Beudel, M., Zrinzo, L., Limousin, P., Hariz, M., Foltynie, T., Litvak, V., and Brown, P. (2016). Deep brain stimulation modulates synchrony within spatially and spectrally distinct resting state networks in parkinson's disease. *Brain*, 139:1482.

Oswal, A., Brown, P., and Litvak, V. (2013). Synchronized neural oscillations and the pathophysiology of parkinson's disease. *Current Opinion in Neurology,*, 26:662–670.

Palmer, C. E., Auksztulewicz, R., Ondobaka, S., and Kilner, J. M. (2019). Sensorimotor beta power reflects the precision-weighting afforded to sensory prediction errors. *NeuroImage*, 200:59–71.

Paulo, D. L., Qian, H., Subramanian, D., Johnson, G. W., Zhao, Z., Hett, K., Kang, H., Kao, C. C., Roy, N., Summers, J. E., Claassen, D. O., Dhima, K., and Bick, S. K. (2023). Corticostriatal beta oscillation changes associated with cognitive function in parkinson's disease. *Brain*, 146:3662–3675.

Perbal, S., Deweer, B., Pillon, B., Vidailhet, M., Dubois, B., and Pouthas, V. (2005). Effects of internal clock and memory disorders on duration reproductions and duration productions in patients with parkinson's disease. *Brain and Cognition*, 58:35–48.

Pfurtscheller, G., Graimann, B., Huggins, J. E., Levine, S. P., and Schuh, L. A. (2003). Spatiotemporal patterns of beta desynchronization and gamma synchronization in corticographic data during self-paced movement. *Clinical Neurophysiology*, 114:1226–1236.

Pillon, B., Ardouin, C., Damier, P., Krack, P., Houeto, J. L., Klinger, H., Bonnet, A. M., Pollak, P., Benabid, A. L., and Agid, Y. (2000). Neuropsychological changes between "off" and "on" stn or gpi stimulation in parkinson's disease. *Neurology*, 55:411–418.

Polverino, P., Ajčević, M., Catalan, M., Mazzon, G., Bertolotti, C., and Manganotti, P. (2022). Brain oscillatory patterns in mild cognitive impairment due to alzheimer's and parkinson's disease: An exploratory high-density eeg study. *Clinical Neurophysiology*, 138:1–8.

Radecke, J. O., Khan, A., Engel, A. K., Wolters, C. H., and Schneider, T. R. (2020). Individual targeting increases control over inter-individual variability in simulated transcranial electric fields. *IEEE Access*, 8:182610–182624.

Rammsayer, T. and Classen, W. (1997). Impaired temporal discrimination in parkinson's disease: Temporal processing of brief durations as an indicator of degeneration of dopaminergic neurons in the basal ganglia. *International Journal of Neuroscience*, 91:45–55.

Rao, S. M., Mayer, A. R., and Harrington, D. L. (2001). The evolution of brain activation during temporal processing. *Nature Neuroscience*, 4(3):317–23.

Ray, N. J., Jenkinson, N., Wang, S., Holland, P., Brittain, J. S., Joint, C., Stein, J. F., and Aziz, T. (2008). Local field potential beta activity in the subthalamic nucleus of patients with parkinson's disease is associated with improvements in bradykinesia after dopamine and deep brain stimulation. *Experimental Neurology*, 213:108–113.

Rea, R. C., Berlot, R., Martin, S. L., Craig, C. E., Holmes, P. S., Wright, D. J., Bon, J.,

Pirtošek, Z., and Ray, N. J. (2021). Quantitative eeg and cholinergic basal forebrain atrophy in parkinson's disease and mild cognitive impairment. *Neurobiology of Aging*, 106:37–44.

Reitan, R. (1956). Trail making test. manual for administration, scoring, and interpretation. Technical report, Indiana University Press.

Riecke, L., Formisano, E., Sorger, B., Başkent, D., and Gaudrain, E. (2018). Neural entrainment to speech modulates speech intelligibility. *Current Biology*, 28:161–169.e5.

Righetti, L., Buchli, J., and Ijspeert, A. J. (2006). Dynamic hebbian learning in adaptive frequency oscillators. *Physica D: Nonlinear Phenomena*, 216(2):269–281.

Rohenkohl, G. and Nobre, A. C. (2011). Alpha oscillations related to anticipatory attention follow temporal expectations. *Journal of Neuroscience*, 31:14076–14084.

Romei, V., Gross, J., and Thut, G. (2012). Sounds reset rhythms of visual cortex and corresponding human visual perception. *Current Biology*, 22(9):807–13.

Ronconi, L., Melcher, D., Junghöfer, M., Wolters, C. H., and Busch, N. A. (2022). Testing the effect of tacs over parietal cortex in modulating endogenous alpha rhythm and temporal integration windows in visual perception. *European Journal of Neuroscience*, 55:3438–3450.

Ronconi, L., Vitale, A., Federici, A., Mazzoni, N., Battaglini, L., Molteni, M., and Casartelli, L. (2023). Neural dynamics driving audio-visual integration in autism. *Cerebral Cortex*, 33:543–556.

Roth, M. J., Synofzik, M., and Lindner, A. (2013). The cerebellum optimizes perceptual predictions about external sensory events. *Current Biology*, 23(10):930–935.

Sack, A. T. (2006). Transcranial magnetic stimulation, causal structure-function mapping and networks of functional relevance. *Current Opinion in Neurobiology*, 16(5):593–9.

Samaha, J., Bauer, P., Cimaroli, S., and Postle, B. R. (2015). Top-down control of the phase of alpha-band oscillations as a mechanism for temporal prediction. *Proceedings of the National Academy of Sciences of the United States of America*, 112:8439–8444.

Santos-García, D., de Deus Fonticoba, T., Bartolomé, C. C., Painceiras, M. J. F., Castro, E. S., Canfield, H., Miró, C. M., Jesús, S., Aguilar, M., Pastor, P., Planellas, L.,

Cosgaya, M., Caldentey, J. G., Caballol, N., Legarda, I., Hernández-Vara, J., Cabo, I., Manzanares, L. L., Aramburu, I. G., Rivera, M. A. , Mayordomo, V. G., Nogueira, V., Puente, V., García-Soto, J. D., Borrué, C., Vila, B. S., Sauco, M. , Vela, L., Escalante, S., Cubo, E., Padilla, F. C., Castrillo, J. C. M., Alonso, P. S., Losada, M. G. A., Ariztegui, N. L., Gastón, I., Kulisevsky, J., Estrada, M. B., Seijo, M., Martínez, J. R., Valero, C., Kurtis, M., de Fábregues, O., Ardura, J. G., Redondo, R. A., Ordás, C., Díaz, L. M. L., McAfee, D., Martinez-Martin, P., Mir, P., and Group, C. S. (2022). Motor fluctuations development is associated with non-motor symptoms burden progression in parkinson's disease patients: A 2-year follow-up study. *Diagnostics*, 12(5).

Sauseng, P., Klimesch, W., Schabus, M., and Doppelmayr, M. (2005). Fronto-parietal eeg coherence in theta and upper alpha reflect central executive functions of working memory. *International Journal of Psychophysiology*, 57:97–103.

Schroeder, C. E. and Lakatos, P. (2009). Low-frequency neuronal oscillations as instruments of sensory selection. *Trends in Neurosciences*, 32:9–18.

Schroeder, C. E., Lakatos, P., Kajikawa, Y., Partan, S., and Puce, A. (2008). Neuronal oscillations and visual amplification of speech. *Trends in Cognitive Sciences*, 12:106–113.

Schroeder, C. E., Wilson, D. A., Radman, T., Scharfman, H., and Lakatos, P. (2010). Dynamics of active sensing and perceptual selection. *Current Opinion in Neurobiology*, 20:172–176.

Senkowski, D. and Engel, A. K. (2024). Multi-timescale neural dynamics for multisensory integration. *Nature Reviews Neuroscience 2024*, 25:625–642.

Sharott, A., Magill, P. J., Harnack, D., Kupsch, A., Meissner, W., and Brown, P. (2005). Dopamine depletion increases the power and coherence of beta-oscillations in the cerebral cortex and subthalamic nucleus of the awake rat. *European Journal of Neuroscience*, 21:1413–1422.

Singhal, I. (2021). No sense in saying 'there is no sense organ for time'. *Timing & Time Perception*, 9:229–240.

Smith, J. G., Harper, D. N., Gittings, D., and Abernethy, D. (2007). The effect of parkinson's disease on time estimation as a function of stimulus duration range and modality. *Brain and Cognition*, 64:130–143.

Stefanics, G., Hangya, B., Hernádi, I., Winkler, I., Lakatos, P., and Ulbert, I. (2010). Phase entrainment of human delta oscillations can mediate the effects of expectation on reaction speed. *Journal of Neuroscience*, 30:13578–13585.

Stolk, A., Todorovic, A., Schoffelen, J. M., and Oostenveld, R. (2013). Online and offline tools for head movement compensation in meg. *NeuroImage*, 68:39–48.

Storch, A., Schneider, C. B., Wolz, M., Stürwald, Y., Nebe, A., Odin, P., Mahler, A., Fuchs, G., Jost, W. H., Chaudhuri, K. R., Koch, R., Reichmann, H., and Ebersbach, G. (2013). Nonmotor fluctuations in parkinson disease. *Neurology*, 80(9):800–809.

Summerfield, C. and Egner, T. (2009). Expectation (and attention) in visual cognition. *Trends in Cognitive Sciences*, 13:403–409. doi: 10.1016/j.tics.2009.06.003.

te Woerd, E. S., Oostenveld, R., de Lange, F. P., and Praamstra, P. (2014). A shift from prospective to reactive modulation of beta-band oscillations in parkinson's disease. *NeuroImage*, 100:507–519.

ten Oever, S., Schroeder, C. E., Poeppel, D., van Atteveldt, N., and Zion-Golumbic, E. (2014). Rhythmicity and cross-modal temporal cues facilitate detection. *Neuropsychologia*, 63:43–50.

Terranova, S., Botta, A., Putzolu, M., Bonassi, G., Cosentino, C., Mezzarobba, S., Ravizzotti, E., Pelosin, E., and Avanzino, L. (2023). Cerebellar direct current stimulation reveals the causal role of the cerebellum in temporal prediction. *Cerebellum*, 23:1386–1398.

Tinkhauser, G., Pogosyan, A., Little, S., Beudel, M., Herz, D. M., Tan, H., and Brown, P. (2017). The modulatory effect of adaptive deep brain stimulation on beta bursts in parkinson's disease. *Brain*, 140:1053–1067.

Todorovic, A., Schoffelen, J. M., Ede, F. V., Maris, E., and Lange, F. P. D. (2015). Temporal expectation and attention jointly modulate auditory oscillatory activity in the beta band. *PLoS ONE*, 10.

Tomassini, A., Pollak, T. A., Edwards, M. J., and Bestmann, S. (2019). Learning from the past and expecting the future in parkinsonism: Dopaminergic influence on predictions about the timing of future events. *Neuropsychologia*, 127:9–18.

Tort, A. B., Komorowski, R., Eichenbaum, H., and Kopell, N. (2010). Measuring phase-

amplitude coupling between neuronal oscillations of different frequencies. *Journal of Neurophysiology*, 104(2):1195–210.

van Ede, F., de Lange, F., Jensen, O., and Maris, E. (2011). Orienting attention to an upcoming tactile event involves a spatially and temporally specific modulation of sensorimotor alpha- and beta-band oscillations. *Journal of Neuroscience*, 31:2016–2024.

van Wassenhove, V. (2016). Temporal cognition and neural oscillations. *Current Opinion in Behavioral Sciences*, 8:124–130.

Weinberger, M., Mahant, N., Hutchison, W. D., Lozano, A. M., Moro, E., Hodaie, M., Lang, A. E., and Dostrovsky, J. O. (2006). Beta oscillatory activity in the subthalamic nucleus and its relation to dopaminergic response in parkinson's disease. *Journal of Neurophysiology*, 96:3248–3256.

Whitmer, D., de Solages, C., Hill, B., Yu, H., Henderson, J. M., and Bronte-Stewart, H. (2012). High frequency deep brain stimulation attenuates subthalamic and cortical rhythms in parkinson's disease. *Frontiers in Human Neuroscience*, 6:21531.

Wilsch, A., Henry, M. J., Herrmann, B., Maess, B., and Obleser, J. (2015). Slow-delta phase concentration marks improved temporal expectations based on the passage of time. *Psychophysiology*, 52:910–918.

Witt, K., Pulkowski, U., Herzog, J., Lorenz, D., Hamel, W., Deuschl, G., and Krack, P. (2004). Deep brain stimulation of the subthalamic nucleus improves cognitive flexibility but impairs response inhibition in parkinson disease. *Archives of Neurology*, 61:697–700.

Wojtecki, L., Elben, S., Timmermann, L., Reck, C., Maarouf, M., Jörgens, S., Ploner, M., Südmeyer, M., Groiss, S. J., Sturm, V., Niedeggen, M., and Schnitzler, A. (2011). Modulation of human time processing by subthalamic deep brain stimulation. *PLOS ONE*, 6:e24589.

Xu, X. M., Olivas, N. D., Ikrar, T., Peng, T., Holmes, T. C., Nie, Q., and Shi, Y. L. (2016). Primary visual cortex shows laminar-specific and balanced circuit organization of excitatory and inhibitory synaptic connectivity. *Journal of Physiology-London*, 594(7):1891–1910.

Yamanaka, T., Ishii, F., Umemura, A., Miyata, M., Horiba, M., Oka, Y., Yamada, K., Okita, K., Matsukawa, N., and Ojika, K. (2012). Temporary deterioration of

executive function after subthalamic deep brain stimulation in parkinson's disease. *Clinical Neurology and Neurosurgery*, 114:347–351.

Zhao, Y., Cai, J., Song, J., Shi, H., Kong, W., Li, X., Wei, W., and Xue, X. (2025). Peak alpha frequency and alpha power spectral density as vulnerability markers of cognitive impairment in parkinson's disease: an exploratory eeg study. *Front Neurosci*, 19:1575815.

Zoefel, B., Davis, M. H., Valente, G., and Riecke, L. (2019). How to test for phasic modulation of neural and behavioural responses. *NeuroImage*, 202:116175.

Zoefel, B., ten Oever, S., and Sack, A. T. (2018). The involvement of endogenous neural oscillations in the processing of rhythmic input: More than a regular repetition of evoked neural responses. *Frontiers in Neuroscience*, 12.

APPENDIX

APPENDIX A

ABSTRACTS

A.1. English abstract

The human ability to estimate time plays a central role in cognitive and motor processes. However, the underlying neural mechanisms and their modifiability through external influences are not yet fully understood. This dissertation investigated temporal prediction from three different methodological perspectives: (1) using magnetoencephalography (MEG) to examine oscillatory mechanisms specific to crossmodal temporal prediction, (2) through non-invasive brain stimulation to modulate temporal prediction, and (3) via invasive brain stimulation to directly influence neural networks. In the first study, previously established neural correlates of time estimation were examined using MEG to ensure the reproducibility of earlier findings and to further characterize the underlying oscillatory mechanisms of crossmodal time estimation. The results showed that delta-band phase alignment increased during temporal prediction and correlated with behavioral performance. Building on these insights, the second study investigated whether non-invasive brain stimulation, such as transcranial alternating current stimulation (tACS), can influence subjective temporal prediction. This approach showed that behavioral performance was modulated in a phase-dependent, sinusoidal manner, supporting the functional role of low-frequency delta phase in temporal prediction. However, the tACS-induced effects did not extend to a crossmodal task, suggesting increased cognitive demands and differ-

ent network requirements for multimodal integration. Finally, the third study employed invasive brain stimulation in patients with PD to determine whether a direct modulation of the basal ganglia induces even more targeted effects on temporal prediction. We found that subthalamic DBS enhances temporal prediction performance in PD patients by modulating oscillatory mechanisms, particularly through beta power suppression. Together, these studies underscore the importance of oscillatory phase dynamics, particularly delta phase alignment, in temporal prediction. They also demonstrate that these mechanisms can be modulated through external stimulation, offering both theoretical advances and translational potential. The integration of MEG, tACS, and DBS within a single research program provides a comprehensive framework for probing the neural, oscillatory structure of non-rhythmic unimodal and crossmodal temporal prediction.

A.2. Deutsche Zusammenfassung

Die menschliche Fähigkeit zur Zeitschätzung spielt eine zentrale Rolle in kognitiven und motorischen Prozessen. Dennoch sind die zugrunde liegenden neuronalen Mechanismen und ihre Modulierbarkeit durch externe Einflüsse noch nicht vollständig erforscht. In dieser Dissertation wurde die zeitliche Wahrnehmung aus drei unterschiedlichen methodischen Perspektiven untersucht: (1) mittels Magnetoenzephalographie (MEG), um oszillatorische Mechanismen von crossmodalen zeitlichen Vorhersageprozessen zu untersuchen, (2) durch nicht-invasive Hirnstimulation, zur gezielten Modulation der Zeitschätzung und (3) durch invasive Hirnstimulation bei Patient:innen mit Parkinson zur direkten Beeinflussung neuronaler Netzwerke. In der ersten Studie wurden bereits etablierte neuronale Korrelate der Zeitschätzung mit MEG überprüft, um die Reproduzierbarkeit früherer Ergebnisse zu gewährleisten und die zugrunde liegenden oszillatorischen Mechanismen der crossmodalen Zeitschätzung weiter zu charakterisieren. Die Ergebnisse bestätigten, dass Delta-Band-Phasensynchronisation während der Zeitschätzung zunimmt und mit der Verhaltensleistung korreliert. Aufbauend auf diesen Erkenntnissen wurde in der zweiten Studie untersucht, ob nicht-invasive Hirnstimulation, wie transkranielle Wechselstromstimulation (tACS), die subjektive Zeitschätzung beeinflussen kann. Dieser Ansatz zeigte, dass die Verhaltensleistung in einer phasenabhängigen, sinusförmigen Weise moduliert wurde, was die funktionelle Rolle der niederfrequenten Delta-Phase bei der zeitlichen Vorhersage unterstützt. Die tACS-induzierten Effekte ließen sich jedoch nicht auf die crossmodale Aufgabe erweitern, was auf erhöhte kognitive Anforderungen und unterschiedliche Netzwerkanforderungen für die multimodale Integration hindeuten könnte. Schließlich wurde in der dritten Studie mit invasiver Hirnstimulation bei Patient:innen mit Parkinson getestet, ob eine direkte Beeinflussung der Basalganglien noch gezieltere Modulationseffekte auf die Zeitschätzung hervorruft. Wir fanden heraus, dass subthalamische Tiefenhirnstimulation die zeitliche Vorhersageleistung bei

Patient:innen mit Parkinson-Krankheit durch die Modulation oszillatorischer Mechanismen, insbesondere durch Unterdrückung der Beta-Power, verbessert. Insgesamt unterstreichen diese Studien die Bedeutung der oszillatorischen Phasendynamik, insbesondere der Delta- Phasensynchronisation, für Zeitschätzung. Sie zeigen auch, dass diese neuronalen Mechanismen durch externe Stimulation moduliert werden können, was sowohl theoretische Fortschritte als auch translationales Potenzial bietet. Durch die kombinierte Anwendung von MEG, tACS und DBS entsteht ein integrativer Forschungsansatz, der tiefere Einblicke in die neuronalen, oszillatorischen Grundlagen crossmodaler und unimodaler Zeitschätzung ermöglicht.

ACKNOWLEDGMENTS, PUBLICATIONS, AND CURRICULUM VITAE

ACKNOWLEDGEMENTS

This project flourished through the funding organisation, collaboration, generosity, and expertise of my supervisor and colleagues. Your shared knowledge enriched my research with depth and breadth. Andreas, your supervision allowed me to take ownership of my work and develop confidence in my direction, while knowing support was always nearby. Till, your calm nature created a work environment where I could pursue my research without the fear of judgment or pressure. Your supervision brought a sense of ease, allowing ideas to grow in their own time. Marina, you welcomed me with open arms from day one, leaving a lasting impact on both, my scientific and personal path. Your ability to understand situations holistically and meet others with empathy, combined with your deep scientific insight and inquisitive questions, has been a constant source of support, perspective, and inspiration to me. Marleen, you always motivated me to face things head-on, with vigor and clarity. Your energy helped me to keep moving no matter the obstacles. Jonas, thank you for offering both direction and comfort when I felt stuck during my first project and beyond. Karin, thank you for your never-ending supply of coffee, your open heart, and our thoughtful conversations always kept me energized and inspired. Many thanks to the department of Neurology, especially Monika Pötter-Nerger and Alessandro Gulberti, who helped us tirelessly with patient recruitment and without whom this project would've not been possible.

During my time in Hamburg, I spun a social web, strong and steady, that gave me the strength to keep growing. Despite starting my PhD during the first lockdown, my flatmates made the silence and social distancing bearable. Alena, Alex, Bene, Lara, and Marlene, thank you for all the laughter, the good food and for making the everyday feel extraordinary. Most of all, Alex and Lara, both of you inspire me to approach life with softness and courage and being seen and supported by you is a treasured gift. The comfort of our friendship feels like a summer evening breeze in the South of France:

warm, steady, and soothing. Fabrizio, thank you for being there for me for most of my PhD, always reminding me to believe in myself when my confidence wavered. You've always inspired me with your ability to speak up for what you believe in and it's a quiet force that pushes me to do the same. Kayson and Tatia, from fellow master students to PhD companions, I couldn't have asked for better company on this journey. Kaysito, your humor, love for coffee and watermelon, and your ability to bring people together made every day lighter. Tatuki, your unique view of the world reminds me constantly to notice the strange and beautiful undergrowth of life, things others may overlook. Your way of seeing has deeply enriched mine. Both of you have a gift for making others feel at home and I hope you know how much our friendship means to me. I've been fortunate to be surrounded by so many more wonderful people, each of whom has impacted me in their unique way: Alex, Alina, Fatemeh, Masha, Tahmine, Mareike, Laura, and Lucas. I'm truly grateful to have met you along the way.

And above all, I am rooted in the unwavering support of my family. Christina, Theresa, Michael, and Magdalena, knowing that I can always lean on you has grounded me more than you might know. Mama & Papa, thank you for giving me the space to grow freely, slowly and in my own way. You provided a safe, rich soil that I've drawn strength from my whole life. You've always stood behind, quietly nurturing, never asking for light, but always giving it. Finally, to Gina, whose absence echoes in these words. You were the seed that led me into clinical research, in the hope of understanding just one piece of the illness that cast shadows over your life. Your wit, kindness, and philosophical nature shaped the very core of who I am. Though you're no longer here to read these lines, you are part of everything I do.

This work is not just my thesis, it is a testament to the vibrant, intricate ecosystem of people who surrounded me, lifted me, and walked with me. I may fall short in words, but I hope the gratitude in my heart reaches you nevertheless.

USE OF AI ASSISTANCE

A generative large language model, specifically, UHHGPT, a locally run instance of ChatGPT-4, was used for text correction and editing. Specifically, Artificial Intelligence (AI) tools were employed with the goal of identifying grammatical errors and enhancing readability of already written text. Importantly, the model was *not* used to create scientific content, generate ideas, or interpret findings. AI was used for debugging of LaTeXand MATLAB errors, but not for the generation of code for analyses.

PUBLICATIONS

The following articles resulted directly from the work on this dissertation:

- **Burke, R.,** Maÿe, A., Misselhorn, J., Fiene, M., Engelhardt, F. J., Schneider, T. R., and Engel, A. K. (2024). The role of delta phase for temporal predictions investigated with bilateral parietal tacs. *Brain Stimulation*, 18:103–113. doi: https://doi.org/10.1016/j.brs.2024.12.1476.

- **Burke, R.,** Daume, J., Schneider, T. R., and Engel, A. K. (2025). Differential contributions of low-frequency phase and power in temporal prediction: A crossmodal MEG study. *bioRxiv*, doi: https://doi.org/10.1101/2025.05.26.656128.

- **Burke, R.,** Schoenfeld, M.J., Gulberti, A., Moll, C., Pötter-Nerger, M., and Engel, A. K. (2025). Modulation of temporal prediction by STN-DBS in Parkinson's disease: Links between behavior and cortical oscillations. *bioRxiv*, https://doi.org/10.1101/2025.05.29.656824.

- Schoenfeld, M.J., **Burke, R.,** Schneider, T. R., and Engel, A. K. (2025). Predicting time across age: Comparing performance of younger and older adults in a temporal prediction task *in preparation*.

CURRICULUM VITAE

REBECCA BURKE

About Me

How we think and perceive the world has always been a question I've been drawn to. My resumé is a reflection of the different angles from which I've tried to approach it. An attempt to understand the mind through abstract and philosophical lenses made me curious about how mental processes emerge from brain function and, most recently, how we can shape and influence these brain functions through electrical brain stimulation.

Personal

Rebecca Burke
German
1992

Areas of Specialization

Neuroscience · Cognitive Science · Neurophilosophy · Neuromodulation ·

Programming

MATLAB
R
LaTeX
python

Languages

German	C2	mother tongue
English	C1	
French	B1	
Spanish	A1	

Short Resumé

since 03/2020 — **Doctoral Researcher**
University Medical Center Hamburg-Eppendorf (UKE) · Hamburg, Germany
Research Focus: Investigation and modulation of temporal prediction using non-invasive and invasive electrical brain stimulation

03/2019–10/2019 — **Research Assistant**
Applied Neurocognitive Psychology Lab, Carl von Ossietzky University · Oldenburg, Germany
Tutor for Computational Neuroscience: Statistical Learning

09/2018–02/2019 — **Research Assistant**
BANCO, Institut de Neurosciences de la Timone · Marseille, France
Research focus: Speech production, fMRI

08/2017–08/2018 — **Research Assistant**
Biological Psychology, Carl von Ossietzky University · Oldenburg, Germany
Research focus: ADHD and sports, fMRI

10/2015–03/2016 — **Psychological Assistant - Internship**
Vitanas Dementia Center · Magdeburg, Germany
Psychological assistance in special dementia care center

02/2015–05/2015 — **Psychological Assistant - Internship**
St. George's Hospital · London, Great Britain
Neuropsychological diagnostics and therapy on stroke and neurorehabilitation wards

Education

since 2020 — **PhD Candidate**
University Medical Center Hamburg-Eppendorf (UKE) ·
Research Focus: Neuromodualation of temporal prediction using non-invasive and invasive electrical brain stimulation

2019 — **M.Sc. Neurocognitive Psychology**
Carl-von-Ossietzky University, Oldenburg ·
Thesis: Connectivity analysis of cortical and subcortical regions in auditory processing using EEG and iEEG data

2016 — **B.A. Philosophy, Neuroscience, Cognition**
Otto-von-Guericke University, Magdeburg ·
Thesis: Between paternalism and autonomy: An ethical view on the use of psycho-active drugs in caring for people with dementia

Certificates & Grants

2023 DGKN Best Poster Award
2017 A*Midex fellowship (€4,000)

Publications

2024 *The role of delta phase in temporal predictions using bilateral parietal tACS*, Brain Stimulation
2025 *Differential contributions of low-frequency phase and power in temporal prediction*, bioRxiv
2025 *Modulation of temporal prediction by STN-DBS in Parkinson's disease: Links between behavior and cortical oscillations*, bioRxiv

Rebecca Burke r.burke@uke.de Hamburg

EIDESSTATTLICHE ERKLÄRUNG

Ich versichere ausdrücklich, dass ich die Arbeit selbständig und ohne fremde Hilfe, insbesondere ohne entgeltliche Hilfe von Vermittlungs- und Beratungsdiensten, verfasst, andere als die von mir angegebenen Quellen und Hilfsmittel nicht benutzt und die aus den benutzten Werken wörtlich oder inhaltlich entnommenen Stellen einzeln nach Ausgabe (Auflage und Jahr des Erscheinens), Band und Seite des benutzten Werkes kenntlich gemacht habe. Das gilt insbesondere auch für alle Informationen aus Internetquellen. Soweit beim Verfassen der Dissertation KI-basierte Tools („Chatbots“) verwendet wurden, versichere ich ausdrücklich, den daraus generierten Anteil deutlich kenntlich gemacht zu haben. Die „Stellungnahme des Präsidiums der Deutschen Forschungsgemeinschaft (DFG) zum Einfluss generativer Modelle für die Text- und Bilderstellung auf die Wissenschaften und das Förderhandeln der DFG“ aus September 2023 wurde dabei beachtet. Ferner versichere ich, dass ich die Dissertation bisher nicht einem Fachvertreter an einer anderen Hochschule zur Überprüfung vorgelegt oder mich anderweitig um Zulassung zur Promotion beworben habe. Ich erkläre mich damit einverstanden, dass meine Dissertation vom Dekanat der Medizinischen Fakultät mit einer gängigen Software zur Erkennung von Plagiaten überprüft werden kann.

Unterschrift: